



*Molecular mechanisms of forgetting  
in *Caenorhabditis elegans**

**Inauguraldissertation**  
zur  
Erlangung der Würde  
eines Doktors der Philosophie  
vorgelegt der  
Fakultät für Psychologie  
der Universität Basel

von

Nils Omar Hadziselimovic

aus Basel-Land, Schweiz

Basel, Mai 2014

Genehmigt von der Fakultät für Psychologie  
auf Antrag von

Prof. Dr. Andreas Papassotiropoulos

Prof. Dr. Dominique J-F. de Quervain

Basel, den 27.01.2014

Prof. Dr. Alexander Grob

Dekan



Miyamoto Musashi, from the series Sixty-nine Stations of the Kisokaidô Road  
by Utagawa Kuniyoshi, 1852

## **Acknowledgments**

I would like to thank my supervisors Professors Andreas Papassotiropoulos and Dominique de Quervain as well as Dr. Attila Stetak. Their trust and guidance was essential to the work, without which this thesis would not have been possible.

I would like to thank my parents and my wife for their support and encouragement.

Finally I would like to give thanks to the entire research group for providing a very fruitful environment.

## Table of contents

Introduction.....	6
Theoretical Background	
Definition of forgetting.....	7
Theoretical models of forgetting.....	8
Molecular mechanisms of learning and memory.....	8
Synaptic plasticity and the actin cytoskeleton.....	13
RNA binding proteins and synaptic plasticity.....	15
Molecular mechanisms of forgetting.....	17
<i>C. elegans</i> as a model organism.....	19
References.....	21
Original Research Paper	
Forgetting is regulated via Musashi-mediated translational control of the Arp2/3 complex.....	26
Declaration.....	58
Curriculum Vitae.....	59

## Introduction

“Memory is the scribe of the soul.”

Aristotle

Forgetting is a process that accompanies us every day of our lives, most of the time unnoticed, yet when it is noticed it is usually associated with negative connotations. To forget a telephone number or an acquaintance’s name or birthday is usually experienced as uncomfortable. Most instances of conscious forgetting are not readily accepted, yet at the same time forgetting allows for the erasure of unnecessary or unpleasant memories, updating of old inaccurate memories or for the generalization of similar memories and thus their abstraction and application in other mental processes. The necessity and helpfulness of functional forgetting becomes clear when one considers, for example, post-traumatic stress disorder, a condition in which patients are unable to let go of traumatic memories.

This thesis attempts to further the knowledge on forgetting based on the following original research paper:

### **Forgetting is regulated via Musashi-mediated translational control of the Arp2/3 complex.**

Nils Hadziselimovic, Vanja Vukojevic, Fabian Peter, Annette Milnik, Matthias Fastenrath, Bank Fenyves, Petra Hieber, Philippe Demougin, Christian Vogler, Dominique J-F. de Quervain, Andreas Papassotiropoulos, Attila Stetak, *Cell*. 2014 Mar 13;156(6):1153-66.

## **Theoretical Background**

### **Definition of forgetting**

The definition of forgetting is, even though a very old concept, still very much debated. Generally, forgetting is seen as the opposite of learning and memory, a process in which memory is lost. But is it really and if so how? What exactly do we forget and what happens when we do? Are memories actually erased, deleted or merely not retrieved, while actually still present?

One reason why this debate is still going on very strongly is the fact that it is still impossible to prove complete erasure of memories. The opposite, complete recollection, has been reported however and may help shed light on this problem. The case of A.J. was recently reported by Parker, Cahill and McGaugh [1] which shows that one can exhibit what is now called “Highly Superior Autobiographical Memory” (HSAM). HSAM is an ability to recall dates and personal events that happened as far back as the childhood in great detail and without application of mnemonic techniques or in fact any greater cognitive effort. Most of those memories would have been of events happening only once, carrying no special emotional relevance, leaving out the possibility of stronger encoding through repetition or emotional gravity.

If then the capacity for “total recall” exists, the inability to recall memories could likely play a more important role in the process of forgetting than erasure.

Arguing in favour of this point is for example Tulving and Pearlstone’s experiment of cue-dependent retrieval [2]. In this experiment, probands were presented with words that were arranged in categories and later asked to remember them. If given cues related to the category, probands were able to remember significantly more words than without cues. Importantly, giving cues after the first recall without cues increased the amount of words recalled later.

Another report in favour of forgetting being a retrieval failure comes from an experiment performed by Erdelyi and Becker. Presenting subjects with pictures and asking them to recall the pictures immediately after presentation, then again two times after incrementing intervals produced increasing numbers of recalled pictures [3]. It’s possible therefore, that forgetting represents a limited capacity retrieval system [4].

As such Tulving’s definition of forgetting as “the inability to recall something now, that could be recalled on an earlier occasion” [5] seems the most appropriate.

## **Theoretical models of forgetting**

Two main theories about the nature of forgetting are currently discussed in psychology: trace decay and interference [6].

Trace decay itself is not as much a scientific theory that had once been proposed, as it is the general implication of lost memory due to decay much like ice vanishes in hot air. Numerous papers have attacked trace decay and brought forward good arguments as to why trace decay can't be the main mechanism of forgetting. Most important among others is the argument of reminiscence, the act of remembering items that couldn't be remembered previously [7]. While trace decay is under debate, it still proves to be exceptionally difficult to demonstrate the existence or absence of trace decay.

Interference theory states that forgetting happens due to interfering memory, or, as McGeoch put it, the wrong memory being accessed by a particular cue [8].

Two forms of interference are generally distinguished: retroactive interference and proactive interference.

Retroactive interference refers to the more difficult retrieval of older memories when similar newer memory contents have been acquired after the original memory that is supposed to be retrieved. Proactive interference is basically the inverse, whereby newly acquired memories are also more difficult to retrieve if the subject has previously acquired similar memory items [9].

## **Molecular mechanisms of learning and memory**

To investigate forgetting as the reversal of learning and memory on a cellular and molecular level requires to first understand the process of learning and memory retention.

Until Ramon y Cajals investigations into the cellular brain structure at the end of the 19<sup>th</sup> century, it was unclear whether the brain was made up of discrete cells, as had been proposed for other tissues only decades before. Laying the foundation of the neuron doctrine with his work, demonstrating not only intricate details of the neuronal cellular network, Ramon y Cajal furthermore proposed that these discrete neurons possessed polarity, allowing communication only in one direction [10].

Building upon this framework, Donald Hebb put forward his theory whereby memory was stored in the synapses, the contact between the neurons themselves [11], which is often summarized with a quote of his: "What wires together, fires together."



Thanks to the vast amount of research performed on several different model organisms, including invertebrates as well as vertebrates and mammals [12, 13], we now know not only that Hebb was right in his assumption, but perhaps more importantly also that the molecular mechanisms of learning and memory are highly conserved between species [12, 13].

Habituation as the simplest form of learning and memory requires only one synapse for the acquisition and retention of the behaviour. The gill withdrawal reflex of the sea slug *Aplysia* has successfully been used to study habituation. This reflex requires only two neurons, a sensory neuron registering the touch input and a motor neuron executing the gill withdrawal output. Upon repeated activation of the sensory neuron through touch, the gill withdrawal reflex attenuates, showing habituation to the touch. Castellucci et al. were able to demonstrate that this habituation was due to less excitatory neurotransmitter released per activation of the sensory neuron, thereby decreasing synaptic transmission efficiency [14].

Sensitization or dishabituation refers to the opposite phenomenon whereby the gill withdrawal reflex is heightened through application of a single noxious stimulus. This stronger gill withdrawal was found to be due to an interneuron modulating the primary sensory neuron thereby increasing the release of the same excitatory neurotransmitter [14].

Investigating the molecular mechanisms of facilitation, which underlies sensitization, Castellucci et al. found that the modulating interneuron releases serotonin upon activation by the noxious stimulus, which binds to receptors on the primary sensory neuron. This in turn activates the enzyme adenylyl cyclase, which produces the second messenger cAMP. cAMP in turn activates among others PKA, which phosphorylates various targets thereby enhancing synaptic transmission. One target for example is a potassium channel, which closes upon phosphorylation and thereby lengthens the action potential, enhancing the release of neurotransmitters (Figure1)[14].

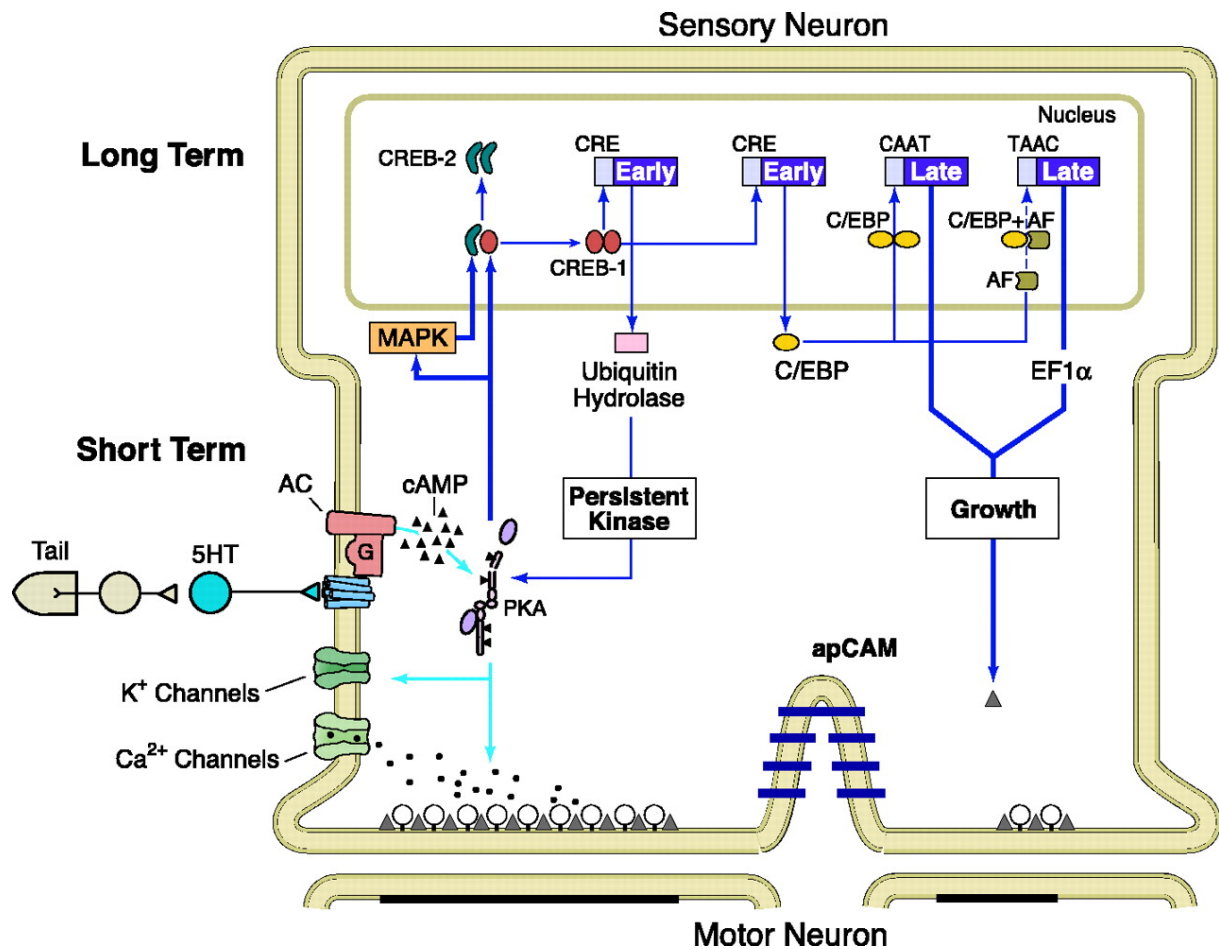


**Figure 1.** (adapted from Kandel, 2001 [15]) Presynaptic facilitation is governed by serotonin stimulation, which activates the adenylyl cyclase, which in turn activates PKA. PKA phosphorylates various proteins, resulting in closure of potassium channels and enhanced neurotransmitter release among others. Longer lasting activation of PKA leads to phosphorylation and thus activation of transcription factors, which results in protein synthesis and synaptic growth.

Interestingly, *Aplysia* can also be classically conditioned using the same stimuli and the same neuronal network as with sensitization, with the exception of different timing. Timing the noxious (unconditioned) stimulus appropriately with the touch (conditioned) stimulus results in much stronger cAMP production in the primary sensory neuron through calcium enhanced activation of the adenylyl cyclase [16].

Post-synaptically, i.e. in the motor neuron in *Aplysia*, transmission can be enhanced as well, interestingly using similar molecular mechanisms as in the pre-synaptic neuron. The excitatory neurotransmitter glutamate can bind to two different types of receptors termed AMPA- and NMDA-type. Upon binding of glutamate, AMPA-receptors open allowing sodium and potassium to pass freely. This leads to local depolarizations, termed excitatory post-synaptic potentials (EPSPs). If the post-synaptic neuron is

depolarized enough and NMDA-receptors bind glutamate and thus open, calcium can enter the neuron. This influx of calcium through NMDA receptors is responsible for the enhancement of synaptic transmission [17] by activating different calcium-dependent kinases such as calcium/calmodulin-dependent kinase II [18], protein kinase C [19] and tyrosine kinase Fyn [20]. These kinases phosphorylate, much like PKA, various proteins including AMPA-receptors, enhancing their response to neurotransmitters. They also induce incorporation of more AMPA-receptors into the post-synaptic membrane, thus enhancing the response to released neurotransmitters.

The behavioural distinction between short- and long-term memories can be correlated with further molecular mechanisms found in synaptic plasticity. While short-term adaptations (habituation as well as sensitization) in *Aplysia*, lasting a few hours, are based in large parts on phosphorylation of existing structures, long-term adaptation was found to require protein degradation or synthesis.

Long-term habituation in *Aplysia* for example leads to reduction of synaptic terminals and the amount of certain proteins, while long-term sensitization produces synaptic growth [21]. Similarly, intracerebral injection of puromycin, a protein synthesis inhibitor, after acquisition of new behaviour, prevents long-term memory formation in mice [22].

Formation and retention of long-term memory employs molecular mechanisms that are based on and expand those in use in short-term memory. Enhancing and prolonging the levels of cAMP through repeated sensitization trials for example results in prolonged activity of PKA, which then recruits p42 MAPK. Both kinases together phosphorylate transcription factors and thus enhance gene expression, which results in enhanced protein synthesis. One transcription factor in particular, CREB1, which is activated by PKA, plays a key role by promoting expression of immediate-response genes such as ubiquitin hydrolase [23], which hydrolyses the regulatory subunit of PKA thus prolonging its activity, and C/EBP [24], which leads to the expression of as yet unidentified proteins necessary for the growth of new synaptic connections (Figure 1).

Since Squires summary description [25], long-term memory has generally been divided into explicit (or declarative) memory and implicit (or non-declarative) memory. Implicit memory describes memories that are not consciously recollected, such as the previously mentioned habituation, sensitization and classical conditioning as well as skill learning. Explicit memory on the other hand describes consciously recollected memories and is divided again into episodic and semantic memory. This distinction can also be made

anatomically, as the different memory classes can be ascribed to different but overlapping anatomic areas. Most prominently the hippocampus features as the essential integration site for episodic memory in mammals, which became dramatically clear in the case of patient H.M. as reported by Scoville and Milner [26]. Having undergone bilateral excision of the hippocampus due to severe uncontrollable temporal epilepsy, patient H.M. was no longer able to form new declarative memories. H.M. could however still remember old events that happened long before the surgery and form new implicit memory. As such the hippocampus gained considerable attention in the research on learning and memory.

Bliss and Lømo discovered a type of synaptic plasticity in cultured hippocampal slices from rabbits they termed long-term potentiation (LTP) [27]. Tetanic stimulation of the perforant pathway led to increased response to subsequent single stimuli (Figure 2A). Similar to short- and long-term facilitation, early- and late-LTP can also be distinguished based on duration of potentiated response and requirement for protein synthesis (Figure 2B)[28]. Furthermore, the molecular mechanics of induction are strikingly similar, requiring the activation of NMDA receptors, CamKII, PKA and CREB-1 (Figure 2C)[15].

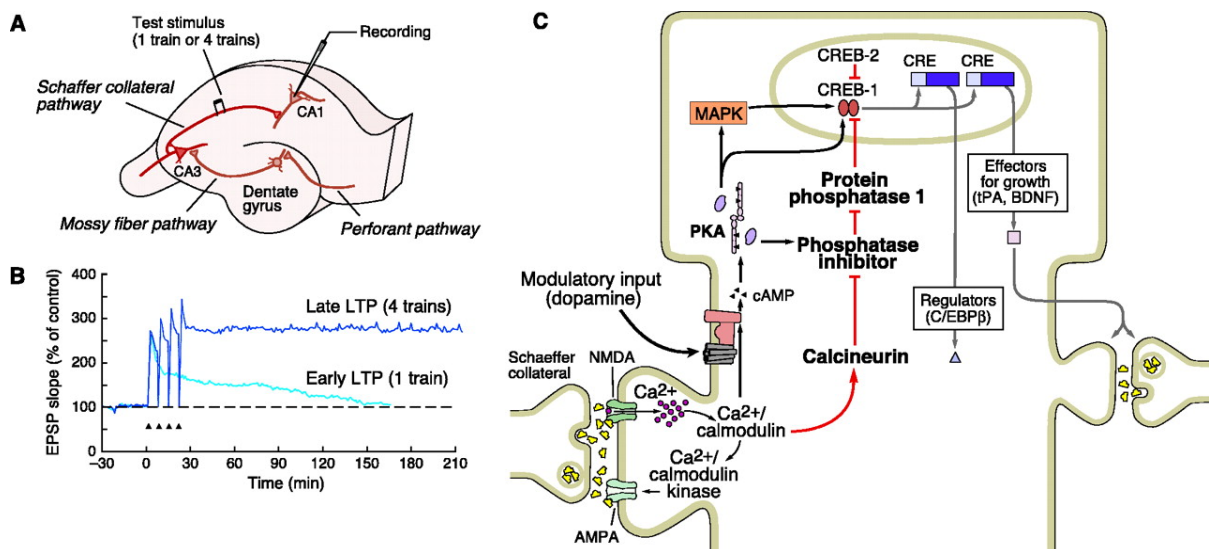


**Figure 2.** (adapted from Kandel, 2001 [15]) **A.** Long-Term Potentiation can be induced in cultured hippocampal slices by tetanic stimulation. **B.** Depending on the number of tetanic stimuli, early or late LTP can be induced. **C.** LTP is initiated by calcium-influx through NMDA-receptors, which activates the kinases CaMKII and PKA among others. The early phase of LTP expression results among others from phosphorylation and externalization of AMPA-receptors. The late phase of LTP is a result of protein synthesis due to enhanced transcription by phosphorylated transcription factors such as CREB1.

Induction of LTP however only enhances synaptic strength. The discovery of long-term depression (LTD) added the possibility of modulating synaptic strength in opposing ways [29-32]. LTD leads to reduction in synaptic strength through, among others, internalization of AMPA receptors. Surprisingly, LTD employs the same pathways as LTP, albeit in different ways. Induction of LTP occurs after short but high frequency tetanic bursts, resulting in strong calcium influx, while induction of LTD happens after application of long but low frequency electric currents, resulting in far less calcium influx [30]. This lower level of calcium in LTD is thought to be responsible for the different outcomes while applying the same pathways because the participating enzymes have different calcium affinities [32]. For example the phosphatase calcineurin is activated at much lower calcium levels than CaMKII and thus shows relatively greater activity at lower calcium levels, which leads to AMPA-receptors being dephosphorylated and internalized, rather than phosphorylated and incorporated into the post-synaptic cell membrane.

A possibly more physiological representation of synaptic plasticity was the discovery of spike-timing-dependent plasticity (STDP). STDP incorporates both concepts, LTP as well as LTD, in the same model, however not making them dependent on different tetanic stimuli, rather on the timing of action potentials with EPSPs and the activation of NMDA receptors thereof [33-35]. NMDA receptor activation through depolarization after presynaptic activation results in enhancement, NMDA receptor activation through depolarization before presynaptic activation results in weakening of synaptic strength, both thought to be mediated by different levels of calcium [34].

### **Synaptic plasticity and the actin cytoskeleton**

Synaptic plasticity relies in large parts on the ability to change the structure of dendritic spines. Dendritic spines come in three general types: the stubby type with a small head and no neck, the thin type with a long thin neck and a small head and the mushroom type with a neck and a big head [36]. These types however rather represent a continuum than distinct classes, as the spines can change morphology according to activity [37].

An important driving force behind the morphological change is the regulation of the actin network, which forms the central infrastructure of dendritic spines [38].

Beyond driving morphological change, the actin network in synapses participates in the organization of the postsynaptic density [39], anchoring of receptors [40], synaptic transport of organelles and vesicles [41] and local protein synthesis [42].

Filamentous actin, f-actin, is polymerized from globular, g-actin monomers, in an activity-dependent manner [43]. Actin filaments are polar structures, growing at the so-called “barbed” end, where monomers are added, and depolymerizing at the “pointed” end, where g-actin is removed. Based on this process, f-actin can “treadmill” by removing and adding g-actin at the same time, keeping the filaments in a high turnover allowing for very dynamic structural adaptations, unless its stabilized by actin capping proteins [44]. In the dendritic spine, f-actin is found in three pools, which allow for regulated morphological growth or shrinkage (Figure 3) [45]. Regulation of the actin network plays an important part in synaptic plasticity. Interfering with the actin capping activity of adducin for example reduces the stability of synaptic size increase and thereby reduces memory retention [46].

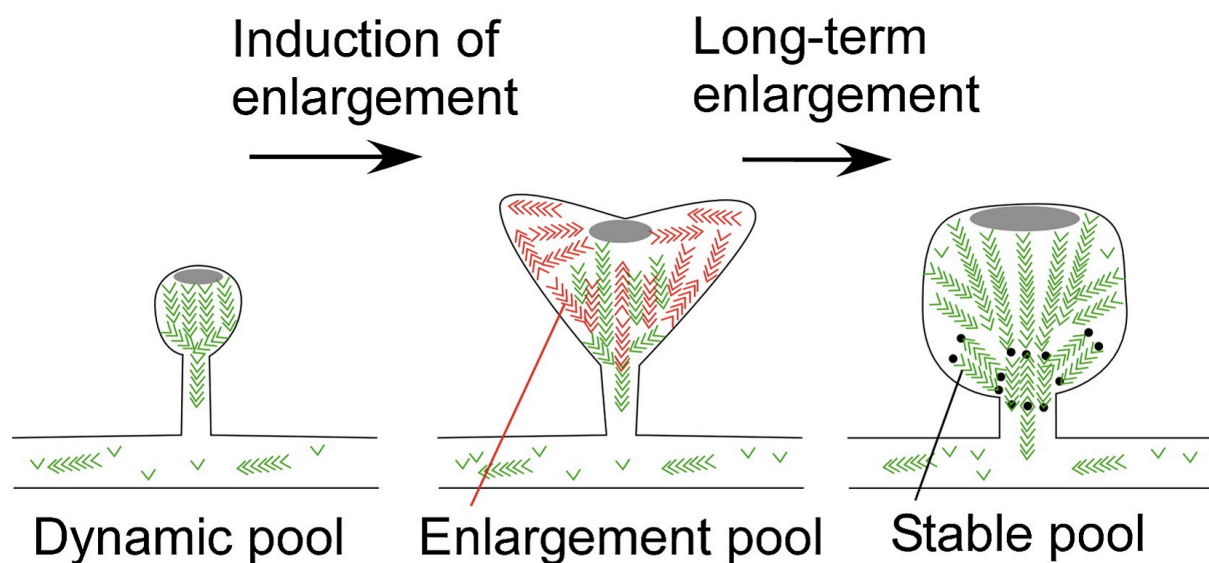


**Figure 3.** (adapted from Honkura et al., 2008 [45]) F-actin is found in three pools in dendritic spines, a dynamic, an enlargement and a stable pool, which together participate in the morphological change of dendritic spines.

Proper organization of the actin network in dendritic spines requires the function of among others the Arp2/3 complex [47]. The Arp2/3 complex is a protein complex consisting of seven subunits that together bind to the side of actin filaments and, upon activation among others by WASP [48, 49], induce actin branching, serving as the

nucleation core [50]. Synaptic plasticity involves the active regulation of the Arp2/3 complex. Disruption of WAVE-1, an Arp2/3 activator, leads to impaired learning and memory [51, 52] and knock-down of the Arp2/3 inhibitor PICK1, leads to reduced LTD in cultured hippocampal slices [53].

### **RNA binding proteins and synaptic plasticity**

Martin et al. were able to demonstrate that only activated or “tagged” synapses undergo structural change upon increased synaptic activity, while other synapses on the same neuron, that weren’t active, did not [54]. These local structural changes required protein synthesis, however RNA transcription is an obligatory central process. Memory formation was soon found to be independent of RNA transcription [55] and localized protein synthesis was discovered in dendritic spines [56-58]. This allows certain synapses to grow while others, on the same neuron, do not, hence making differentiated synaptic efficiency possible.

As such RNA-binding proteins (RBPs) play an important role in synaptic plasticity, regulating gene expression locally. RBPs form RNA-protein-granules, transporting mRNA from the nucleus to their destination while inhibiting their translation, store them release them to allow or even enhance protein synthesis upon cues and organize their degradation [59-63]. Three types of RNA granules are found in dendrites: Ribonucleoprotein particles (RNPs), which mainly transport and store mRNA; stress granules (SGs), which isolate certain mRNAs upon stress signals, shifting translation in favour of other mRNAs; and processing bodies (P-bodies), which participate in the degradation of mRNAs.

An example of a prominent RBP playing a major role in synaptic plasticity is CPEB [63-65]. CPEB, cytoplasmic polyadenylation element binding protein, is a RBP that regulates mRNA translation in different tissues including dendrites. By binding to the cytoplasmic polyadenylation element (CPE) in the 3'UTR region of target mRNAs, CPEB first prevents their polyadenylation and subsequent translation. Upon phosphorylation and thus activation CPEB undergoes a conformational change and activates translation permitting polyadenylation of the target mRNA [63, 66]. Furthermore it has been proposed, that CPEB needs a certain threshold of activation after which it is able to activate other CPEB proteins and keep this activated state in a prion-like fashion, thereby supporting prolonged translation und thus long-term memory [67].

The RBP of interest for this thesis belongs to the musashi family. This family is a group of highly conserved RBPs, having been described functionally first in *drosophila* [68], where *msi* was found to be required for the proper development of adult external sensory organs. Since then, representatives of this family have been found in several other species including humans [69] and *C. elegans* [70]. Mammalian genomes encode two separate forms of musashi, MSI1 and MSI2, which have a high degree of sequence similarity and thus likely share many targets, however MSI-1 is expressed predominantly in neuronal stem cells [71] while MSI-2 shows a more ubiquitous expression pattern, including differentiated interneurons in the hippocampus [72].

Musashi family members possess two tandem RNA recognition motifs (RRMs), while their target mRNAs in turn contain a conserved so called musashi binding element (MBE) (G/A)U<sub>1-3</sub> AGU found in their 3' untranslated region [73] through which interaction is established. The MBE sequence is widely distributed in the genome identifying roughly 8000 potential targets containing at least one MBE however so far only a few have been confirmed to be *in vivo* musashi targets [74]. Interestingly musashi family members can inhibit translation of their targets, as has been reported for *m-numb* [73], but also enhance translation as for example of *c-mos* in *Xenopus laevis* [75]. This capacity of differential regulation seems to be independent of the target as another elegant experiment has shown, where musashi inhibited or enhanced translation of the same artificial target in the same cellular context depending only on environmental cues [76]. It is not fully understood how musashi family members regulate translation, however recent work by Kawahara et al. showed that the vertebrate MSI-1 (but not MSI-2) associates with the poly [A] binding protein (PABP) preventing PABP interaction with the eIF4G initiation factor and thus the recruitment of ribosomes [77] in a similar way to CPEB.

A recent microarray analysis of potential MSI-1 targets identified among others ACTR2 [74], one of seven subunits of the highly conserved Arp2/3 complex. However, the microarray analysis was performed with musashi ectopically expressed in HEK cells and the action of musashi in synaptic plasticity has thus far not been described. Since the Arp2/3 complex could play an important part in synaptic plasticity and is a potential target of musashi, this interaction is of considerable interest with regard to learning and memory.



## **Molecular mechanisms of forgetting**

Clear-cut evidence for mechanisms involved in the observable behaviour of forgetting is still sparse but what is available offers excellent first insight into the regulation of memory loss.

A recent study found the TIR-1/JNK-1 MAPK pathway to be involved in the regulation of forgetting in *C. elegans* [78]. TIR-1/JNK-1 pathway mutants showed prolonged retention of adaptation to diacetyl. Interestingly, even though the sensory neuron AWA is necessary for sensation and adaptation to diacetyl, it seems that the AWC sensory neuron is responsible for initiating forgetting in AWA via a suggested neurosecretory mechanism. TIR-1/JNK-1 mutants furthermore exhibit prolonged retention of associative memory as well. However in this setting, expression of TIR-1 in sensory neurons was not able to rescue the phenotype, while expression in a subset of interneurons was, suggesting that the TIR-1/JNK-1 pathway is involved in the regulation of different types of behavioural plasticity in different sets of neurons. Another study found the modulating activity of dopamine to be responsible for learning and forgetting in *Drosophila* [79]. Delivering an unconditioned stimulus via the dopamine receptor dDA1, dopaminergic neurons (DANs) participate in the acquisition of associative memory. After fulfilling this role, they continue to release dopamine, activating however only the DAMB dopamine receptors, which results in forgetting of recently acquired labile memory. Particularly interesting is the fact that blocking the action of DANs after learning results in enhanced memory expression, while stimulation of DANs leads to accelerated memory decay, demonstrating the specific effect of DANs on the regulation of forgetting, separately from their effect on learning. On their own, while difficult to make further conclusions, these two studies clearly show, that forgetting is an induced and regulated behaviour, that at least in these settings is not solely due to passive decay. Evidence for regulation of forgetting has also been found in connection with synaptic structures. Shuai et al. demonstrated how Rac, a GTPase from the Rho family, is responsible for induced forgetting [80]. Rac inhibition has no effect on learning or short-term retention of memory in *Drosophila* but leads to prolonged retention of labile (but not consolidated) memory and overexpression to accelerated loss. This prolonged memory retention is achieved by disinhibition of the actin depolymerizing enzyme cofilin and *vice versa*, which implies that the actin network not only participates in

learning and memory, but is also actively regulated in forgetting. Interestingly this slower forgetting is also found in assays that produce interference-induced forgetting and not just, as the authors claim, forgetting due to decay. Finally the study found reversal learning in which the flies are trained to forget incorrect memories by reversal of the training conditions; when impaired the mutant flies were unable to forget old, “outdated” memories. Taken together, the authors argue, that decay and interference-induced forgetting might share the same molecular mechanisms, implying that decay and interference are not as distinct as originally thought.

As much as phosphorylation is a key action in learning and memory, the opposite, dephosphorylation, seems to be important in loss of memory, with the phosphatases calcineurin as well as its downstream target protein phosphatase 1 being key players. Transiently expressing inhibitors of the phosphatase calcineurin in mice, Malleret et al. were able to produce LTP easier and prolong memory retention [81]. In a similar way, inhibition of calcineurin enhances sensitization in *Aplysia* by activation of MAPK after only a single pulse of serotonin [82]. Adding to this, Genoux et al. could demonstrate that inhibiting protein phosphatase 1 leads to fewer necessary trainings to achieve long-term memory in mice and importantly, inhibition of protein phosphatase 1 after learning resulted in longer memory retention, implicating its role in forgetting [83]. Demonstrating the importance of continuous phosphorylation, Shema et al. showed that conditioned taste aversion memory could be effectively erased at any time-point after acquisition by inhibiting the kinase PKMzeta [84].

Cao et al demonstrated a different very interesting direct link between the molecular mechanisms and the behaviour of forgetting. While the participation of CaMKII in LTP has been mentioned previously, its overexpression specifically at the timepoint of recall of certain memories selectively erases them in mice [85]. This fits well with the theory of reconsolidation, whereby once consolidated memories are made labile again through recall to be adapted after which they are reconsolidated [86]. As such, reconsolidation could be seen as a forgetting mechanism of decay as well as interference, whereby the recall presents as its own interference.

If the hypothesis on the molecular mechanisms of forgetting is extended beyond the observations linked to the actual forgetting *in vivo*, then on the surface it would be compelling to equate LTP with memory and LTD with forgetting, as LTP has been equated with memory storage. However, not only does interfering with both LTP and

LTD disturb learning and memory but also neither LTP nor LTD could thus far be shown to directly underlie specific behaviours or memory traces, even though the indirect evidence is overwhelming. Nevertheless, if the reduction in synaptic efficiency is assumed to be part of forgetting, then certain elements of LTD likely participate. Moreover if, as previously theorized, trace decay is at least in part caused by interference and interference itself is due to learning of similar information, then forgetting could be a form of “unlearning”, a concept similar to extinction of classically conditioned behaviours, which is thought to be a form of learning dependent on NMDA-receptors [87].

### ***C. elegans* as a model organism**

Reducing the number of neurons that participate in a given learning and memory network is of great advantage when studying the molecular mechanisms of synaptic plasticity. As Castellucci wrote: “We have indeed found that once the wiring diagram of the behaviour is known, the analysis of its modifications becomes greatly simplified” [14]. As a basic premise, *C. elegans* not only offers a completely sequenced genome [88] with roughly 80% of the protein coding genes being homologous to humans [89], but also a complete connectome, i.e. a complete mapping and characterization of its neurons, with all its connections. Every wild type *C. elegans* hermaphrodite worm has exactly 959 somatic cells, of which 302 are neurons [90]. The hermaphrodite can self-fertilize, which effectively allows the investigator to keep a line of perfect genetically homogenous population, thus controlling the influence of the genetic variability. Genes can easily be modified, either by adding genetic material through microinjection or through mutagenesis by irradiation, the use of chemicals or transposons or as recently reported through the targeted use of endonucleases [91]. *C. elegans* can furthermore easily be treated with RNAi which allows for comfortable and selective knock-down of gene expression [92]. As another advantage, *C. elegans* is transparent throughout life, which allows *in vivo* examinations of fluorescently labelled proteins of interest [93]. *C. elegans* has a fast life-cycle, growing to adult form within 2 to 3 days under given temperature conditions, lives for 2 weeks and is comparably cheap to maintain.

Finally, *C. elegans* is able to learn, not only by habituation or sensitization but also by association, and together with the low amount of neurons, makes it particularly interesting for studies on learning and memory. Taking these advantages into

consideration, we chose *C. elegans* as the model organism to examine the effects of musashi in the learning and memory processes.

## References

1. Parker, E.S., L. Cahill, and J.L. McGaugh, *A case of unusual autobiographical remembering*. *Neurocase*, 2006. **12**(1): p. 35-49.
2. Tulving, E. and Z. Pearlstone, *Availability Versus Accessibility of Information in Memory for Words*. *Journal of Verbal Learning and Verbal Behaviour*, 1966. **5**(4): p. 381-391.
3. Erdelyi, M. and J. Becker, *Hypermnesia for pictures: Incremental memory for pictures but not words in multiple recall trials*. *Cognitive Psychology*, 1974. **6**(1): p. 159-171.
4. Tulving, E., *The effects of presentation and recall of material in free-recall learning*. *Journal of Verbal Learning and Verbal Behavior*, 1967. **6**(2): p. 175-184.
5. Tulving, E., *Cue-dependent forgetting*. *American Scientist*, 1974. **62**(1): p. 74-82.
6. Wixted, J.T., *The psychology and neuroscience of forgetting*. *Annual review of psychology*, 2004. **55**: p. 235-69.
7. Brown, W., *To what extent is memory measured by a single recall?* *Psychonomic Science*, 1923. **6**: p. 377-382.
8. McGeoch, J.A., *the psychology of human learning* 1942, Oxford: Longmans, Green and Co.
9. Underwood, B.J., *Interference and forgetting*. *Psychological Review*, 1957. **64**(1): p. 49-60.
10. Ramon y Cajal, S. *La fine structure des centres nerveux*. in *Croonian Lecture*. 1894. London: Royal Society.
11. Hebb, D., *The Organization of Behaviour*. 1949, New York: Wiley & Sons.
12. Kandel, E.R., *The molecular biology of memory: cAMP, PKA, CRE, CREB-1, CREB-2, and CPEB*. *Molecular brain*, 2012. **5**: p. 14.
13. Mayford, M., S.A. Siegelbaum, and E.R. Kandel, *Synapses and memory storage*. *Cold Spring Harbor perspectives in biology*, 2012. **4**(6).
14. Castellucci, V., et al., *Neuronal mechanisms of habituation and dishabituation of the gill-withdrawal reflex in Aplysia*. *Science*, 1970. **167**(3926): p. 1745-8.
15. Kandel, E.R., *The molecular biology of memory storage: a dialogue between genes and synapses*. *Science*, 2001. **294**(5544): p. 1030-8.
16. Hawkins, R.D., et al., *A cellular mechanism of classical conditioning in Aplysia: activity-dependent amplification of presynaptic facilitation*. *Science*, 1983. **219**(4583): p. 400-5.
17. Lynch, G., et al., *Intracellular injections of EGTA block induction of hippocampal long-term potentiation*. *Nature*, 1983. **305**(5936): p. 719-21.
18. Malenka, R.C., et al., *An essential role for postsynaptic calmodulin and protein kinase activity in long-term potentiation*. *Nature*, 1989. **340**(6234): p. 554-7.
19. Routtenberg, A., *Synaptic plasticity and protein kinase C*. *Progress in brain research*, 1986. **69**: p. 211-34.
20. Grant, S.G., et al., *Impaired long-term potentiation, spatial learning, and hippocampal development in fyn mutant mice*. *Science*, 1992. **258**(5090): p. 1903-10.
21. Bailey, C.H. and M. Chen, *Structural plasticity at identified synapses during long-term memory in Aplysia*. *Journal of neurobiology*, 1989. **20**(5): p. 356-72.
22. Flexner, J.B., L.B. Flexner, and E. Stellar, *Memory in mice as affected by intracerebral puromycin*. *Science*, 1963. **141**(3575): p. 57-9.

23. Hegde, A.N., et al., *Ubiquitin C-terminal hydrolase is an immediate-early gene essential for long-term facilitation in Aplysia*. Cell, 1997. **89**(1): p. 115-26.
24. Alberini, C.M., et al., *C/EBP is an immediate-early gene required for the consolidation of long-term facilitation in Aplysia*. Cell, 1994. **76**(6): p. 1099-114.
25. Squire, L., *Memory and brain*. 1987, New York: Oxford University Press.
26. Scoville, W.B. and B. Milner, *Loss of recent memory after bilateral hippocampal lesions*. Journal of neurology, neurosurgery, and psychiatry, 1957. **20**(1): p. 11-21.
27. Bliss, T.V. and T. Lomo, *Long-lasting potentiation of synaptic transmission in the dentate area of the anaesthetized rabbit following stimulation of the perforant path*. The Journal of physiology, 1973. **232**(2): p. 331-56.
28. Krug, M., B. Lossner, and T. Ott, *Anisomycin blocks the late phase of long-term potentiation in the dentate gyrus of freely moving rats*. Brain research bulletin, 1984. **13**(1): p. 39-42.
29. Dudek, S.M. and M.F. Bear, *Homosynaptic long-term depression in area CA1 of hippocampus and effects of N-methyl-D-aspartate receptor blockade*. Proceedings of the National Academy of Sciences of the United States of America, 1992. **89**(10): p. 4363-7.
30. Mulkey, R.M. and R.C. Malenka, *Mechanisms underlying induction of homosynaptic long-term depression in area CA1 of the hippocampus*. Neuron, 1992. **9**(5): p. 967-75.
31. Mulkey, R.M., C.E. Herron, and R.C. Malenka, *An essential role for protein phosphatases in hippocampal long-term depression*. Science, 1993. **261**(5124): p. 1051-5.
32. Mulkey, R.M., et al., *Involvement of a calcineurin/inhibitor-1 phosphatase cascade in hippocampal long-term depression*. Nature, 1994. **369**(6480): p. 486-8.
33. Markram, H., et al., *Regulation of synaptic efficacy by coincidence of postsynaptic APs and EPSPs*. Science, 1997. **275**(5297): p. 213-5.
34. Bi, G.Q. and M.M. Poo, *Synaptic modifications in cultured hippocampal neurons: dependence on spike timing, synaptic strength, and postsynaptic cell type*. The Journal of neuroscience : the official journal of the Society for Neuroscience, 1998. **18**(24): p. 10464-72.
35. Song, S., K.D. Miller, and L.F. Abbott, *Competitive Hebbian learning through spike-timing-dependent synaptic plasticity*. Nature neuroscience, 2000. **3**(9): p. 919-26.
36. Peters, A. and I.R. Kaiserman-Abramof, *The small pyramidal neuron of the rat cerebral cortex. The perikaryon, dendrites and spines*. The American journal of anatomy, 1970. **127**(4): p. 321-55.
37. Rochefort, N.L. and A. Konnerth, *Dendritic spines: from structure to in vivo function*. EMBO reports, 2012. **13**(8): p. 699-708.
38. Kasai, H., et al., *Structural dynamics of dendritic spines in memory and cognition*. Trends in neurosciences, 2010. **33**(3): p. 121-9.
39. Sheng, M. and C.C. Hoogenraad, *The postsynaptic architecture of excitatory synapses: a more quantitative view*. Annual review of biochemistry, 2007. **76**: p. 823-47.
40. Renner, M., D. Choquet, and A. Triller, *Control of the postsynaptic membrane viscosity*. The Journal of neuroscience : the official journal of the Society for Neuroscience, 2009. **29**(9): p. 2926-37.
41. Schlager, M.A. and C.C. Hoogenraad, *Basic mechanisms for recognition and transport of synaptic cargos*. Molecular brain, 2009. **2**: p. 25.

42. Bramham, C.R., *Local protein synthesis, actin dynamics, and LTP consolidation*. Current opinion in neurobiology, 2008. **18**(5): p. 524-31.
43. Okamoto, K., et al., *Rapid and persistent modulation of actin dynamics regulates postsynaptic reorganization underlying bidirectional plasticity*. Nature neuroscience, 2004. **7**(10): p. 1104-12.
44. Cingolani, L.A. and Y. Goda, *Actin in action: the interplay between the actin cytoskeleton and synaptic efficacy*. Nature reviews. Neuroscience, 2008. **9**(5): p. 344-56.
45. Honkura, N., et al., *The subspine organization of actin fibers regulates the structure and plasticity of dendritic spines*. Neuron, 2008. **57**(5): p. 719-29.
46. Vukojevic, V., et al., *A role for alpha-adducin (ADD-1) in nematode and human memory*. The EMBO journal, 2012. **31**(6): p. 1453-66.
47. Kim, I.H., et al., *Disruption of Arp2/3 results in asymmetric structural plasticity of dendritic spines and progressive synaptic and behavioral abnormalities*. The Journal of neuroscience : the official journal of the Society for Neuroscience, 2013. **33**(14): p. 6081-92.
48. Machesky, L.M., et al., *Scar, a WASp-related protein, activates nucleation of actin filaments by the Arp2/3 complex*. Proceedings of the National Academy of Sciences of the United States of America, 1999. **96**(7): p. 3739-44.
49. Rohatgi, R., et al., *The interaction between N-WASP and the Arp2/3 complex links Cdc42-dependent signals to actin assembly*. Cell, 1999. **97**(2): p. 221-31.
50. Welch, M.D., A. Iwamatsu, and T.J. Mitchison, *Actin polymerization is induced by Arp2/3 protein complex at the surface of Listeria monocytogenes*. Nature, 1997. **385**(6613): p. 265-9.
51. Soderling, S.H., et al., *Loss of WAVE-1 causes sensorimotor retardation and reduced learning and memory in mice*. Proceedings of the National Academy of Sciences of the United States of America, 2003. **100**(4): p. 1723-8.
52. Soderling, S.H., et al., *A WAVE-1 and WRP signaling complex regulates spine density, synaptic plasticity, and memory*. The Journal of neuroscience : the official journal of the Society for Neuroscience, 2007. **27**(2): p. 355-65.
53. Nakamura, Y., et al., *PICK1 inhibition of the Arp2/3 complex controls dendritic spine size and synaptic plasticity*. The EMBO journal, 2011. **30**(4): p. 719-30.
54. Martin, K.C., et al., *Synapse-specific, long-term facilitation of aplysia sensory to motor synapses: a function for local protein synthesis in memory storage*. Cell, 1997. **91**(7): p. 927-38.
55. Ghirardi, M., P.G. Montarolo, and E.R. Kandel, *A novel intermediate stage in the transition between short- and long-term facilitation in the sensory to motor neuron synapse of aplysia*. Neuron, 1995. **14**(2): p. 413-20.
56. Steward, O. and W.B. Levy, *Preferential localization of polyribosomes under the base of dendritic spines in granule cells of the dentate gyrus*. The Journal of neuroscience : the official journal of the Society for Neuroscience, 1982. **2**(3): p. 284-91.
57. Tiedge, H. and J. Brosius, *Translational machinery in dendrites of hippocampal neurons in culture*. The Journal of neuroscience : the official journal of the Society for Neuroscience, 1996. **16**(22): p. 7171-81.
58. Steward, O. and E.M. Schuman, *Protein synthesis at synaptic sites on dendrites*. Annual review of neuroscience, 2001. **24**: p. 299-325.
59. Martin, K.C. and A. Ephrussi, *mRNA localization: gene expression in the spatial dimension*. Cell, 2009. **136**(4): p. 719-30.

60. Richter, J.D. and E. Klann, *Making synaptic plasticity and memory last: mechanisms of translational regulation*. *Genes & development*, 2009. **23**(1): p. 1-11.
61. Kiebler, M.A. and G.J. Bassell, *Neuronal RNA granules: movers and makers*. *Neuron*, 2006. **51**(6): p. 685-90.
62. Thomas, M.G., et al., *RNA granules: the good, the bad and the ugly*. *Cellular signalling*, 2011. **23**(2): p. 324-34.
63. Wang, D.O., K.C. Martin, and R.S. Zukin, *Spatially restricting gene expression by local translation at synapses*. *Trends in neurosciences*, 2010. **33**(4): p. 173-82.
64. Alarcon, J.M., et al., *Selective modulation of some forms of schaffer collateral-CA1 synaptic plasticity in mice with a disruption of the CPEB-1 gene*. *Learning & memory*, 2004. **11**(3): p. 318-27.
65. Si, K., et al., *A neuronal isoform of CPEB regulates local protein synthesis and stabilizes synapse-specific long-term facilitation in aplysia*. *Cell*, 2003. **115**(7): p. 893-904.
66. Fernandez-Miranda, G. and R. Mendez, *The CPEB-family of proteins, translational control in senescence and cancer*. *Ageing research reviews*, 2012. **11**(4): p. 460-72.
67. Si, K., S. Lindquist, and E.R. Kandel, *A neuronal isoform of the aplysia CPEB has prion-like properties*. *Cell*, 2003. **115**(7): p. 879-91.
68. Nakamura, M., et al., *Musashi, a neural RNA-binding protein required for Drosophila adult external sensory organ development*. *Neuron*, 1994. **13**(1): p. 67-81.
69. Good, P., et al., *The human Musashi homolog 1 (MSI1) gene encoding the homologue of Musashi/Nrp-1, a neural RNA-binding protein putatively expressed in CNS stem cells and neural progenitor cells*. *Genomics*, 1998. **52**(3): p. 382-4.
70. Yoda, A., H. Sawa, and H. Okano, *MSI-1, a neural RNA-binding protein, is involved in male mating behaviour in Caenorhabditis elegans*. *Genes to cells : devoted to molecular & cellular mechanisms*, 2000. **5**(11): p. 885-895.
71. Sakakibara, S., et al., *Mouse-Musashi-1, a neural RNA-binding protein highly enriched in the mammalian CNS stem cell*. *Developmental biology*, 1996. **176**(2): p. 230-42.
72. Sakakibara, S., et al., *Rna-binding protein Musashi2: developmentally regulated expression in neural precursor cells and subpopulations of neurons in mammalian CNS*. *The Journal of neuroscience : the official journal of the Society for Neuroscience*, 2001. **21**(20): p. 8091-107.
73. Imai, T., et al., *The neural RNA-binding protein Musashi1 translationally regulates mammalian numb gene expression by interacting with its mRNA*. *Molecular and cellular biology*, 2001. **21**(12): p. 3888-900.
74. de Sousa Abreu, R., et al., *Genomic analyses of musashi1 downstream targets show a strong association with cancer-related processes*. *The Journal of biological chemistry*, 2009. **284**(18): p. 12125-35.
75. Charlesworth, A., et al., *Musashi regulates the temporal order of mRNA translation during Xenopus oocyte maturation*. *The EMBO journal*, 2006. **25**(12): p. 2792-801.
76. MacNicol, M.C., C.E. Cragle, and A.M. MacNicol, *Context-dependent regulation of Musashi-mediated mRNA translation and cell cycle regulation*. *Cell cycle*, 2011. **10**(1): p. 39-44.
77. Kawahara, H., et al., *Neural RNA-binding protein Musashi1 inhibits translation initiation by competing with eIF4G for PABP*. *The Journal of cell biology*, 2008. **181**(4): p. 639-53.



78. Inoue, A., et al., *Forgetting in C. elegans is accelerated by neuronal communication via the TIR-1/JNK-1 pathway*. Cell reports, 2013. **3**(3): p. 808-19.
79. Berry, J.A., et al., *Dopamine is required for learning and forgetting in Drosophila*. Neuron, 2012. **74**(3): p. 530-42.
80. Shuai, Y., et al., *Forgetting is regulated through Rac activity in Drosophila*. Cell, 2010. **140**(4): p. 579-89.
81. Malleret, G., et al., *Inducible and reversible enhancement of learning, memory, and long-term potentiation by genetic inhibition of calcineurin*. Cell, 2001. **104**(5): p. 675-86.
82. Sharma, S.K., et al., *Inhibition of calcineurin facilitates the induction of memory for sensitization in Aplysia: requirement of mitogen-activated protein kinase*. Proceedings of the National Academy of Sciences of the United States of America, 2003. **100**(8): p. 4861-6.
83. Genoux, D., et al., *Protein phosphatase 1 is a molecular constraint on learning and memory*. Nature, 2002. **418**(6901): p. 970-5.
84. Shema, R., T.C. Sacktor, and Y. Dudai, *Rapid erasure of long-term memory associations in the cortex by an inhibitor of PKM zeta*. Science, 2007. **317**(5840): p. 951-3.
85. Cao, X., et al., *Inducible and selective erasure of memories in the mouse brain via chemical-genetic manipulation*. Neuron, 2008. **60**(2): p. 353-66.
86. Nader, K. and O. Hardt, *A single standard for memory: the case for reconsolidation*. Nature reviews. Neuroscience, 2009. **10**(3): p. 224-34.
87. Davis, M., *NMDA receptors and fear extinction: implications for cognitive behavioral therapy*. Dialogues in clinical neuroscience, 2011. **13**(4): p. 463-74.
88. *Genome sequence of the nematode C. elegans: a platform for investigating biology*. Science, 1998. **282**(5396): p. 2012-8.
89. Lai, C.H., et al., *Identification of novel human genes evolutionarily conserved in Caenorhabditis elegans by comparative proteomics*. Genome research, 2000. **10**(5): p. 703-13.
90. Sulston, J.E. and H.R. Horvitz, *Post-embryonic cell lineages of the nematode, Caenorhabditis elegans*. Developmental biology, 1977. **56**(1): p. 110-56.
91. Friedland, A.E., et al., *Heritable genome editing in C. elegans via a CRISPR-Cas9 system*. Nature methods, 2013. **10**(8): p. 741-3.
92. Fire, A., et al., *Potent and specific genetic interference by double-stranded RNA in Caenorhabditis elegans*. Nature, 1998. **391**(6669): p. 806-11.
93. Chalfie, M., et al., *Green fluorescent protein as a marker for gene expression*. Science, 1994. **263**(5148): p. 802-5.

# Forgetting Is Regulated via Musashi-Mediated Translational Control of the Arp2/3 Complex

Nils Hadziselimovic,<sup>1,2,3</sup> Vanja Vukojevic,<sup>1,2,3</sup> Fabian Peter,<sup>1,2,3</sup> Annette Milnik,<sup>1,2</sup> Matthias Fastenrath,<sup>4</sup> Bank Gabor Fenyves,<sup>5</sup> Petra Hieber,<sup>1,2,3</sup> Philippe Demougin,<sup>1,2,3</sup> Christian Vogler,<sup>1,6</sup> Dominique J.-F. de Quervain,<sup>1,4,6</sup> Andreas Papassotiropoulos,<sup>1,2,3,6</sup> and Attila Stetak<sup>1,2,3,6,\*</sup>

<sup>1</sup>Transfaculty Research Platform Molecular and Cognitive Neurosciences, University of Basel, Birmannsgasse 8, 4055 Basel, Switzerland

<sup>2</sup>Division of Molecular Neuroscience, Department of Psychology, University of Basel, Birmannsgasse 8, 4055 Basel, Switzerland

<sup>3</sup>Biozentrum, Life Sciences Training Facility, University of Basel, Klingelbergstrasse 50/70, 4056 Basel, Switzerland

<sup>4</sup>Division of Cognitive Neuroscience, Department of Psychology, University of Basel, Birmannsgasse 8, 4055 Basel, Switzerland

<sup>5</sup>Department of Medical Chemistry, Semmelweis University, Tüzoltó u. 37-47, 1094 Budapest, Hungary

<sup>6</sup>University Psychiatric Clinics, University of Basel, Wilhelm Klein-Strasse 27, 4055 Basel, Switzerland

\*Correspondence: [a.stetak@unibas.ch](mailto:a.stetak@unibas.ch)

<http://dx.doi.org/10.1016/j.cell.2014.01.054>

## SUMMARY

A plastic nervous system requires the ability not only to acquire and store but also to forget. Here, we report that *musashi* (*msi-1*) is necessary for time-dependent memory loss in *C. elegans*. Tissue-specific rescue demonstrates that MSI-1 function is necessary in the AVA interneuron. Using RNA-binding protein immunoprecipitation (IP), we found that MSI-1 binds to mRNAs of three subunits of the Arp2/3 actin branching regulator complex in vivo and downregulates ARX-1, ARX-2, and ARX-3 translation upon associative learning. The role of *msi-1* in forgetting is also reflected by the persistence of learning-induced GLR-1 synaptic size increase in *msi-1* mutants. We demonstrate that memory length is regulated cooperatively through the activation of *adducin* (*add-1*) and by the inhibitory effect of *msi-1*. Thus, a GLR-1/MSI-1/Arp2/3 pathway induces forgetting and represents a novel mechanism of memory decay by linking translational control to the structure of the actin cytoskeleton in neurons.

## INTRODUCTION

Animals receive and respond to environmental challenges throughout their life. This vast amount of information is retained in the nervous system and ensures the behavioral plasticity of the organism. In order to maintain a highly flexible nervous system, not only the generation of memories but also forgetting (memory loss) is essential to adapt to a constantly changing environment (McGaugh, 2000).

Molecular mechanisms that underlie learning and memory formation are extensively studied, and our current knowledge provides a complex picture on the regulation of synaptic plasticity.

The activity-dependent Ca<sup>2+</sup> influx during long-term potentiation (LTP), for example, activates a multitude of signaling pathways, trafficking and rearrangements of scaffold proteins (Kessels et al., 2009), protein degradation and synthesis, gene expression changes (Carlezon et al., 2005), and subsequent structural modifications of the actin cytoskeleton (Wang et al., 2006). Modulation of the actin dynamics during learning and memory mediates morphological changes of synaptic areas and is also necessary for the formation of new synaptic connections in vertebrates (Bosch and Hayashi, 2012). However, until now, the molecular mechanisms that link LTP- or long-term depression-regulated signaling cascades to the structural changes of the actin cytoskeleton during learning and memory are poorly investigated.

The two classical psychological concepts of forgetting, decay and interference, are usually thought of as two distinct processes (Jonides et al., 2008; Wixted, 2004). The decay model suggests that memory passively disappears over time, whereas the interference model claims that forgetting results from competition with other memory traces (Jonides et al., 2008; Wixted, 2004). Recent studies demonstrated that active regulation of forgetting likely takes place (Berry et al., 2012; Inoue et al., 2013; Shuai et al., 2010) and that retention and loss of memory does not depend solely upon the activity of kinases and phosphatases. Active regulators of forgetting also include the small guanosine-triphosphate-binding protein Rac in *Drosophila* (Shuai et al., 2010) and a TIR-1/JNK-1 pathway in the sensory neurons in *C. elegans* (Inoue et al., 2013). These findings suggest that multiple different signaling cascades are regulating the retention and loss of memories.

RNA-binding proteins (RBPs) have recently emerged as essential modulators of mRNA distribution, translation, and degradation during proper synaptic function (Holt and Bullock, 2009). In vertebrates, *musashi1* (*msi1*) and *musashi2* (*msi2*) are two closely related members of the *musashi* (*msi*) gene family, which belongs to the RNA-recognition motif (RRM) containing proteins that interact with single-stranded RNAs (Sakakibara et al., 2002). Both MSIs are expressed in the developing and

adult nervous system. In mammals, MSI1 is mainly expressed in stem and progenitor cells and its expression decreases during differentiation (Sakakibara et al., 2001), whereas MSI2 is present also in differentiated neurons of the adult brain (Sakakibara et al., 2001). In nematodes, the sole *musashi* (*msi-1*) is widely expressed during embryogenesis and remains present in differentiated mature neurons of the adult nervous system similar to *musashi* in *Drosophila* (Hirota et al., 1999; Yoda et al., 2000). In *C. elegans*, loss of the *msi-1* gene causes a defect in male mating behavior (Yoda et al., 2000), suggesting that MSI may regulate the activity of differentiated neurons.

MSIs bind to the (G/A)<sub>n</sub>AGU (n = 1–3) motif located in the 3' UTR of the target mRNA. Although MSI binding to this RNA sequence in vitro is well documented (Ohshima et al., 2012), so far only few in vivo targets were identified, such as *m-numb* (Imai et al., 2001), CDKN1A (Battelli et al., 2006), doublecortin (Horisawa et al., 2009), and *c-mos* in *Xenopus leavis* (Charlesworth et al., 2006). Beside these, an immunoprecipitation of RNA-binding protein coupled to microarray (RIP-ChIP) approach recently identified 64 mRNAs that were interacting with MSI in transfected human embryonic kidney 293 cells (de Sousa Abreu et al., 2009). These MSI-binding partners are mainly genes involved in proliferation, apoptosis, cell differentiation, and post-translational modification and, interestingly, include a component of the Arp2/3 actin branching regulator protein complex (*ACTR2*). Thus, its expression pattern in the nervous system and its interaction with the *ACTR2/ax-2* mRNA make *Musashi* a likely candidate that may regulate memory.

Here, we show that the *C. elegans* neuronal *musashi* gene ortholog *msi-1* regulates forgetting. Although MSI-1 is expressed in several neurons, memory length depends on the action of MSI-1 only in the AVA interneuron. We demonstrate that MSI-1 binds in vivo to the mRNA of three members of the actin branching ARP2/3 complex and regulates their protein levels via a 3' UTR-dependent translational repression. The inhibitory function of *msi-1* is also reflected in persistence of GLR-1-positive synapse size increase induced by associative learning in *msi-1(lf)* mutants. Finally, GLR-1 signaling possibly regulates both actin capping through the activity of *adducin* (*add-1*) and inhibition of actin branching mediated by *msi-1*, and these two parallel mechanisms act in concert to establish the proper memory trace. Our results suggest that MSI-1 regulates forgetting and point to a novel aspect of memory regulation linking translational repression to regulation of the actin cytoskeleton structure.

## RESULTS

### MSI-1 Function Accelerates Memory Loss

In an effort to identify potential genes regulating actin cytoskeleton remodeling during associative learning and memory, we performed a candidate-gene-based test using learning and memory assays in *C. elegans* (Kauffman et al., 2010; Nuttley et al., 2002; Vukojevic et al., 2012). MSI-1 represented a likely candidate based on its expression pattern and interaction with the *ACTR2/ax-2* mRNA. Thus, we investigated the potential role of a loss-of-function deletion allele *msi-1(os1)* of the sole *C. elegans* *Musashi* ortholog (Yoda et al., 2000). Because olfactory conditioning relies on normal detection of volatile attrac-

tants, we first tested the chemotaxis of *msi-1(lf)* animals toward different odorants. The chemotaxis of *msi-1(lf)* mutants to three different volatile attractants and a repellent was comparable to the response of the wild-type strain (Figure S1A available online). Furthermore, both wild-type and *msi-1(lf)* mutants showed normal locomotor behavior and responded similarly to food, indicating that *msi-1(lf)* mutants have no obvious sensory or motor defects (Figure S1B). In the negative olfactory learning assay, unconditioned wild-type and *msi-1(lf)* animals both exhibited strong chemotaxis toward diacetyl (DA) (Figure S1C). Furthermore, after a 1 hr starvation period in the presence of DA (conditioning), both wild-type and *msi-1* mutant animals displayed a strongly reduced attraction to DA, whereas starvation or DA alone (in presence of abundant food) had only a mild effect (Figure S1C). *msi-1(lf)* mutants showed normal associative learning toward DA when compared to wild-type (Figure S1C). Finally, we tested the role of *msi-1* in the ability of the animals to retain a conditioned behavior over time (short-term associative memory [STAM] and long-term associative memory [LTAM]). In STAM, animals were subjected to conditioning and tested every 10 min over a period of 1 hr for their DA preference (Figure 1A). In wild-type animals, the negative association of DA with starvation persisted during the recovery period tested (Figure 1A). *msi-1(lf)* worms showed a strong increase in memory retention (Figure 1A). Reintroduction of a wild-type 16 kb genomic fragment of the *msi-1* gene into the mutant worms fully rescued the memory phenotype (Figure 1B). Finally, we observed a similar effect of *msi-1* on memory in a salt gustatory associative learning assay (Wicks et al., 2000) (Figure S1D). The effect observed was not due to developmental defects, because RNAi silencing of *msi-1* following neuronal differentiation phenocopied the *msi-1(lf)* phenotype (Figure 1C). To further confirm a sensory-input-independent role of *msi-1*, we tested animals for their short-term positive associative memory, as described previously (Kauffman et al., 2010). In this assay, a simultaneous exposure to 2-butanone and food as a reward dramatically increased chemotaxis toward the attractant in both wild-type and *msi-1(lf)* worms to a similar extent (Figure 1D). However, the 1 hr recovery phase resulted in a recovery to almost naive behavior in wild-type animals, whereas *msi-1(lf)* mutants still exhibited strong attraction toward 2-butanone (Figure 1D). Thus, deletion of *msi-1* inhibits memory loss independently of the sensory input. Finally, we tested the effect of *msi-1* on aversive LTAM as described previously (Vukojevic et al., 2012). Although learning (aversion to DA immediately following the conditioning phase) was effective in all genotypes, we observed significant differences in LTAM retention in *msi-1(lf)* mutants compared to the wild-type worms after a 24 hr or 32 hr delay period (Figure 1E). Altogether, these results demonstrate that the *C. elegans* ortholog of *Musashi* induces a sensory-input-independent memory loss both in STAM and LTAM.

### MSI-1 Function Is Necessary in the AVA Interneuron

Previously, *msi-1* expression in GABAergic neurons of the adult *C. elegans* nervous system was demonstrated (Yoda et al., 2000). In order to study in more detail the expression of MSI-1 in adult worms, we generated an *msi-1* minigene construct by fusing the 7.7 kb promoter region with *msi-1* cDNA, tag red

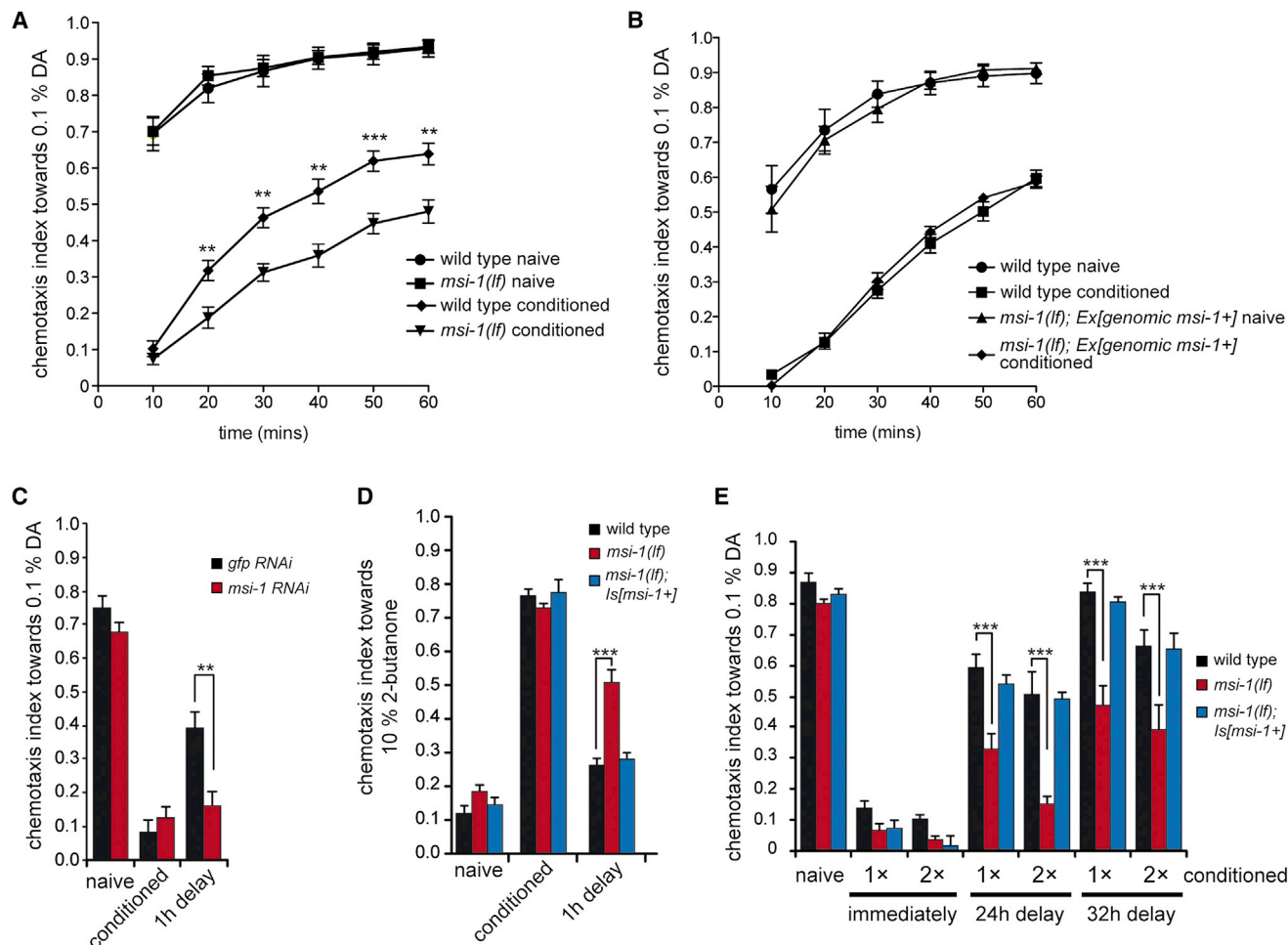


**Figure 1. Loss of *C. elegans* MSI-1 Interferes with Memory Loss**

(A) The STAM was tested in worms without (naive) or with conditioning, and DA preference was recorded every 10 min for 1 hr.

(B) STAM was tested in wild-type and *msi-1(lf)* mutant worms rescued with the genomic *msi-1* locus. Graph shows the sum of three independent lines.

(C) STAM conditioning of RNAi-hypersensitive worms (*nre-1 lin15b*) treated with *msi-1* or *gfp* RNAi from early L3 until adulthood. Worms were assayed toward DA without (naive) or with (conditioned) preincubation with DA or after 1 hr (1h delay).

(D) Positive STAM in different genotypes was tested as described elsewhere (Kauffman et al., 2010) toward 2-butanone immediately (conditioned) or after a 1 hr delay.

(E) Negative LTAM in the different genotypes was tested following one (1×) or two (2×) consecutive conditioning phases and DA preference was tested immediately, after 24 hr (24h delay) or 32 hr (32h delay) recovery period.

All experiments were done in triplicates and repeated at least three times. Bars represent mean ± SEM. \*\**p* < 0.01, \*\*\**p* < 0.001. See also Figure S1 and Table S1.

fluorescent protein (tRFP), and the *msi-1* 3' UTR. The expression of MSI-1::tRFP was investigated in an AMPA-type glutamate-receptor-expressing GLR-1::GFP transgenic background (Figures 2A–2F). As shown on Figure 2, MSI-1 expression partially overlapped with GLR-1 expression in the adult nervous system. Besides the GABAergic neurons (RMEL, RMER, RMEV, RMED) (Yoda et al., 2000), we identified AVA, AFD, and RMD neurons that are expressing MSI-1 (Figures 2D–2F). We previously showed that the GLR-1-expressing AVA neuron is a key regulator of olfactory associative memory in *C. elegans* (Stetak et al., 2009; Vukojevic et al., 2012). In order to define the cellular requirement for MSI-1, we performed tissue-specific rescue experiments by expressing the *msi-1* cDNA under the control of the endogenous, *nmr-1*, *lim-4*, *rig-3*, or the *unc-47* promoters in the

*msi-1(lf)* mutant. The activity of these promoters overlaps with certain subsets of MSI-1-expressing neurons (Figure 2G), allowing us to pinpoint the cellular focus of *msi-1*. In the STAM test, the endogenous promoter as well as the *P<sub>nmr-1</sub>* and *P<sub>rig-3</sub>*-driven *msi-1* cDNA rescued the memory phenotype of *msi-1(lf)* mutants (Figures 2H, 2J, and 2K), whereas no rescue was observed when using *P<sub>lim-4</sub>* or *P<sub>unc-47</sub>* (Figures 2I and 2L).

### MSI-1 Interacts with *arx-1*, *arx-2*, and *arx-3* mRNAs of the Arp2/3 Complex

Besides the identification of the cellular focus of *msi-1*, we investigated the requirement for the interaction of *msi-1* with RNA in forgetting. We generated an RNA-binding mutant form in both RRM domains of the rescuing *msi-1* cDNA by altering all three

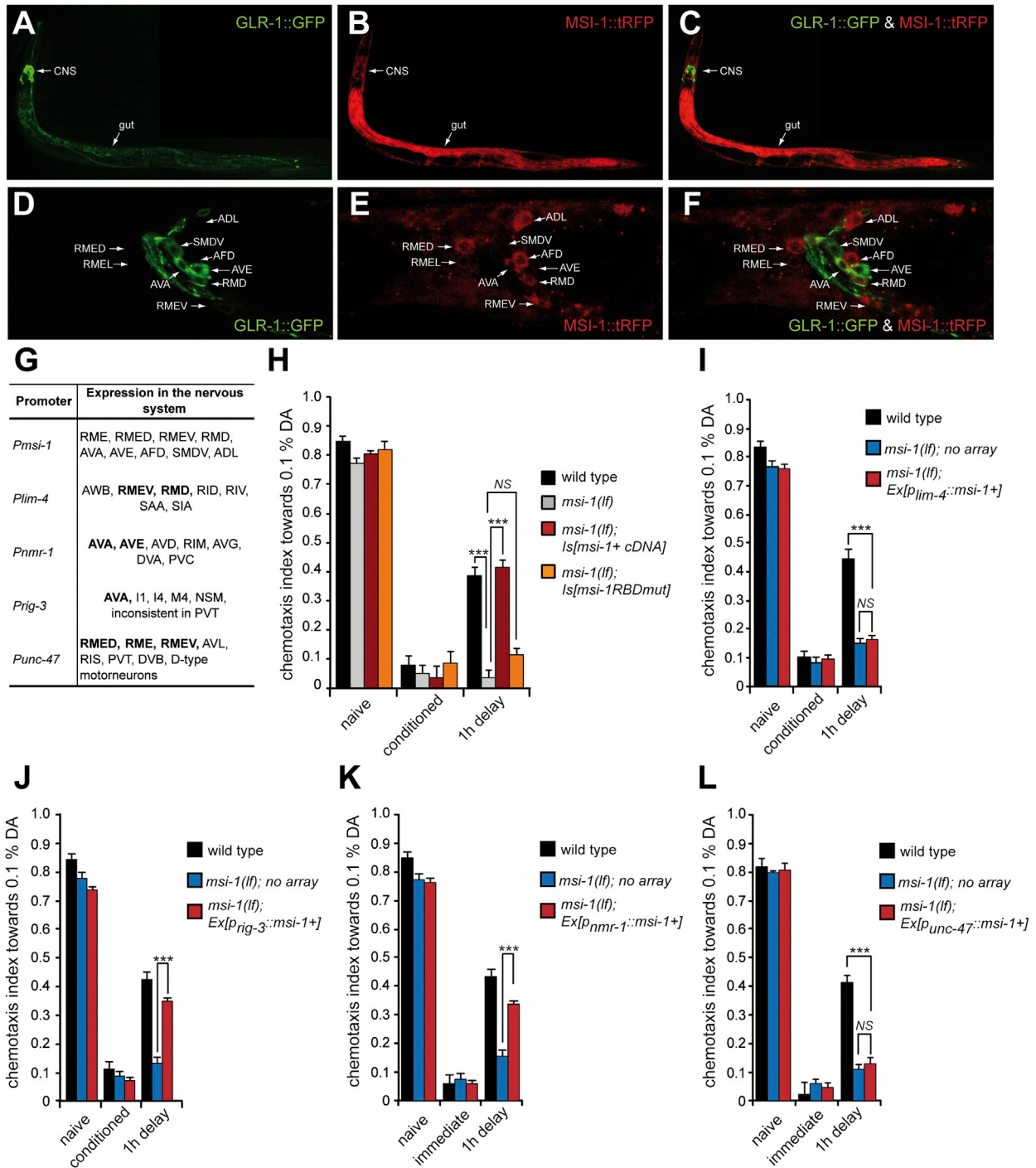


**Figure 2. MSI-1 Regulates Memory Loss in the AVA Interneuron**

(A–C) MSI-1 expression in the adult worm is detected in the gut and in multiple head neurons (red in A and C). MSI-1 partially overlaps with the GLR-1 expression (green in B and C). Panels shown were constructed by merging three overlapping images to reconstruct the whole animal. The black box in the top right was added using Photoshop to complete the rectangular image.

(D–F) In the head region, MSI-1 (red) was found in previously identified GABAergic neurons (RMEs) and in some GLR-1-expressing (green) cells (AVA, RMD).

(G) Expression pattern of the different neural promoters used in (H)–(L). Overlap with the *msi-1*-expressing neurons is highlighted in bold.

(H) Rescue of the forgetting defect of *msi-1(lf)* mutant worms carrying the wild-type (*msi-1+*) or an RNA-binding mutant (*RBDmut*) *msi-1* cDNA fused to Myc-tag under the control of the endogenous *msi-1* promoter.

(legend continued on next page)

conserved K to A in each domain (Figure S2) previously found to be essential for Musashi1-RNA interaction (Miyanoiri et al., 2003). In accord with the known function of MSI-1, the RNA-binding mutant *msi-1* was unable to rescue the memory phenotype of the *msi-1(lf)* mutants (Figure 2H). Thus, MSI-1 exerts its memory-related function by interacting with target RNA molecules. Among the previously identified MSI mRNA-binding partners (de Sousa Abreu et al., 2009), 14 genes are conserved in nematodes. One of these is the ACTR2/ARX-2, a member of the Arp2/3 protein complex that induces actin branching (Machesky and Gould, 1999). Because actin remodeling has a known role in synaptic plasticity (Okamoto et al., 2004), ACTR2/ARX-2 may represent a link to synapse remodeling, cortical actin structure modification, and maintenance of memory. To investigate the physical interaction between MSI-1 and the Arp2/3 protein complex, we used the integrated *msi-1(lf); ls[msi-1 minigene::myc-tag]* or as control the *msi-1(lf); ls[msi-1RBDmutant::myc-tag]* *C. elegans* strains (Figure 2H). The different MYC-tagged proteins were immunoprecipitated, the associated RNA was isolated, and the mRNA levels of the different subunits of the Arp2/3 protein complex (*arx-1* to *arx-7*) were quantified using quantitative RT-PCR (qRT-PCR). Equal amounts of bacterial reference RNAs were added to the isolated RNA before the reverse transcription and used for the quantitative PCR normalization. The relative amounts of the *arxs* RNA were compared to mock immunoprecipitations from the N2 strain (Figure 3A). We found that MSI-1 interacted with *arx-1*, *arx-2*, and *arx-3* mRNA, but not with the other four members of the Arp2/3 complex. In addition, mutation of both RNA-binding domains in MSI-1 inhibited interaction of MSI with target mRNAs (Figure 3B). Finally, we could not detect any learning-induced change in MSI-1 expression levels and alteration of the interaction between MSI-1 and its targets, suggesting that the in vivo binding of MSI-1 to the target mRNAs (*arx-1*, *arx-2*, and *arx-3*) is constitutive.

### MSI-1 Regulates Translation from the *arx-1*, *arx-2*, and *arx-3* mRNAs Depending on Neuronal Activity

Next, we studied the potential regulation of the ubiquitously expressed different ARX protein levels by MSI-1. In order to monitor 3' UTR-mediated translational control in the *msi-1*-expressing set of neurons, we generated reporter constructs by fusing the promoter of *msi-1* to GFP and the 3' UTR region of the different *arx* members and established stable integrated transgenic lines. We analyzed the changes of the GFP protein levels controlled by different *arx* 3' UTRs during associative learning and short-term memory by measuring the GFP intensity of transgenic worms either in the head region or within the AVA interneuron of the treated worms. Consistent with our hypothesis, we found a strong reduction of the fluorescence signal upon STAM when GFP was under the control of the *arx-1*, *arx-2*, or *arx-3* 3' UTR (Figures 3C–3E). The 3' UTR-mediated repression was specific to associative learning, because food

withdrawal (starved) or DA alone (adapted) did not influence the GFP signal. Furthermore, the reduction in the amount of protein persisted over at least 1 hr (60 min recovery). At the same time, the GFP levels under the control of the *arx-4* or *arx-5* 3' UTR were not affected (Figures 3F and 3G). We obtained similar results when we analyzed the GFP intensities specifically in the AVA neuron (Figure S3). Finally, we tested the *gfp* mRNA levels under the control of different *arxs* 3' UTRs using qRT-PCR in order to exclude potential changes in the amount of RNA upon conditioning (Figure 3H). We found that the *gfp* mRNA levels were not affected by conditioning, further supporting the idea that the protein levels of ARX-1, ARX-2, and ARX-3 are regulated at the translational level by MSI-1.

Next, we analyzed the role of MSI-1 in the regulation of ARX-1, ARX-2, and ARX-3 protein levels by comparing GFP signals of the transgenes in wild-type or *msi-1(lf)* mutant worms. As expected, we observed a significant increase of the GFP signal in *msi-1(lf)* worms when the *gfp* was under the control of the *arx-1*, *arx-2*, or *arx-3* 3' UTR (Figures 4A–4C), whereas the levels under the regulation of the *arx-4* or *arx-5* 3' UTR were unaffected (Figures 4D and 4E). Furthermore, we could not detect a decrease of the GFP signal after conditioning when *msi-1* was deleted [*msi-1(lf)* cond]. The effect of *msi-1* deletion was rescued by the reintroduction of the wild-type copy of *msi-1* cDNA in the mutant background. Finally, the *gfp* mRNA levels were not different in the *msi-1(lf)* mutant when compared to wild-type animals (Figure 4F). Our findings show that loss of *msi-1* causes elevated protein levels and loss of downregulation of the Arp2/3 complex upon learning. Thus, translational inhibition should suppress the phenotype observed in *msi-1(lf)* worms. Indeed, cycloheximide treatment directly after conditioning fully suppressed *msi-1(lf)* memory phenotype without influencing memory in wild-type worms (Figure 4G). In contrast, cycloheximide treatment prior to conditioning interfered with memory in all genotypes, suggesting that memory acquisition and stabilization occur during the 1 hr conditioning phase independently of *msi-1* function (Figure 4H).

### Increase in Arp2/3 Complex Activity in the AVA Interneuron Inhibits Memory Loss

Our results established a link between the presence of MSI-1 and the protein amount of the Arp2/3 complex. Next, we postulated that the *msi-1(lf)* memory phenotype caused by the increased amount of the Arp2/3 protein complex will be suppressed by the simultaneous reduction of the MSI-1 target RNAs. Thus, we performed RNA silencing of *arx-2* in RNAi hypersensitive strains with or without *msi-1* function and tested the memory of the treated worms. To exclude a developmental defect caused by the removal of the Arp2/3 complex, we treated nematodes with double-stranded RNA (dsRNA) after the full differentiation of the nervous system. Silencing *arx-2* in *msi-1(lf)* efficiently suppressed the mutant phenotype, whereas it had no effect in *msi-1+* worms (Figure 5A). The Arp2/3 complex

(L–L) Tissue-specific rescue of the memory loss defect of *msi-1(lf)* mutant worms carrying the *msi-1* minigene under the control of different promoters as indicated. Worms of each transgenic line were conditioned and their preference toward DA was tested immediately (conditioned) or following 1 hr recovery (1h delay). All experiments were done in triplicate and repeated in three independent experiments. Bars represent the average of three independent transgenic lines with (as indicated) or without array (no array) for each construct. Bars represent mean  $\pm$  SEM. NS, nonsignificant, \*\*\* $p < 0.001$ . See also Figure S2 and Table S2.

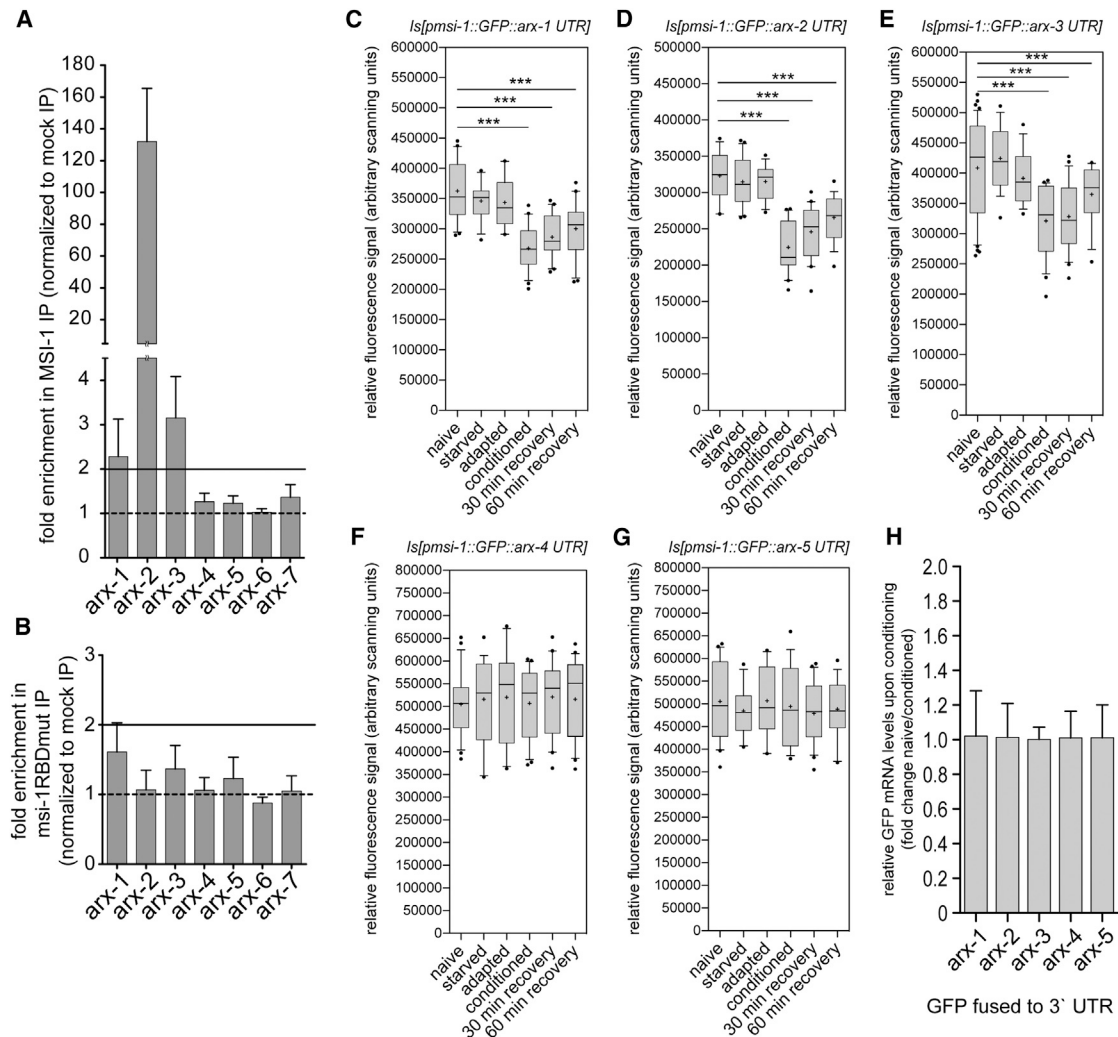


**Figure 3. Translational Control of ARX-1, ARX-2, and ARX-3 during Olfactory-Associative Learning and Memory**

(A) MSI-1/RNA complexes from wild-type (mock) or *msi-1(lf)*; *Is[msi-1 minigene::myc-tag]* were precipitated using anti-Myc antibody, and the amounts of the different *arx* mRNAs were quantified using qRT-PCR compared to mock immunoprecipitation (IP). Dotted line represents no change; solid line shows the 2-fold enrichment threshold.

(B) The enrichment of the different *arx* mRNAs in MSI-1 IPs were measured using qRT-PCR from wild-type (mock) or *msi-1(lf)*; *Is[msi-1 RDB mutant::myc-tag]* strain. Bars in (A) and (B) indicate mean  $\pm$  SEM.

(C–G) GFP intensity in integrated transgenic worms carrying 7.7 kb *msi-1* promoter, GFP, and 3' UTR of *arx-1* (C), *arx-2* (D), *arx-3* (E), *arx-4* (F), or *arx-5* (G). GFP signal was measured in untreated worms (naive), after starvation (starved), following exposure to DA alone (adapted), or immediately after DA conditioning (conditioned). GFP intensity during short-term memory was tested 30 min (30 min recovery) or 1 hr (60 min recovery) after conditioning with DA. For each condition, at least 20 animals from three independent treatments were recorded.

(H) Relative *gfp* mRNA levels were measured using qRT-PCR from total RNA isolated from naive or conditioned transgenic worms carrying different *pmsi-1::GFP::arx* 3' UTR arrays as indicated. The RNA levels were obtained in four technical replicates and three independent biological replicates.

Bars represent 10th and 90th percentile  $\pm$  whiskers in (C)–(G) and mean  $\pm$  SD in (H). \*\*\* $p < 0.001$ . See also Table S3.

consists of seven subunits that interact to form the active complex (Machesky and Gould, 1999; Pollard and Beltzner, 2002). Therefore, we performed RNAi silencing of several other members of the Arp2/3 complex and found that removal of any of the subunits tested suppressed the *msi-1(lf)* phenotype to a similar extent (Figure 5B). This result suggests that MSI-1 may inhibit actin cytoskeleton branching by decreasing the amount of the Arp2/3 protein complex.

The members of the N-WASP protein family, such as WSP-1, induce the activity of the Arp2/3 complex. Based on our hypothesis, a decrease in WSP-1 activity would suppress the *msi-1(lf)* phenotype, whereas constitutive activation of the Arp2/3 complex would lead to increased actin branching and inhibition of memory loss, similar to loss of MSI-1 function. To decrease WSP-1 activity, we performed RNAi silencing of *wsp-1* after differentiation of the nervous system. In accord with our

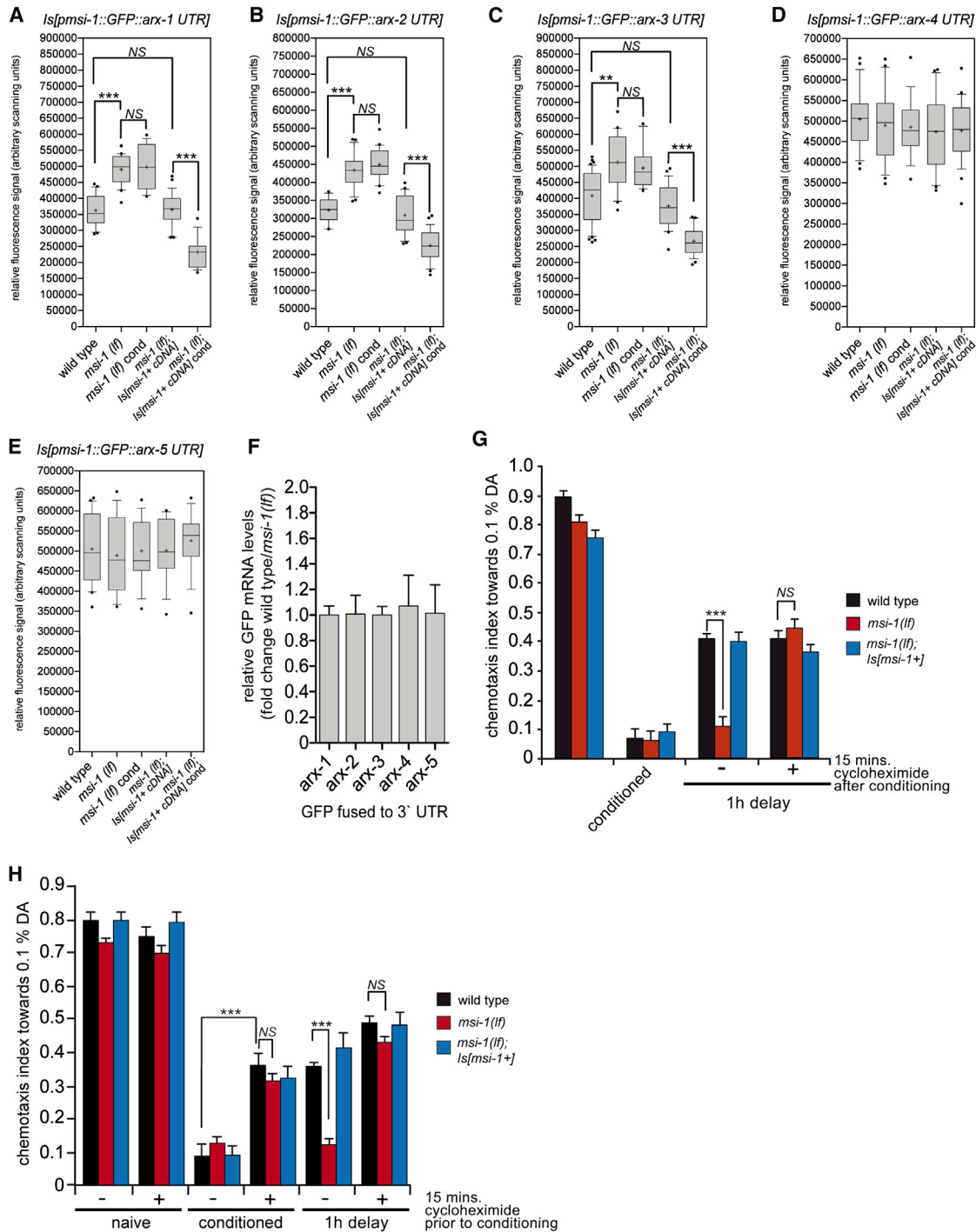


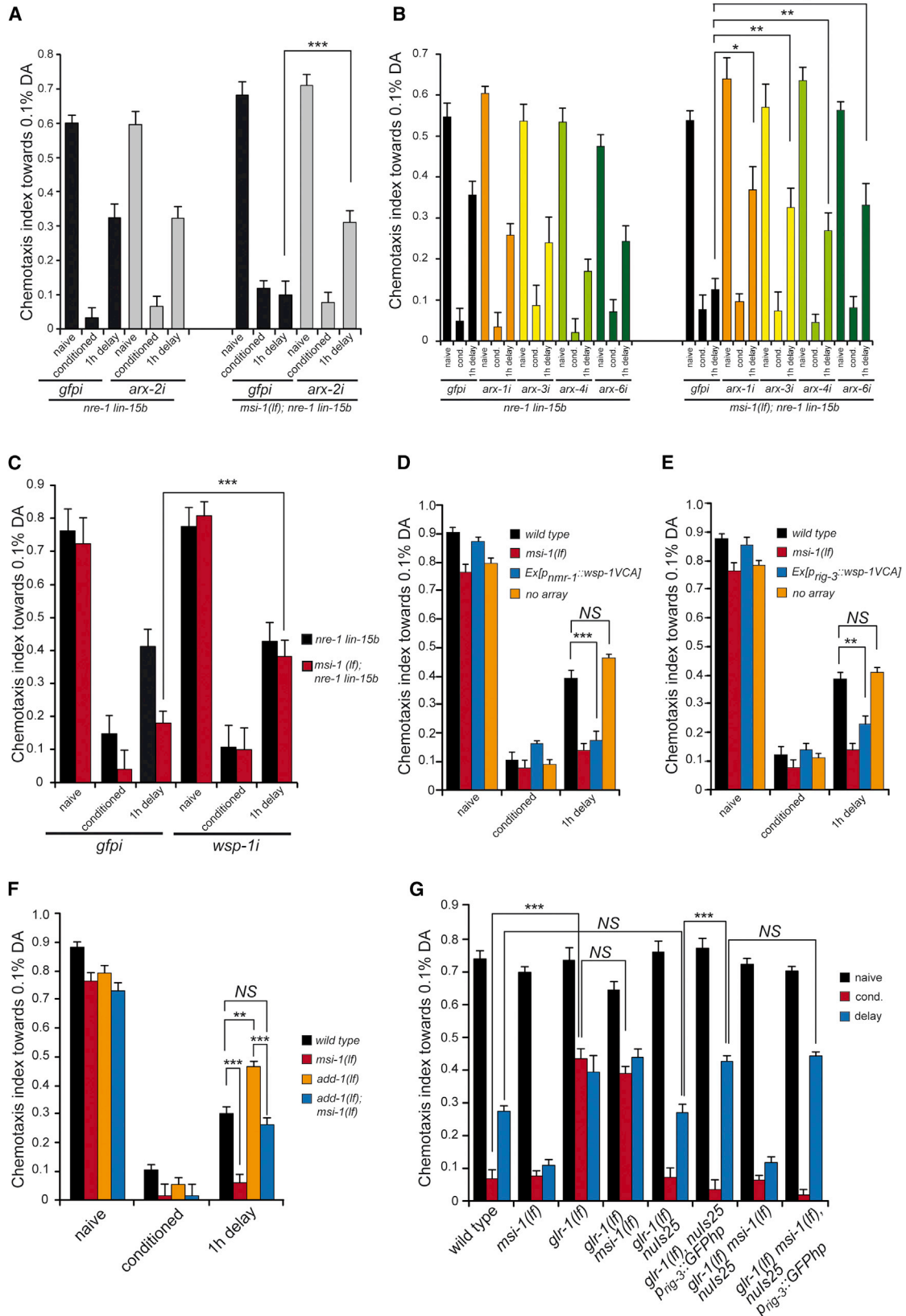
**Figure 4. Translational Repression of ARX-1, ARX-2, and ARX-3 Depends on the MSI-1 Activity**

(A–E) GFP intensity in integrated transgenic worms carrying 7.7 kb *msi-1* promoter, GFP and 3'UTR of *arx-1* (A), *arx-2* (B), *arx-3* (C), *arx-4* (D), or *arx-5* (E). GFP signal was measured on z-projected confocal images in untreated wild-type or *msi-1(lf)* mutants and in *msi-1(lf)* mutant worms that were conditioned with DA [*msi-1(lf)* cond]. At least 20 animals from three independent treatments were analyzed.

(F) Relative *gfp* mRNA levels were measured using qRT-PCR from total RNA isolated from wild-type or *msi-1(lf)* mutant transgenic worms carrying different *pmi-1::GFP::arx* 3' UTR arrays. The RNA levels were measured in quadruplicates for three biological samples.

(G and H) Worms with genotypes indicated were treated with 800  $\mu$ g/ml cycloheximide for 15 min (H) before or (G) immediately after conditioning, washed, and tested for chemotaxis toward DA. Bars indicate 10th and 90th percentile  $\pm$  whiskers in (A)–(E) and mean  $\pm$  SD in (F)–(H). NS, nonsignificant, \*\* $p < 0.01$ , \*\*\* $p < 0.001$ . See also Figure S3 and Table S4.





(legend on next page)

hypothesis, silencing *wsp-1* in *msi-1(lf)* efficiently suppressed the mutant phenotype (Figure 5C).

WSP-1 contains a C-terminal verprolin-, cofilin-homology, acidic region (VCA), which constitutively activates the Arp2/3 complex (Yamaguchi et al., 2000). To overactivate the Arp2/3 complex, we expressed the WSP-1 VCA fragment under the control of the *nmr-1* or *rig-3* promoters in wild-type worms. In accord with our hypothesis, expression of the WSP-1 VCA fragment under the *nmr-1* or *rig-3* promoters increased memory retention in wild-type worms similar to *msi-1* deletion (Figures 5D and 5E). This result shows that increased activity of the Arp2/3 complex in the AVA neuron is sufficient to inhibit memory loss.

### Opposing Regulation Mechanisms of Actin Branching and Capping Modulate Memory Retention

In light of the role of the actin cytoskeleton in shaping synapse morphology, we next investigated the interplay between actin capping and branching in memory maintenance. We simultaneously inactivated *add-1*, an actin-capping protein that regulates memory (Vukojevic et al., 2012), and *msi-1*, which modulates the amount of the Arp2/3 complex. Although loss of *add-1* alone impaired memory (Figure 5F), the simultaneous deletion of *msi-1* suppressed this phenotype and the *msi-1(lf); add-1(lf)* double mutant showed a memory similar to wild-type animals (Figure 5F). This result shows that the two genes act in a parallel but opposing manner and that the correct balance between actin capping and branching is likely to be essential for memory regulation. We previously showed that the remodeling of actin structure through the effect of *add-1*-capping function is possibly linked to GLR-1 activity (Vukojevic et al., 2012). Here, we demonstrated that MSI-1 acts in parallel to ADD-1. We therefore tested if GLR-1 also regulates memory loss through MSI-1 by monitoring learning and memory in both *glr-1(lf) msi-1(lf)* double-mutant animals and in mutants where the *glr-1* function was deleted only in the AVA neuron [*rig-3* promoter-driven *gfp-hairpin* in *glr-1(lf)* rescued with the *glr-1::gfp* construct (*glr-1(lf), nuls25*)], in combination with removal of *msi-1*. Deletion of *glr-1* results in impaired learning that is not affected by the simultaneous deletion of *msi-1* (Figure 5G). Furthermore, AVA-specific deletion of the *glr-1* function using a previously established GFP-hairpin (Vukojevic et al., 2012) was not suppressed by the concurrent removal of *msi-1* function (Figure 5G). These results

suggest that *msi-1* acts downstream of *glr-1* in parallel to *add-1* in the AVA interneuron.

### Persistence of Memory-Related Activity of AVA in *msi-1(lf)* Mutants

We measured  $Ca^{2+}$  currents upon DA stimulation at different stages of learning and memory and observed a long-lasting effect of the *msi-1(lf)* mutation on memory-related activity of AVA (Figures 6A and S4). AVA is a command interneuron characterized by high basal activity. Here, we studied AVA activity with and without DA stimulation. As shown in Figure 6A, DA reduced AVA activity in naive animals, whereas we observed a marked genotype-independent DA-induced increase in  $Ca^{2+}$  transients after conditioning. Importantly, the DA-induced elevated activity of AVA remained high in *msi-1(lf)* mutants, whereas it decreased significantly in wild-type or rescued animals after a 2 hr delay time.

### Inhibition of the Arp2/3 Complex Activity Suppresses the *msi-1(lf)* Phenotype

To gain insight in the temporal requirement of *msi-1* function and to confirm that *msi-1* induces forgetting through modulation of the Arp2/3 complex, we used a selective pharmacological inhibitor (CK-666) (Nolen et al., 2009) that interferes with Arp2/3 activity and acts on actin-dependent processes in worms (Figures S4J and S4K). We applied the inhibitor to block the Arp2/3 activity at different times during STAM and LTAM. Addition of different concentrations of CK-666 prior to conditioning had no obvious effect on learning and memory acquisition but efficiently blocked the *msi-1(lf)* phenotype without influencing the wild-type behavior following a 1 hr delay (Figure 6B). We obtained similar results when the inhibitor was applied for 15 min directly after conditioning (Figure 6C), 15 or 30 min following conditioning, or even after a 23 hr delay (Figure 6D). Thus, in accord with our previous results, loss of *msi-1* function increases Arp2/3 activity, which is responsible for the observed enhanced memory in *msi-1(lf)* mutants. These results also show that *msi-1* is regulating forgetting rather than memory acquisition or consolidation.

### MSI-1 Stabilizes Synaptic Size Increase upon Associative Learning

Our data suggest that *msi-1* may act on the actin cytoskeleton at the synapses of the AVA neuron. AVA projects its axon along the

#### Figure 5. Genetic Interaction of MSI-1 with the Arp2/3 Complex, WSP-1, and the Actin-Capping Process

(A) STAM conditioning of *arx-2* or, as a control, *gfp* RNAi-treated RNAi-hypersensitive worms with (*nre-1 lin15b*) or without *msi-1* [*msi-1(lf); nre-1 lin15b*] as indicated without (naive) or with (conditioned) preincubation with DA or after 1 hr delay following conditioning (delay).  
 (B) STAM conditioning of RNAi-hypersensitive worms with (*nre-1 lin15b*) or without *msi-1* function (*msi-1; nre-1 lin15b*) treated against *gfp* or the different Arp2/3 subunits as indicated. Worms were assayed toward DA without (naive) or with (cond.) preincubation with DA in absence of food. STAM was tested after 1 hr delay following conditioning (1h delay).  
 (C) STAM performance of *gfp* or *wsp-1* RNAi-treated *nre-1 lin15b* or *msi-1; nre-1 lin15b* worms as indicated were assayed toward DA prior (naive) following preincubation with DA in absence of food (conditioned) or after a 1 hr delay (1h delay).  
 (D and E) STAM performance in wild-type (black), *msi-1(lf)* mutant (red), or in *msi-1(lf)* worms overexpressing constitutive active *wsp-1* VCA fragment (blue) under the control of *nmr-1* (D) or *rig-3* (E) promoter. Bars represent the average of three independent transgenic lines with (as indicated) or without array (no array).  
 (F) STAM was tested in worms of genotype indicated, and DA attraction was tested prior to (naive) or following preincubation with DA in absence of food (conditioned) or after a 1 hr delay (1h delay).  
 (G) STAM was tested in wild-type or mutant worms as indicated. Attraction toward DA was tested prior (naive), following preincubation with DA in absence of food (cond.) or after a 1 hr recovery (delay).  
 All experiments were done in triplicate and repeated at least three times. For (D), (E), and (G), three independent transgenic lines were tested. Bars indicate mean  $\pm$  SEM. NS, nonsignificant, \* $p < 0.05$ , \*\* $p < 0.01$ , \*\*\* $p < 0.001$ . See also Table S5.

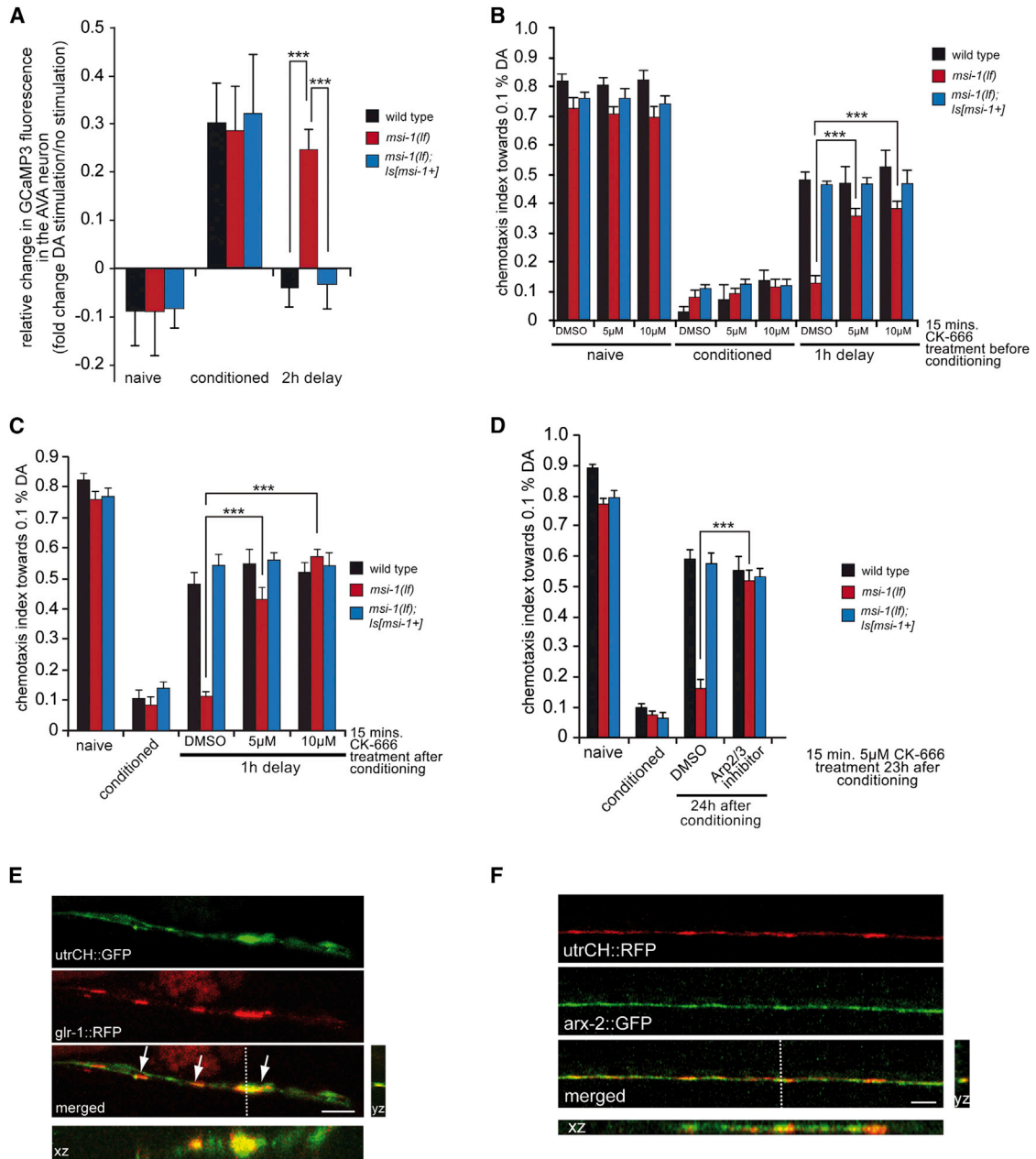


**Figure 6. MSI-1 Influences Persistent Synaptic Plasticity and Acts through the Arp2/3 Complex to Regulate Forgetting**

(A)  $Ca^{2+}$  was detected in transgenic animals carrying GCaMP3 under the control of the *rig-3* promoter in different genotypes as indicated. Worms were unstimulated or DA treated before (naive) or immediately after conditioning (conditioned) or after a 2 hr delay. GCaMP3 fluorescence signal was normalized to the signal of unstimulated worms ( $n > 9$  for each genotype and treatment).

(B and C) Worms with indicated genotypes were treated with 5 or 10  $\mu$ M CK-666 for 15 min before (B) or immediately after (C) conditioning and DA preference was tested in naive, conditioned worms, or after 1 hr delay following conditioning.

(D) Worms with indicated genotypes were treated with DMSO or 5  $\mu$ M CK-666 for 15 min after 23 hr following conditioning and DA preference was tested 24 hr total delay time after conditioning as indicated. Bars represent mean  $\pm$  SEM. \*\*\* $p < 0.001$ .

(E) Distribution of F-actin along the VNC was detected with utropin CH-domain fused to GFP (utrCH::GFP, upper panel) together with GLR-1::RFP (middle panel; arrows point to GLR-1 synapses). The position of yz-projection is marked with dotted line.

(F) Distribution of F-actin (UtrCH::RFP, upper panel) and ARX-2 (ARX-2::GFP, middle panel) along the VNC. The position of yz-projection is marked with dotted line.

Scale bar represents 1  $\mu$ m. See also Figure S4 and Table S6.

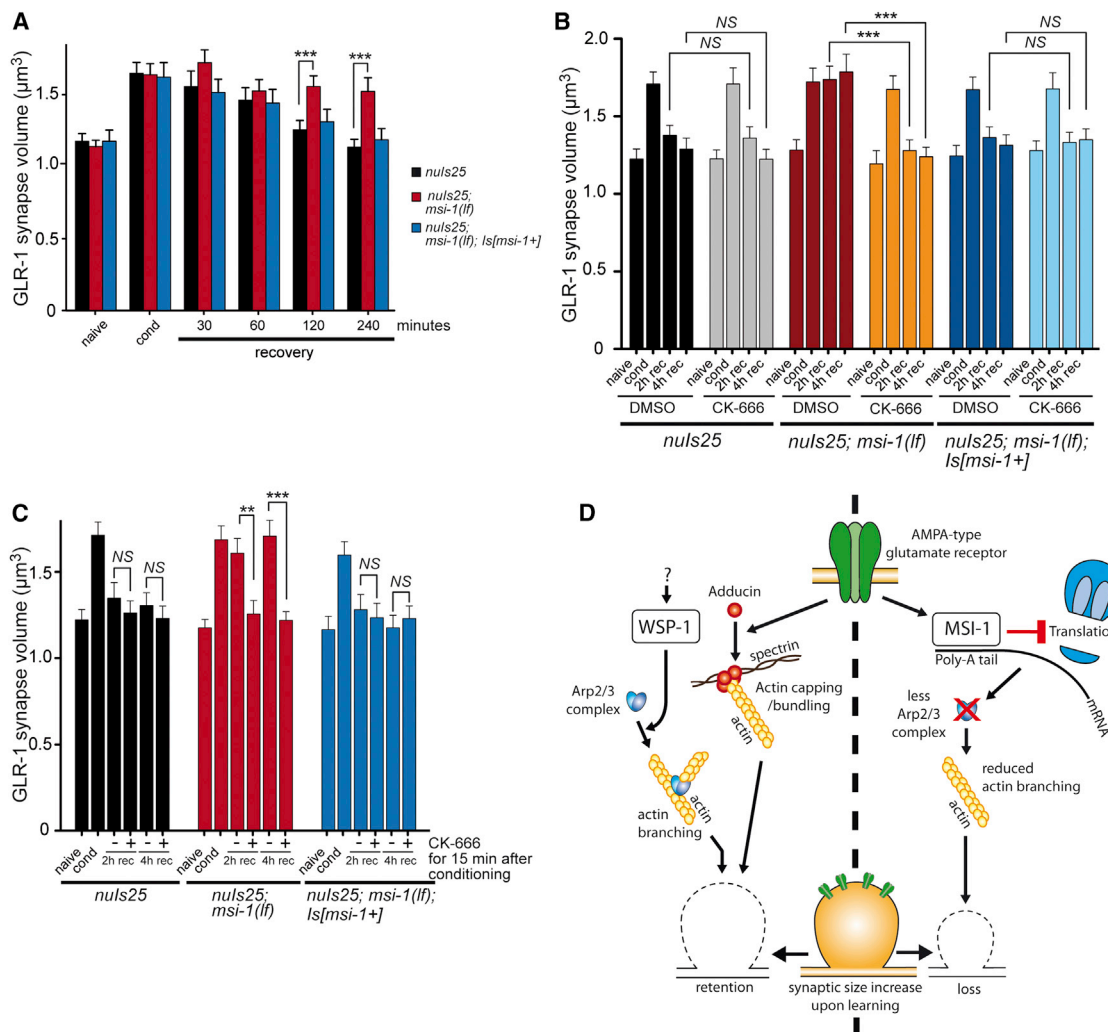


**Figure 7. Deletion of MSI-1 Causes an Arp2/3-Dependent Persistent Enlargement of GLR-1-Positive Synapses Induced by Associative Learning**

(A) Average volume of GLR-1::GFP synapses in the posterior VNC in wild-type and *msi-1(lf)* naive, DA-conditioned (cond) animals or following a recovery period as indicated.

(B and C) Worms with genotypes indicated were treated with 5  $\mu$ M CK-666 for 15 min before (B) or immediately after (C) conditioning and synapse volumes were measured in naive, conditioned (cond), or after 2 or 4 hr delay (2h rec, 4h rec) following conditioning. At least 100 synapses were recorded for each treatment and genotype. Bars indicate mean  $\pm$  SEM. NS, nonsignificant, \*\* $p < 0.01$ , \*\*\* $p < 0.001$ .

(D) Model for regulation of memory loss by the MSI-1 pathway.

See also Figure S5 and Table S7.

ventral nerve chord, where it receives inputs from a large variety of neurons. Therefore, we first tested if synapses of the AVA neuron are enriched in F-actin and contain elevated levels of the Arp2/3 complex. Using confocal microscopy, we found that enriched F-actin colocalizes with GLR-1-positive synapses (Figure 6E). Furthermore, increased F-actin coincides with elevated levels of the Arp2/3 complex (Figure 6F).

Previously, we demonstrated that GLR-1-positive synapses in the *C. elegans* ventral nerve cord change their size upon associative learning (Vukojevic et al., 2012). Furthermore, persistent alteration in synaptic size correlates with memory retention. Among the GLR-1-expressing neurons projecting their axons

posterior to the vulva (AVA, AVB, AVD, and PVC), AVA receives most of the synaptic input. Laser ablation of AVA (Figure S5) deletes virtually all GLR-1 synapses representing inputs to AVA along the VNC. To measure changes in synapse morphology, we investigated GLR-1 punctae volumes posterior to the vulva in naive, DA-conditioned, and memory-consolidated wild-type and *msi-1(lf)* mutant worms. Loss of *msi-1* had no effect on GLR-1 punctae number (Figure S5G). We could not detect a difference in synapse volume between naive wild-type and mutant worms (Figure S5H). Associative learning caused a genotype-independent increase in GLR-1::GFP-positive punctae volume (Figure S5H). In contrast, GLR-1::GFP synapse

volume in wild-type animals reverted to a nearly naive level after 2 hr but remained enlarged in *msi-1(lf)* animals for the tested 4 hr period (Figure 7A). Finally, inhibition of the Arp2/3 complex with CK-666 prior to (Figure 7B) or immediately after (Figure 7C) conditioning reverted the sustained synapse enlargement observed in *msi-1(lf)* worms without influencing synapse-volume increase during learning. In summary, MSI-1 likely inhibits the persistence of the learning-induced size increase of GLR-1-positive punctae volume through the Arp2/3 complex. These results are in accord with the behavioral data and establish a link between forgetting and sustained synapse volume increase in *msi-1(lf)* mutants.

## DISCUSSION

Forgetting is an essential hallmark of behavioral plasticity, although little evidence shows how memory loss is actively regulated at the molecular level (Berry et al., 2012; Inoue et al., 2013; Shuai et al., 2010). In the current study, we demonstrated that the *C. elegans musashi* (*msi-1*) is involved in forgetting independently of the sensory input or the type of memory task. Our data also imply that memory loss is actively regulated and that the learning process induces not only memory acquisition and consolidation but also forgetting. The later observation is in accord with both the proposed role of *Drosophila* Rac during memory loss (Shuai et al., 2010) and the function of the TIR-1/JNK-1 pathway in *C. elegans* (Inoue et al., 2013), suggesting that multiple molecular pathways are actively inducing the decay of memories. Although the TIR-1/JNK-1 pathway is needed in the sensory neurons (Inoue et al., 2013) to eliminate sensory memory, the data presented here propose a mechanism present in the interneurons.

Ablation of AVA, presumably the main regulator of backward movement, was previously found to abolish long reversals (Chalfie et al., 1985). Associative learning, which involves reversals and backward movement upon exposure to a chemoattractant during starvation, could lead to a sustained synaptic sensitivity of this neuron. Therefore, increase in AVA activity could be the direct mediator of avoidance behavior. This is supported by the observation that in naive animals, Ca<sup>2+</sup> transients in AVA decrease upon exposure to DA whereas conditioning increases DA-dependent Ca<sup>2+</sup> transients in AVA. Our results suggest that conditioning-induced activity changes in AVA likely mediate avoidance behavior. Here, we demonstrate that MSI-1 is necessary in the AVA interneuron to induce forgetting. This implies that signaling pathways in the AVA interneuron play a central role in acquisition of memories, as well as in the elimination of them, and that the balance between the two mechanisms defines the duration of memory. This hypothesis is further supported by the analysis of the *add-1*, *msi-1* double-mutant behavioral phenotype. The memory defect of the *add-1* single mutant is rescued to wild-type levels by the simultaneous deletion of *msi-1*, suggesting that the two genes act in parallel in an opposing way during regulation of memory (Figure 7D).

Among the previously identified Musashi mRNA-binding partners, ACTR2 is one of seven subunits of the Arp2/3 protein complex that serves as a nucleation core for the branching of the actin cytoskeleton (Mullins et al., 1998). Here, we found that MSI-1 interacts with the mRNAs of three subunits of the Arp2/3 complex and regulates their protein levels. Several

studies demonstrated that the function of the Arp2/3 protein complex and its proper regulation is necessary for growth of spines and establishment of synapses in vertebrates and that tight control of actin bundling and branching are required during development (Hotulainen et al., 2009). In a mature spine, the neck and the head regions contain a mixture of branched and linear actin filaments, with most of the actin bundles located in the neck and the branched actin in the head region (Korobova and Svitkina, 2010). Besides the different actin composition in synaptic spines, the cortical actin network at the synaptic membranes is also tightly regulated and modulates, for example, AMPA receptor trafficking during synaptic plasticity (Gu et al., 2010). MSI-1 likely influences, in an activity-dependent manner, the structure of the actin network at the synapse, thereby regulating the long-term persistence of size and activity increase of the synaptic areas (Figure 7D). In accordance with this, reduction of the mRNA levels of the Arp2/3 complex, or inhibition of Arp2/3 activity, suppressed the *msi-1(lf)* phenotype, suggesting that the increase of the protein levels observed in *msi-1(lf)* mutants is responsible for the inhibition of memory loss. Furthermore, overactivation of *wsp-1*, a main activator of the Arp2/3 complex (Machesky and Gould, 1999), in the AVA neuron of wild-type worms resulted in a phenotype similar to that of *msi-1* mutants. Interestingly, the activity of the Arp2/3 complex influences memory retention but has no obvious role in memory acquisition. Furthermore, CK-666 was effective 23 hr after conditioning (i.e., at a time point where memory is already consolidated), suggesting a regulation of forgetting rather than memory formation through the Arp2/3 complex. Thus, actin likely plays different roles at various stages of learning and memory. Our results suggest a novel regulation mechanism by which translational inhibition reduces the activity of the Arp2/3 complex, which may result in a less complex cortical actin network. The reduction of the actin network complexity diminishes the persistence time of enlarged synapses. This reduction may represent a structural mechanism of forgetting (Figure 7D).

The complex regulation of the actin cytoskeleton in memory is also reflected in the genetic interaction of actin capping (*add-1* mutant) and actin branching (*msi-1* deletion). Increased capping activity is necessary to stabilize synapses, and an AMPA-type glutamate receptor (GLR-1) signaling pathway in the AVA neuron likely increases actin capping through the activation of adducin (Vukojevic et al., 2012). On the other hand, intact GLR-1 function seems to be a prerequisite for the downstream MSI-1-mediated forgetting machinery (Figure 7D). Thus, activation of the GLR-1 receptor activates memory stabilization and at the same time initiates memory removal. Our results suggest that two parallel mechanisms regulate the complexity of the actin cytoskeleton and that the balance between these mechanisms is crucial for the retention of memories. It is important to stress, however, that at this stage, it is not possible to draw detailed temporal and mechanistic conclusions with regard to how MSI-1- or ADD-1-related molecular changes alter the neural networks involved at different stages of memory maintenance. The elucidation of the precise mechanisms should be a focus of further studies, because an imbalance of these mechanisms may result in altered memory function that could also play a role in memory-related disorders.

## EXPERIMENTAL PROCEDURES

### General Methods and Strains Used

Standard methods were used for maintaining and manipulating *C. elegans* (Brenner, 1974). The *C. elegans* Bristol strain, variety N2, was used as the wild-type reference strain in all experiments. A detailed list of the alleles and transgenes used is provided in [Extended Experimental Procedures](#). Transgenic lines were generated by injecting DNA at a concentration of 10–100 ng/μl into both arms of the syncytial gonad of worms as described previously (Mello et al., 1991). *p<sub>sur-5</sub>::mDsRed* or *pRF4[rol-6D]* was used as a transformation marker at 10 ng/μl concentration. Chromosomal integration of extrachromosomal arrays was done by UV radiation for 10 s. Following integration, generated strains were four-times backcrossed to the wild-type strain. For RNAi experiments, the RNAi-hypersensitive *nre-1(hd20) lin15b(hd126)* strain was used. Early L3 stage worms were fed with bacteria containing dsRNA, and the P<sub>0</sub> generation was tested for behavior.

STAM and LTAM were assessed as described previously (Stetak et al., 2009). Briefly, conditioning was performed for 1 hr without food in the presence of 2 μl undiluted chemoattractant spotted on the lid of 10 cm CTX plates (5 mM KH<sub>2</sub>PO<sub>4</sub>/K<sub>2</sub>HPO<sub>4</sub> [pH 6.0], 1 mM CaCl<sub>2</sub>, 1 mM MgSO<sub>4</sub>, 2% agar). Naive and conditioned worms were given a choice between a spot of 0.1% DA in ethanol with 20 mM sodium-azide and a counter spot with ethanol and sodium-azide. After a delay time, animals were counted and the chemotaxis index was calculated as described previously (Bargmann et al., 1993). A total of 50–200 animals were used in each technical and biological replicate. For the time-course experiment, naive and conditioned worms were given a choice between a spot of 0.1% DA in ethanol with 20 mM sodium-azide and a counter spot with ethanol on 6 cm plates. Animals were counted every 10 min for 1 hr and chemotaxis index was calculated as described previously (Bargmann et al., 1993). The different inhibitors were applied by soaking the worms in M9 supplemented with the inhibitor at the given concentrations.

### Locomotory Rate Assays

Assays were performed on a bacterial lawn as described elsewhere (Stetak et al., 2009). Briefly, worms were grown under uncrowded conditions with or without food for 1 hr and 2 min after transfer to 6 cm plates seeded with OP<sub>50</sub>, and the number of body bends was counted for 1 min for at least ten animals from each strain.

### Fluorescence Microscopy

GFP (or tRFP)-tagged proteins were detected with a Zeiss Axiovert 200 M LSM 5 Pascal confocal microscope as described in [Extended Experimental Procedures](#). For synapse volume measurements, animals were immobilized and GLR-1::GFP were recorded posterior to the vulva. Quantification was performed using the ImageJ Object Counter 3D plugin. Calcium transients using GCaMP3 fluorescence calcium indicator were detected with a Zeiss Axioptan 2 fluorescent microscope and quantified with ImageJ.

### RNA-Binding Protein Immunoprecipitation and Real-Time RT-PCR

Total RNA was isolated from synchronized adult worms using standard protocol. Coimmunoprecipitation was performed as previously described (Roy et al., 2002) from synchronized adult worms, and 400 ng RNA was reverse transcribed using a mix of random decamers (Ambion) and anchored oligo(dT)<sub>20</sub> primer (Invitrogen). Real-time PCR was performed using the SyBr Fast kit (Kapa Biosystems) according to manufacturer's recommendations in a Rotor Gene-6000 instrument (Corbett Research). Expression levels were normalized to *tba-1* and *cdc-42* using a geometric mean of their level of expression, and the fold change was calculated using QBasePlus software (Biogazelle).

### Statistical Analysis

A detailed description of the statistical analysis can be found in [Extended Experimental Procedures](#), and [Tables S1, S2, S3, S4, S5, S6, S7, and S8](#) list statistical significance.

## SUPPLEMENTAL INFORMATION

Supplemental Information includes Extended Experimental Procedures, five figures, and eight tables and can be found with this article online at <http://dx.doi.org/10.1016/j.cell.2014.01.054>.

## ACKNOWLEDGMENTS

We are grateful to Anne Spang and Jean Pieters for generously sharing methods, reagents, and instruments and to Alex Hajnal for his valuable comments on the manuscript and for laser ablation tools. We also like to thank the Caenorhabditis Genetic Center (supported by the National Institutes of Health Office of Research Infrastructure Programs grant P40 OD010440) for providing nematode strains. The Forschungsfonds of the University of Basel (DPE2112 to A.S.) and the Swiss National Science Foundation (Sinergia grants CRSIK0\_122691 and CRSI33\_130080 to D.J.-F.d.Q. and A.P.) supported this work.

Received: July 9, 2013

Revised: November 27, 2013

Accepted: January 17, 2014

Published: March 13, 2014

## REFERENCES

- Bargmann, C.I., Hartwig, E., and Horvitz, H.R. (1993). Odorant-selective genes and neurons mediate olfaction in *C. elegans*. *Cell* **74**, 515–527.
- Battelli, C., Nikopoulos, G.N., Mitchell, J.G., and Verdi, J.M. (2006). The RNA-binding protein Musashi-1 regulates neural development through the translational repression of p21WAF-1. *Mol. Cell. Neurosci.* **31**, 85–96.
- Berry, J.A., Cervantes-Sandoval, I., Nicholas, E.P., and Davis, R.L. (2012). Dopamine is required for learning and forgetting in *Drosophila*. *Neuron* **74**, 530–542.
- Bosch, M., and Hayashi, Y. (2012). Structural plasticity of dendritic spines. *Curr. Opin. Neurobiol.* **22**, 383–388.
- Brenner, S. (1974). The genetics of *Caenorhabditis elegans*. *Genetics* **77**, 71–94.
- Carlezon, W.A., Jr., Duman, R.S., and Nestler, E.J. (2005). The many faces of CREB. *Trends Neurosci.* **28**, 436–445.
- Chalfie, M., Sulston, J.E., White, J.G., Southgate, E., Thomson, J.N., and Brenner, S. (1985). The neural circuit for touch sensitivity in *Caenorhabditis elegans*. *J. Neurosci.* **5**, 956–964.
- Charlesworth, A., Wilczynska, A., Thampi, P., Cox, L.L., and MacNicol, A.M. (2006). Musashi regulates the temporal order of mRNA translation during *Xenopus* oocyte maturation. *EMBO J.* **25**, 2792–2801.
- de Sousa Abreu, R., Sanchez-Diaz, P.C., Vogel, C., Burns, S.C., Ko, D., Burton, T.L., Vo, D.T., Chennasamudaram, S., Le, S.Y., Shapiro, B.A., and Penalva, L.O. (2009). Genomic analyses of musashi1 downstream targets show a strong association with cancer-related processes. *J. Biol. Chem.* **284**, 12125–12135.
- Gu, J., Lee, C.W., Fan, Y., Komlos, D., Tang, X., Sun, C., Yu, K., Hartzell, H.C., Chen, G., Bamberg, J.R., and Zheng, J.Q. (2010). ADF/cofilin-mediated actin dynamics regulate AMPA receptor trafficking during synaptic plasticity. *Nat. Neurosci.* **13**, 1208–1215.
- Hirota, Y., Okabe, M., Imai, T., Kurusu, M., Yamamoto, A., Miyao, S., Nakamura, M., Sawamoto, K., and Okano, H. (1999). Musashi and seven in absentia downregulate Tramtrack through distinct mechanisms in *Drosophila* eye development. *Mech. Dev.* **87**, 93–101.
- Holt, C.E., and Bullock, S.L. (2009). Subcellular mRNA localization in animal cells and why it matters. *Science* **326**, 1212–1216.
- Horisawa, K., Imai, T., Okano, H., and Yanagawa, H. (2009). 3'-Untranslated region of doublecortin mRNA is a binding target of the Musashi1 RNA-binding protein. *FEBS Lett.* **583**, 2429–2434.

- Hotulainen, P., Llano, O., Smirnov, S., Tanhuanpää, K., Faix, J., Rivera, C., and Lappalainen, P. (2009). Defining mechanisms of actin polymerization and depolymerization during dendritic spine morphogenesis. *J. Cell Biol.* *185*, 323–339.
- Imai, T., Tokunaga, A., Yoshida, T., Hashimoto, M., Mikoshiba, K., Weinmaster, G., Nakafuku, M., and Okano, H. (2001). The neural RNA-binding protein Musashi1 translationally regulates mammalian numb gene expression by interacting with its mRNA. *Mol. Cell. Biol.* *21*, 3888–3900.
- Inoue, A., Sawatari, E., Hisamoto, N., Kitazono, T., Teramoto, T., Fujiwara, M., Matsumoto, K., and Ishihara, T. (2013). Forgetting in *C. elegans* is accelerated by neuronal communication via the TIR-1/JNK-1 pathway. *Cell Rep.* *3*, 808–819.
- Jonides, J., Lewis, R.L., Nee, D.E., Lustig, C.A., Berman, M.G., and Moore, K.S. (2008). The mind and brain of short-term memory. *Annu. Rev. Psychol.* *59*, 193–224.
- Kauffman, A.L., Ashraf, J.M., Corces-Zimmerman, M.R., Landis, J.N., and Murphy, C.T. (2010). Insulin signaling and dietary restriction differentially influence the decline of learning and memory with age. *PLoS Biol.* *8*, e1000372.
- Kessels, H.W., Kopec, C.D., Klein, M.E., and Malinow, R. (2009). Roles of star-gazin and phosphorylation in the control of AMPA receptor subcellular distribution. *Nat. Neurosci.* *12*, 888–896.
- Korobova, F., and Svitkina, T. (2010). Molecular architecture of synaptic actin cytoskeleton in hippocampal neurons reveals a mechanism of dendritic spine morphogenesis. *Mol. Biol. Cell* *21*, 165–176.
- Machesky, L.M., and Gould, K.L. (1999). The Arp2/3 complex: a multifunctional actin organizer. *Curr. Opin. Cell Biol.* *11*, 117–121.
- McGaugh, J.L. (2000). Memory—a century of consolidation. *Science* *287*, 248–251.
- Mello, C.C., Kramer, J.M., Stinchcomb, D., and Ambros, V. (1991). Efficient gene transfer in *C. elegans*: extrachromosomal maintenance and integration of transforming sequences. *EMBO J.* *10*, 3959–3970.
- Miyanoiri, Y., Kobayashi, H., Imai, T., Watanabe, M., Nagata, T., Uesugi, S., Okano, H., and Katahira, M. (2003). Origin of higher affinity to RNA of the N-terminal RNA-binding domain than that of the C-terminal one of a mouse neural protein, musashi1, as revealed by comparison of their structures, modes of interaction, surface electrostatic potentials, and backbone dynamics. *J. Biol. Chem.* *278*, 41309–41315.
- Mullins, R.D., Heuser, J.A., and Pollard, T.D. (1998). The interaction of Arp2/3 complex with actin: nucleation, high affinity pointed end capping, and formation of branching networks of filaments. *Proc. Natl. Acad. Sci. USA* *95*, 6181–6186.
- Nolen, B.J., Tomasevic, N., Russell, A., Pierce, D.W., Jia, Z., McCormick, C.D., Hartman, J., Sakowicz, R., and Pollard, T.D. (2009). Characterization of two classes of small molecule inhibitors of Arp2/3 complex. *Nature* *460*, 1031–1034.
- Nuttley, W.M., Atkinson-Leadbetter, K.P., and Van Der Kooy, D. (2002). Serotonin mediates food-odor associative learning in the nematode *Caenorhabditis elegans*. *Proc. Natl. Acad. Sci. USA* *99*, 12449–12454.
- Ohyama, T., Nagata, T., Tsuda, K., Kobayashi, N., Imai, T., Okano, H., Yamazaki, T., and Katahira, M. (2012). Structure of Musashi1 in a complex with target RNA: the role of aromatic stacking interactions. *Nucleic Acids Res.* *40*, 3218–3231.
- Okamoto, K., Nagai, T., Miyawaki, A., and Hayashi, Y. (2004). Rapid and persistent modulation of actin dynamics regulates postsynaptic reorganization underlying bidirectional plasticity. *Nat. Neurosci.* *7*, 1104–1112.
- Pollard, T.D., and Beltzner, C.C. (2002). Structure and function of the Arp2/3 complex. *Curr. Opin. Struct. Biol.* *12*, 768–774.
- Roy, P.J., Stuart, J.M., Lund, J., and Kim, S.K. (2002). Chromosomal clustering of muscle-expressed genes in *Caenorhabditis elegans*. *Nature* *418*, 975–979.
- Sakakibara, S., Nakamura, Y., Satoh, H., and Okano, H. (2001). RNA-binding protein Musashi2: developmentally regulated expression in neural precursor cells and subpopulations of neurons in mammalian CNS. *J. Neurosci.* *21*, 8091–8107.
- Sakakibara, S., Nakamura, Y., Yoshida, T., Shibata, S., Koike, M., Takano, H., Ueda, S., Uchiyama, Y., Noda, T., and Okano, H. (2002). RNA-binding protein Musashi family: roles for CNS stem cells and a subpopulation of ependymal cells revealed by targeted disruption and antisense ablation. *Proc. Natl. Acad. Sci. USA* *99*, 15194–15199.
- Shuai, Y., Lu, B., Hu, Y., Wang, L., Sun, K., and Zhong, Y. (2010). Forgetting is regulated through Rac activity in *Drosophila*. *Cell* *140*, 579–589.
- Stetak, A., Hörndli, F., Maricq, A.V., van den Heuvel, S., and Hajnal, A. (2009). Neuron-specific regulation of associative learning and memory by MAGI-1 in *C. elegans*. *PLoS ONE* *4*, e6019.
- Vukojevic, V., Gschwind, L., Vogler, C., Demougin, P., de Quervain, D.J., Papassotiropoulos, A., and Stetak, A. (2012). A role for  $\alpha$ -adducin (ADD-1) in nematode and human memory. *EMBO J.* *31*, 1453–1466.
- Wang, H., Hu, Y., and Tsien, J.Z. (2006). Molecular and systems mechanisms of memory consolidation and storage. *Prog. Neurobiol.* *79*, 123–135.
- Wicks, S.R., de Vries, C.J., van Luenen, H.G., and Plasterk, R.H. (2000). CHE-3, a cytosolic dynein heavy chain, is required for sensory cilia structure and function in *Caenorhabditis elegans*. *Dev. Biol.* *221*, 295–307.
- Wixted, J.T. (2004). The psychology and neuroscience of forgetting. *Annu. Rev. Psychol.* *55*, 235–269.
- Yamaguchi, H., Miki, H., Suetsugu, S., Ma, L., Kirschner, M.W., and Takenawa, T. (2000). Two tandem verprolin homology domains are necessary for a strong activation of Arp2/3 complex-induced actin polymerization and induction of microspike formation by N-WASP. *Proc. Natl. Acad. Sci. USA* *97*, 12631–12636.
- Yoda, A., Sawa, H., and Okano, H. (2000). MSI-1, a neural RNA-binding protein, is involved in male mating behaviour in *Caenorhabditis elegans*. *Genes Cells* *5*, 885–895.

## Extended Experimental procedures

**Alleles and transgenes used:** *msi-1(os1)*, *msi-1(os1)*; *utrEx24*[genomic *msi-1+*, *p<sub>sur-5</sub>::mDsRed*], *utrIs2*[*p<sub>msi-1</sub>::msi-1cDNA::tRFP::3`UTR*, *rol-6D*]; *nuIs25*[*p<sub>glr-1</sub>::glr-1::GFP*], *msi-1(os1)*; *utrIs3*[*p<sub>msi-1</sub>::msi-1cDNA::MYC-tag::3`UTR*, *p<sub>sur-5</sub>::mDsRed*], *msi-1(os1)*; *utrIs4*[*p<sub>msi-1</sub>::msi-1cDNA-RBDmutant::MYC-tag::3`UTR*, *p<sub>sur-5</sub>::mDsRed*], *msi-1(os1)*; *utrEx59*[*p<sub>lim-4</sub>::msi-1cDNA::MYC-tag::3`UTR*, *p<sub>sur-5</sub>::mDsRed*], *msi-1(os1)*; *utrEx60*[*p<sub>rig-3</sub>::msi-1cDNA::MYC-tag::3`UTR*, *p<sub>sur-5</sub>::mDsRed*], *msi-1(os1)*; *utrEx61*[*p<sub>nmr-1</sub>::msi-1cDNA::MYC-tag::3`UTR*, *p<sub>sur-5</sub>::mDsRed*], *msi-1(os1)*; *utrEx70*[*p<sub>unc-47</sub>::msi-1cDNA::MYC-tag::3`UTR*, *p<sub>sur-5</sub>::mDsRed*], *utrIs5*[*p<sub>msi-1</sub>::GFP::arx-1 3`UTR*, *punc-119+*], *utrIs11*[*p<sub>msi-1</sub>::GFP::arx-2 3`UTR*, *punc-119+*], *utrIs6*[*p<sub>msi-1</sub>::GFP::arx-3 3`UTR*, *punc-119+*], *utrIs7*[*p<sub>msi-1</sub>::GFP::arx-4 3`UTR*, *punc-119+*], *utrIs8*[*p<sub>msi-1</sub>::GFP::arx-5 3`UTR*, *punc-119+*], *msi-1(os1)*; *utrIs5*[*p<sub>msi-1</sub>::GFP::arx-1 3`UTR*, *punc-119+*], *msi-1(os1)*; *utrIs11*[*p<sub>msi-1</sub>::GFP::arx-2 3`UTR*, *punc-119+*], *msi-1(os1)*; *utrIs6*[*p<sub>msi-1</sub>::GFP::arx-3 3`UTR*, *punc-119+*], *msi-1(os1)*; *utrIs7*[*p<sub>msi-1</sub>::GFP::arx-4 3`UTR*, *punc-119+*], *msi-1(os1)*; *utrIs8*[*p<sub>msi-1</sub>::GFP::arx-5 3`UTR*, *punc-119+*], *nuIs25*[*p<sub>glr-1</sub>::glr-1::GFP*], *msi-1(os1)*; *nuIs25*[*p<sub>glr-1</sub>::glr-1::GFP*], *nre-1(hd20)* *lin-15b(hd126)*, *msi-1(os1)*; *nre-1(hd20)* *lin-15b(hd126)*, *utrEx63*[*p<sub>nmr-1</sub>::wsp-1VCA::3`UTR*, *p<sub>sur-5</sub>::mDsRed*], *utrEx62*[*p<sub>rig-3</sub>::wsp-1VCA::3`UTR*, *p<sub>sur-5</sub>::mDsRed*], *add-1(tm3760)*, *add-1(tm3760)*; *msi-1(os1)*, *glr-1(n2461)*, *glr-1(n2561)* *msi-1(os1)*, *glr-1(n2461)*; *nuIs*[*glr-1::gfp*], *glr-1(n2561)* *msi-1(os1)*; *nuIs25*[*glr-1::gfp*], *glr-1(n2461)*; *nuIs25*[*glr-1::gfp*]; *utrIs14*[*p<sub>rig-3</sub>::GFPhp*, *p<sub>sur-5</sub>::mDsRed*], *glr-1(n2461)* *msi-1(os1)*; *nuIs25*[*glr-1::gfp*]; *utrIs14*[*p<sub>rig-3</sub>::GFPhp*, *p<sub>sur-5</sub>::mDsRed*], *msi-1(os1)*; *utrIs3*[*p<sub>msi-1</sub>::msi-1cDNA::MYC-tag::3`UTR*, *p<sub>sur-5</sub>::mDsRed*]; *utrIs5*[*p<sub>msi-1</sub>::GFP::arx-1 3`UTR*, *punc-119+*], *msi-1(os1)*; *utrIs3*[*p<sub>msi-1</sub>::msi-1cDNA::MYC-tag::3`UTR*, *p<sub>sur-5</sub>::mDsRed*]; *utrIs11*[*p<sub>msi-1</sub>::GFP::arx-2 3`UTR*, *punc-119+*], *msi-1(os1)*; *utrIs3*[*p<sub>msi-1</sub>::msi-1cDNA::MYC-tag::3`UTR*, *p<sub>sur-5</sub>::mDsRed*]; *utrIs6*[*p<sub>msi-1</sub>::GFP::arx-3 3`UTR*, *punc-119+*], *msi-1(os1)*; *utrIs3*[*p<sub>msi-1</sub>::msi-1cDNA::MYC-tag::3`UTR*, *p<sub>sur-5</sub>::mDsRed*]; *utrIs7*[*p<sub>msi-1</sub>::GFP::arx-4 3`UTR*, *punc-119+*], *msi-1(os1)*; *utrIs3*[*p<sub>msi-1</sub>::msi-1cDNA::MYC-tag::3`UTR*, *p<sub>sur-5</sub>::mDsRed*]; *utrIs8*[*p<sub>msi-1</sub>::GFP::arx-5 3`UTR*, *punc-119+*], *utrEx43*[*p<sub>rig-3</sub>::GCaMP3*, *p<sub>sur-5</sub>::mDsRed*], *msi-1(os1)*; *utrEx66*[*p<sub>rig-3</sub>::GCaMP3*, *rol-6D*], *msi-1(os1)*; *utrEx67*[*p<sub>msi-1</sub>::msi-1cDNA::MYC-tag::3`UTR*, *p<sub>rig-3</sub>::GCaMP3*, *rol-6D*], *nuIs25*; *msi-1(os1)*; *utrIs3*[*p<sub>msi-1</sub>::msi-1cDNA::MYC-tag::3`UTR*], *utrEx68*[*p<sub>nmr-1</sub>::glr-1::RFP*, *prig-3::utrCH::GFP*, *rol-6D*], *utrEx69*[*prig-3::utrCH::RFP*, *prig-3::arx-2::GFP*, *rol-6D*], *oxIs12*[*unc-47::gfp*; *lin-15(+)*].



## **Immunoprecipitation**

Co-Immunoprecipitation was performed as previously described (Roy et al., 2002) with some modifications. Briefly, populations of well-fed young adult worms were suspended and fixed in 5 ml 0.5% formaldehyde in M9 for 1 hour at 4°C, washed once with ice-cold M9 and twice with 750 µl HB buffer (300 mM NaCl, 50 mM HEPES Buffer pH 7.6, 10 mM MgCl<sub>2</sub>, 1 mM EGTA, 30 mM EDTA, 0.2 mg/ml heparin, 10% glycerol, 1 mM DTT, 8 mM vanadyl ribonucleoside complex, 50 U/ml RNasin (Promega) and 1 tablet of EDTA-free Protease inhibitor cocktail/10 ml (Roche). The worms were resuspended in 1 ml HB buffer, shock-frozen in liquid nitrogen and lysed in a TissueLyzer MM 301 Ball Mill Homogenizer (Retsch) three times for 30 seconds at 30 Hz while cooled in liquid nitrogen in between cycles. The homogenate was cleaned with 5 minutes centrifugation at 14.000 rpm at 4°C. RNA bound to MSI-1::MYC or MSI-1(RNA binding mutant)::MYC was precipitated with EZview Red Anti c-Myc agarose beads (Sigma). Prior to addition to the lysates the agarose beads were 2 times equilibrated with 1 ml HB buffer containing 1 µl RNasin and 8 µl vanadyl ribonucleoside complex. The MSI-1/RNA complexes were incubated with the anti cMyc beads for 1 hour at 4°C with constant mixing. The RNA-protein complexes were dissociated by incubating the beads for 30 minutes in 125 µl EB (50 mM Tris-HCl pH 8.0, 10 mM EDTA, 1.3 % SDS, 160 Units/ml RNasin) at 65°C. The RNA was collected by centrifugation and isolated with the Direct-zol RNA MiniPrep kit (Zymo Research Cooperation) and concentrated using the RNA Clean & Concentrator-5 kit (Zymo Research Cooperation) according to the manufacturer's protocol. The final RNA quality was assessed with RNA Nano assay cells using Agilent 2100 Bioanalyzer (Agilent Technologies).

## **Total RNA isolation**

Total RNA was isolated from synchronized adult worms with lysis by vortexing with glass beads in TRI-Reagent. RNA isolation was done with Direct-zol RNA MiniPrep kit (Zymo Research Cooperation) according to manufacturer's recommendations.

## **Real-time PCR**

Reverse transcription was performed with GoScript Reverse Transcription System (Promega Corporation) according to the manufacturer's recommendations using 400 ng of purified RNA. 60 ng spike mRNA of each *B. subtilis* gene *thr* and *phe* was added to the MSI-1 bound RNA prior to the reverse transcription and used as internal control for normalization in the

subsequent Real-time PCR using a geometric mean of their expression levels. Real-time PCR of total RNA was normalized to the expression levels of *tba-1* and *cdc-42*. Real-time PCR was performed using the SyBr Fast Kit (Kapa Biosystems) according to the manufacturer's recommendations in a Rotor-Gene Q instrument (Qiagen).

### **Molecular biology**

Genomic rescue of the *msi-1(lf)* phenotype was performed with a 16.4 kb *EagI* fragment of WRM0618cG08 fosmid covering the *msi-1* genomic locus. Musashi minigene was constructed by fusing a 7.6-kb *msi-1* promoter region with the complete *msi-1* cDNA together with a 1.1-kb *msi-1* 3'UTR. Introducing tRFP or myc-tag sequence before the stop codon of the *msi-1* minigene generated tRFP or myc-tag reporter construct. To abolish the RNA binding capacity of the *msi-1::myc-tag* construct in order to create a control for the Co-IP, 6 point mutations (Figure S3) were created in the RRM of *msi-1* by site-directed mutagenesis. For the tissue-specific rescue experiments, the original *msi-1* cDNA and 3'UTR was fused to a 940-bp fragment of the *nmr-1*, a 2.6-kb fragment of the *lim-4*, a 3.2-kb fragment of the *rig-3* or a 1.2-kb of the *unc-47* promoters. GFP reporters were generated by fusing the 7.6-kb *msi-1* promoter region, to GFP under the control of a 486-bp *arx-1*, a 1.2-kb *arx-2*, a 398-bp *arx-3*, a 1.4-kb *arx-4* or a 233-bp *arx-5* 3' UTR sequence.

### **Detection of calcium transients with fluorescence microscopy**

Calcium transients using GCaMP3 fluorescence calcium indicator (Tian et al., 2009) were detected with a Zeiss Axioplan2 Imaging fluorescent microscope. The measurements were conducted on young adult animals, immobilized with polystyrene microspheres and Ca<sup>2+</sup> transients fluorescence signal was recorded in AVA neuron, every 2 seconds with 150ms exposure, for 400s total time (200 cycles). Recorded images were processed using ImageJ (Schneider et al., 2012). The image stack was segmented to isolate structures of interest and aligned to correct for movement of the specimen (Bolte and Cordelières, 2006; Thévenaz et al., 1998). A mask was created based on the segmentation. Time courses were computed by averaging the intensity values per slice of the image stack within the mask.

### **Laser ablation**

To remove the specific neurons, the nuclei of the cells were ablated in early L4 larvae with a laser microbeam as described (Sulston and White 1980; Kimble 1981). In order to identify the cells, the *nuIs25* transgenic strain carrying *glr-1::GFP* was used. The operated animals were

allowed to develop until the adulthood and successfully operated animals were scored using confocal microscopy.

### **Statistical analysis**

All statistical analyses were done using the identical linear mixed model approach applying the lme-function (Pinheiro, Bates, DebRoy, Sarkar, & R Core Team, 2012) in R (R Core Team, 2012). Independent *C.elegans* samples were set as random effect. Fixed-effects were – depending on the analysis – genotype, condition, treatment, dilution, repetition or time points and the corresponding two-way interactions. In case of more than two possible fixed effects per analysis, data was split in sub-data sets and analyzed in several independent models. In order to be able to account for variance-heterogeneity, we included a variance function (varIdent function) in the additive model of the main effects only. The varIdent function allows accounting for different variances within each subgroup by modeling the variance structure of the within-group errors as covariate. The model including the varIdent function was tested against the simple model without the variance function using a log-likelihood ratio test. If this log-likelihood ratio test comparing the additive models showed at least nominal significance and visual inspection of the residual plot indicated an improvement, the model with the varIdent function was used in all further analyses, otherwise the simple model was used. Main effects and interaction terms were tested using ANOVA. Statistical tests for significance were done with *F*-tests using sums-of-squares type II. The *p*-value threshold was set to nominal significance ( $p < 0.05$ ). In case of a significant main or interaction effects, *post-hoc* tests were calculated using *t*-tests. *P*-values of the *post-hoc* tests were corrected for the number *post-hoc* tests calculated per analysis (Bonferroni-correction per analysis:  $p_{bonf} < 0.05$ ).

## Supplemental Figures

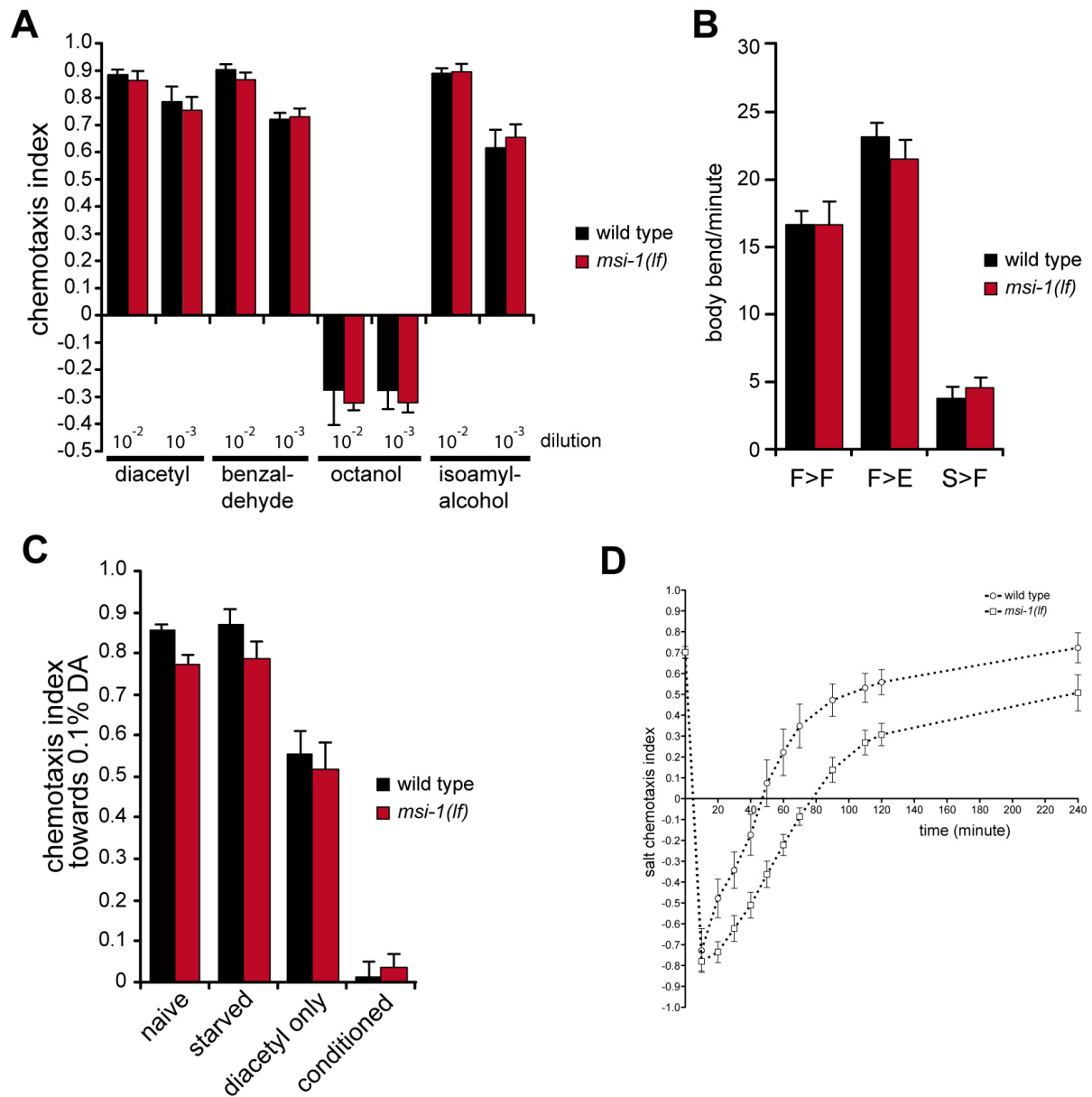


**Figure S1. Loss of *msi-1* does not influence chemotaxis, learning, response to starvation and motoric behaviors, related to Figure 1.** A., chemotaxis towards the indicated chemicals was tested in wild type and *msi-1(lf)* worms as described (Bargmann et al., 1993). B., Locomotory rate of fed (F) or starved worms (S) was tested in presence (>F) or absence of food (>E) (n=14-20). C., Attraction of wild type or mutant worms was assayed towards 0.1% DA without (naïve) or with (conditioned) pre-incubation with DA coupled with starvation. As controls, the effect of starvation (starved) or diacetyl in presence of abundant food (diacetyl only) was tested. D., Salt associative learning, and memory of *msi-1(os1)* and wild type animals during a 4 hours time period. All experiments were done in triplicate and repeated at least three times. Bars represent average  $\pm$  SEM. See also Table S8.

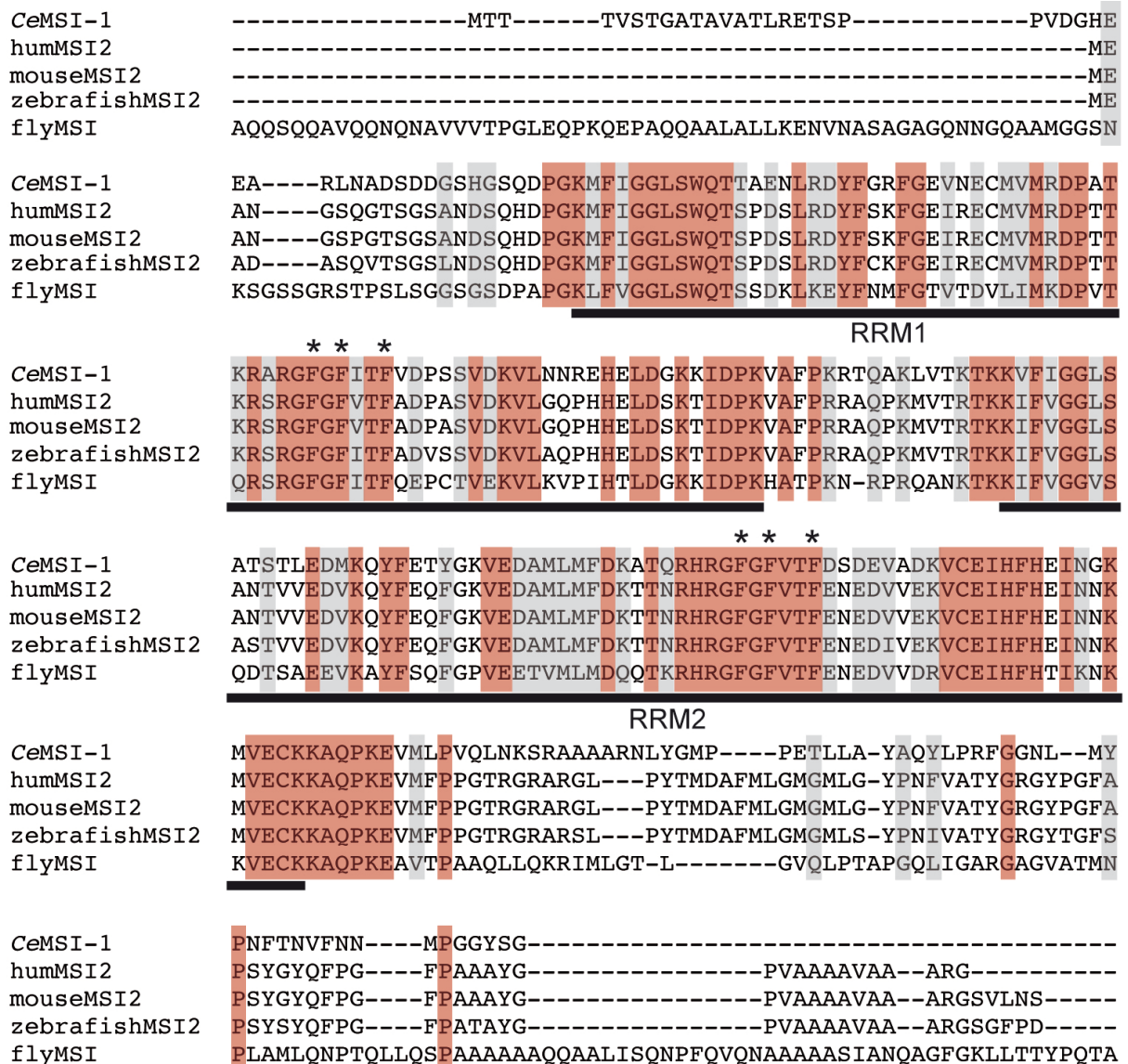


**Figure S2. Sequence alignment of Musashi from different species, related to Figure 2.** Red boxes show identity, grey boxes represent similarity. The two RNA-binding domains (RRM1 and RRM2) are underlined. Stars show highly conserved amino acids that are essential for association with RNA molecules. All these amino acids were mutated in MSI-1 RNA-binding mutant.

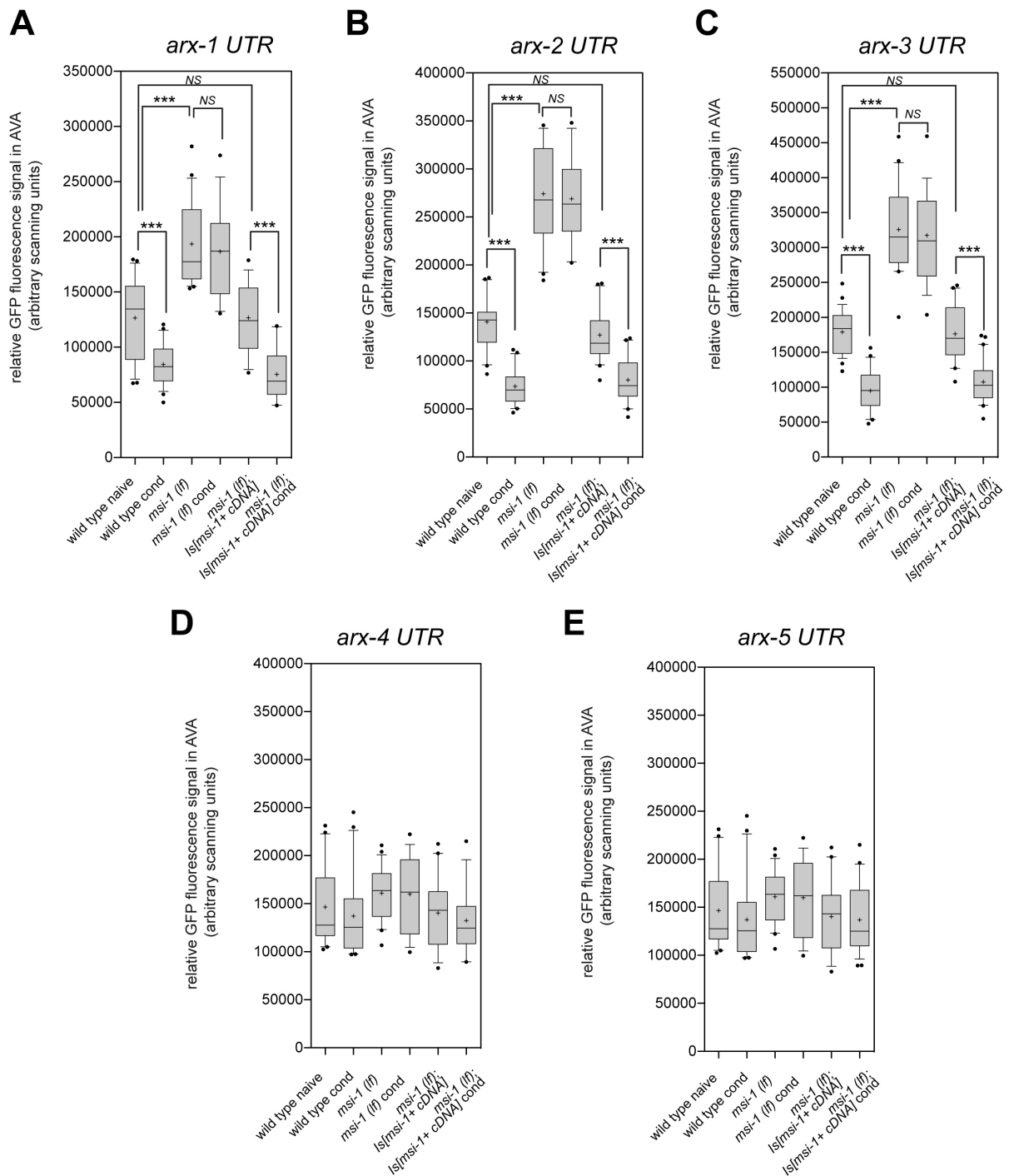


**Figure S3 related to Figure 4. A-E.**, GFP intensity in AVA interneuron in integrated transgenic worms carrying 7.7 kb *msi-1* promoter, GFP and 3' UTR as indicated. GFP signal was measured on z-projected confocal images in untreated wild type (naïve) immediately after DA treatment in the absence of food (conditioned), *msi-1(lf)* mutants (*msi-1(lf)* naïve), or in *msi-1(lf)* mutant worms that were conditioned with DA (*msi-1(lf)* cond). As control, GFP intensities were also measured in naïve or conditioned *msi-1(lf); Is[msi-1+]* rescued line. For each condition, at least 15 animals from 3 independent treatments were recorded with identical microscope settings. The intensity was quantified in projected images using ImageJ software. Bars represent 10 and 90 percentile  $\pm$  SD. \*\*\*:  $p < 0.001$ . See also Table S8.

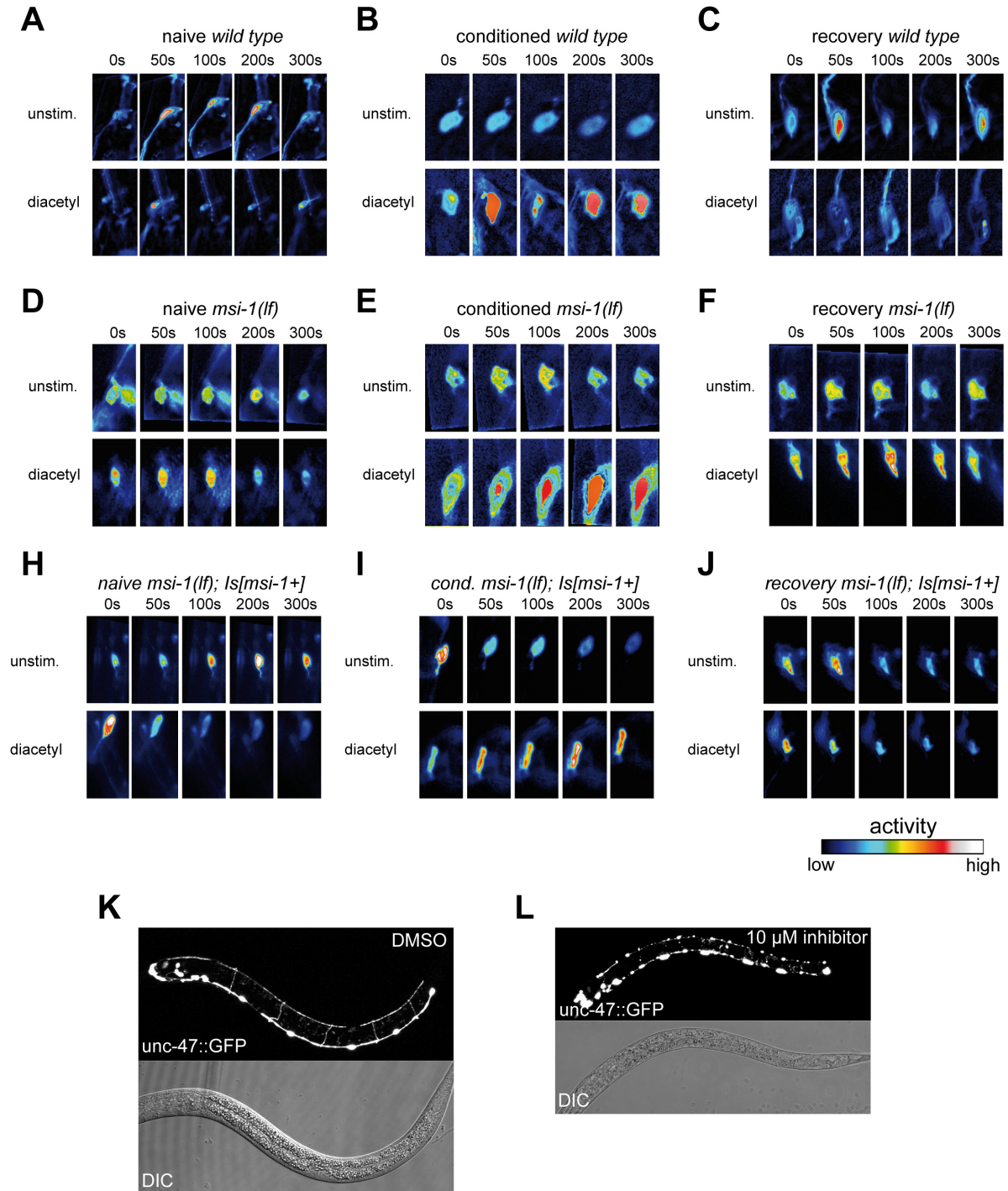


**Figure S4 related to Figure 6.** Representative fluorescence images of AVA interneuron  $\text{Ca}^{2+}$  transients in naïve (**A**, **D**, and **H**) and conditioned (**B**, **E**, and **I**), and after 2h delay (**C**, **F**, and **J**) wild type (**A-C**), *msi-1(lf)* (**D-F**), and *msi-1(lf); Is[msi-1+]* (**H-J**) rescued animals. (**D-E**). Scale represents the relative fluorescence intensity. **K-L**, Adult *unc-47::GFP* worms were put on plates containing DMSO (**K**) or 10  $\mu\text{M}$  CK-666 (**L**) and let lay eggs for 6 hours. GFP signal was recorded in hatched L1-L2 animals. Upper panel shows maximal projection of the GFP channel, lower panel shows phase contrast image.

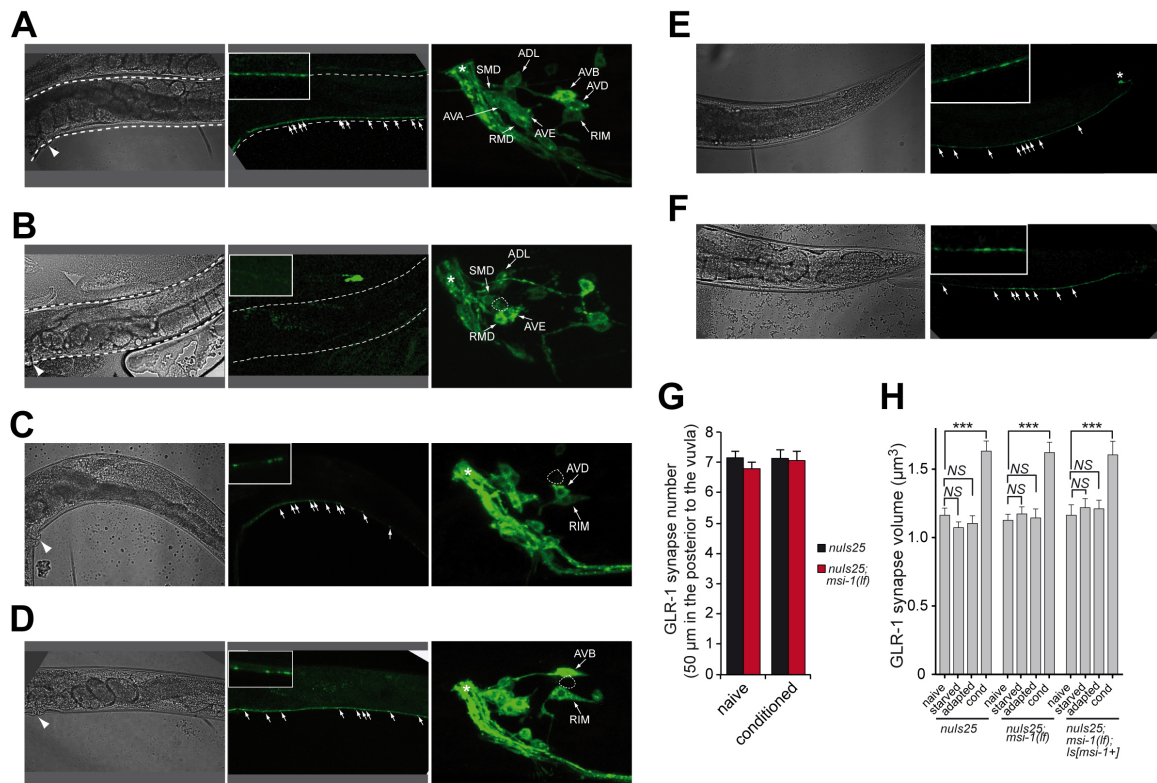


**Figure S5 related to Figure 7.** GLR-1 positive synapses along the posterior part of the ventral nerve chord represent inputs to the AVA command interneuron. **A.**, Expression of GLR-1 in wild type animal. Phase contrast image (left panel) shows the posterior part of an adult worm (arrowhead points to the vulva) where GLR-1 localizes in punctae along the ventral nerve chord (arrows on the middle panel. See also insert). Right panel shows the GLR-1 expressing neurons in the head ganglion. Star labels the nerve ring. **B-F.**, Expression of GLR-1 in laser ablated animals. Laser microbeam was used to remove AVA (**B**), AVB (**C**), AVD (**D**) or PVC (**F**) in L4 *nuls25* transgenic worms. Phase contrast image (left panel) shows the posterior part of an adult worm (arrowhead points to the vulva) where GLR-1 localizes in punctae along the ventral nerve chord (arrows on the middle panel. See also insert). Right panel on **B-D** shows the GLR-1 expressing neurons in the head ganglion. Star labels the nerve ring; dotted line labels the ablated cells. **E.**, Expression of GLR-1 in the posterior part of a wild type animal. Star labels PVC neuron cell body. **G.**, number of GLR-1::GFP containing synapses along the ventral nerve chord in adult wild type (*nuls25*) or *msi-1(lf)* (*nuls25; msi-1(lf)*) mutants. Worms were untreated (naïve) or conditioned with diacetyl (conditioned). Number of synapses were counted on 50 μm length posterior to the vulva **H.**, Average volume of GLR-1::GFP synapses in naïve, upon starvation without (starved), upon treatment with DA in presence of food (adapted) or after conditioning with DA (cond) in wild type (*nuls25*), *msi-1(lf)* (*nuls25; msi-1(lf)*) and *msi-1(lf)* *Is[msi-1+]* rescued animals (*nuls25; msi-1(lf); Is[msi-1+]*). Synapse volumes were measured using ImageJ on confocal images (voxel size: 0.09×0.09×0.28 μm). Bars represent mean ± SEM. \*\*\*: p<0.001. See also Table S8.



Table S1: Statistical Results for Figure 1

Figure	Model	Condition tested	Class	Levels	Test	Test statistic	df	p value	p value bonf	varIdent
1A naïve	Anova	time	IN		F	197.47	1 153	<1e-16		no
1A naïve	Anova	genotype	FA	WT, <i>msi-1(ff)</i>	F	0.07	1 153	0.8		no
1A naïve	Anova	time:genotype	F		F	0.23	1 153	0.63		no
1A conditioned	Anova	time	IN		F	593.61	1 140	<1e-16		no
1A conditioned	Anova	genotype	FA	WT, <i>msi-1(ff)</i>	F	24.75	1 140	3.30E-05		no
1A conditioned	Anova	time:genotype	F	WT, <i>msi-1(ff)</i>	F	10.07	1 140	0.0019		no
1A conditioned	Post-hoc	genotype (time=10)	FA	WT, <i>msi-1(ff)</i>	t	1.48	27	0.15	0.9	no
1A conditioned	Post-hoc	genotype (time=20)	FA	WT, <i>msi-1(ff)</i>	t	<b>3.75</b>	<b>26</b>	<b>9.00E-04</b>	<b>0.0054</b>	no
1A conditioned	Post-hoc	genotype (time=30)	FA	WT, <i>msi-1(ff)</i>	t	4.32	27	<b>0.0019</b>	<b>0.0011</b>	no
1A conditioned	Post-hoc	genotype (time=40)	FA	WT, <i>msi-1(ff)</i>	t	4.34	26	<b>0.0019</b>	<b>0.0012</b>	no
1A conditioned	Post-hoc	genotype (time=50)	FA	WT, <i>msi-1(ff)</i>	t	4.8	27	<b>5.20E-05</b>	<b>0.00031</b>	no
1A conditioned	Post-hoc	genotype (time=60)	FA	WT, <i>msi-1(ff)</i>	t	<b>4.05</b>	<b>26</b>	<b>0.00041</b>	<b>0.0024</b>	no
1B naïve	Anova	time	IN		F	218.08	1 127	<1e-16		no
1B naïve	Anova	genotype	FA	WT, <i>msi-1(ff); ls[msi-1+]</i>	F	0.11	1 127	0.75		no
1B naïve	Anova	time:genotype	F		F	2.06	1 127	0.15		no
1B conditioned	Anova	time	IN		F	1663.24	1 112	<1e-16		no
1B conditioned	Anova	genotype	FA	WT, <i>msi-1(ff); ls[msi-1+]</i>	F	0.31	1 112	0.58		no
1B conditioned	Anova	time:genotype	F		F	1.47	1 112	0.23		no
1C	Anova	condition	FA	naive,cond.,1 h delay	F	106.74	2 47	<1e-16		no
1C	Anova	genotype	FA	<i>gfp</i> RNAi, <i>msi-1</i> RNAi	F	6.55	1 47	0.014		no
1C	Anova	condition:genotype	F		F	6.24	2 47	0.004		no
1C	Post-hoc	genotype (condition=naive)	FA	<i>gfp</i> RNAi, <i>msi-1</i> RNAi	t	1.48	16	0.16	0.47	no
1C	Post-hoc	genotype (condition=cond.)	FA	<i>gfp</i> RNAi, <i>msi-1</i> RNAi	t	-0.82	15	0.42	1	no
1C	Post-hoc	genotype (condition=1 h delay)	FA	<i>gfp</i> RNAi, <i>msi-1</i> RNAi	t	<b>3.69</b>	<b>16</b>	<b>0.002</b>	<b>0.0059</b>	no
1D	Anova	condition	FA	naive,cond.,1 h delay	F	655.06	2 181	<1e-16		yes
1D	Anova	genotype	FA	WT, <i>msi-1(ff); msi-1(ff); ls[msi-1+]</i>	F	1.26	2 181	0.29		yes
1D	Anova	condition:genotype	F		F	9.69	4 181	4.00E-07		yes
1D	Post-hoc	genotype (condition=naive)	FA	WT, <i>msi-1(ff)</i>	t	-2.65	54	0.011	0.064	yes
1D	Post-hoc	genotype (condition=cond.)	FA	WT, <i>msi-1(ff)</i>	t	0.53	52	0.6	1	yes
1D	Post-hoc	genotype (condition=1 h delay)	FA	WT, <i>msi-1(ff)</i>	t	<b>-6.47</b>	<b>51</b>	<b>3.70E-08</b>	<b>2.20E-07</b>	yes
1D	Post-hoc	genotype (condition=naive)	FA	<i>msi-1(ff); msi-1(ff); ls[msi-1+]</i>	t	1.53	31	0.14	0.81	yes
1D	Post-hoc	genotype (condition=cond.)	FA	<i>msi-1(ff); msi-1(ff); ls[msi-1+]</i>	t	-1	31	0.33	1	yes
1D	Post-hoc	genotype (condition=1 h delay)	FA	<i>msi-1(ff); msi-1(ff); ls[msi-1+]</i>	t	5.58	30	4.60E-06	2.70E-05	yes
1E naïve	Anova	genotype	FA		F	1.37	2 24	0.27		no
1E immediate	Anova	repetition	FA	1×, 2×	F	5.23	1 48	0.027		yes
1E immediate	Anova	genotype	FA	WT, <i>msi-1(ff); msi-1(ff); ls[msi-1+]</i>	F	12.82	2 48	3.20E-05		yes
1E immediate	Anova	repetition:genotype	F		F	0.13	2 48	0.87		yes
1E 24h delay	Anova	repetition	FA	1×, 2×	F	8.23	1 48	0.0052		yes
1E 24h delay	Anova	genotype	FA	WT, <i>msi-1(ff); msi-1(ff); ls[msi-1+]</i>	F	72.24	2 48	1.80E-15		yes
1E 24h delay	Anova	repetition:genotype	F		F	2.07	2 48	0.14		yes
1E 24h delay	Post-hoc	genotype	FA	WT, <i>msi-1(ff)</i>	t	<b>6.15</b>	<b>33</b>	<b>6.20E-07</b>	<b>1.90E-06</b>	yes
1E 24h delay	Post-hoc	genotype	FA	<i>msi-1(ff); msi-1(ff); ls[msi-1+]</i>	t	-11.63	33	3.30E-13	9.80E-13	yes
1E 24h delay	Post-hoc	genotype	FA	WT, <i>msi-1(ff); ls[msi-1+]</i>	t	0.98	33	0.34	1	yes
1E 32h delay	Anova	repetition	FA	1×, 2×	F	18.2	1 48	8.90E-05		yes
1E 32h delay	Anova	genotype	FA	WT, <i>msi-1(ff); msi-1(ff); ls[msi-1+]</i>	F	18.13	2 48	1.20E-06		yes
1E 32h delay	Anova	repetition:genotype	F		F	0.32	2 48	0.73		yes
1E 32h delay	Post-hoc	genotype	FA	WT, <i>msi-1(ff)</i>	t	<b>5.89</b>	<b>33</b>	<b>1.30E-06</b>	<b>4.00E-06</b>	yes
1E 32h delay	Post-hoc	genotype	FA	<i>msi-1(ff); msi-1(ff); ls[msi-1+]</i>	t	-5.67	33	2.50E-06	7.60E-06	yes
1E 32h delay	Post-hoc	genotype	FA	WT, <i>msi-1(ff); ls[msi-1+]</i>	t	1.09	33	0.28	0.84	yes

## Abbreviations:

IN: integer

FA: factor

df: degrees of freedom

varIdent: model calculated accounts for heterogeneity of variance

P-values represented on the figure are highlighted in bold.

Table S2: Statistical Results for Figure 2

Figure	Model	Condition.tested	Class	Levels	Test	Test.statistic	df	p.value	p.value bonf	var/dent
2H	Anova	condition	FA	naive,cond.,1 h delay	F	<b>804.47</b>	2 119	<1e-16		yes
2H	Anova	genotype	FA	WT,msi-1(ff),msi-1(ff);:ls[msi-1+cDNA],msi-1(ff);:ls[msi-1RBDmut]	F	<b>3</b>	3 119	<b>0.033</b>		yes
2H	Anova	condition:genotype	FA		F	<b>18.83</b>	6 119	<b>2.6e-15</b>		yes
2H	Post-hoc	genotype (condition=naive)	FA	WT,msi-1(ff)	t	<b>2.58</b>	<b>23</b>	<b>0.017</b>	<b>0.15</b>	yes
2H	Post-hoc	genotype (condition=cond.)	FA	WT,msi-1(ff)	t	<b>0.7</b>	<b>25</b>	<b>0.49</b>		yes
2H	Post-hoc	genotype (condition=naive)	FA	WT,msi-1(ff)	t	<b>9.2</b>	<b>24</b>	<b>2.5e-09</b>	<b>2.2e-08</b>	yes
2H	Post-hoc	genotype (condition=cond.)	FA	msi-1(ff);:ls[msi-1+cDNA],msi-1(ff)	t	<b>1.52</b>	<b>14</b>	<b>0.15</b>		yes
2H	Post-hoc	genotype (condition=cond.)	FA	msi-1(ff);:ls[msi-1+cDNA],msi-1(ff)	t	<b>0.32</b>	<b>16</b>	<b>0.75</b>		yes
2H	Post-hoc	genotype (condition=naive)	FA	msi-1(ff);:ls[msi-1+cDNA],msi-1(ff)	t	<b>11.15</b>	<b>16</b>	<b>5.9e-09</b>	<b>5.3e-08</b>	yes
2H	Post-hoc	genotype (condition=naive)	FA	msi-1(ff);:ls[msi-1RBDmut],msi-1(ff)	t	<b>0.45</b>	<b>14</b>	<b>0.66</b>		yes
2H	Post-hoc	genotype (condition=cond.)	FA	msi-1(ff);:ls[msi-1RBDmut],msi-1(ff)	t	<b>0.73</b>	<b>16</b>	<b>0.48</b>		yes
2H	Post-hoc	genotype (condition=1 h delay)	FA	msi-1(ff);:ls[msi-1RBDmut],msi-1(ff)	t	<b>2.28</b>	<b>15</b>	<b>0.038</b>	<b>0.34</b>	yes
2I	Anova	condition	FA	naive,cond.,1 h delay	F	<b>563.23</b>	2 258	<1e-16		yes
2I	Anova	genotype	FA	WT,msi-1(ff);:Exp[prnc-47::msi-1+],msi-1(ff);:no array	F	<b>12.64</b>	2 258	<b>5.8e-06</b>		yes
2I	Anova	condition:genotype	FA		F	<b>16.92</b>	4 258	<b>2.5e-12</b>		yes
2I	Post-hoc	genotype (condition=naive)	FA	WT,msi-1(ff);:no array	t	<b>3.39</b>	<b>60</b>	<b>0.0012</b>	<b>0.011</b>	yes
2I	Post-hoc	genotype (condition=cond.)	FA	WT,msi-1(ff);:no array	t	<b>1</b>	<b>62</b>	<b>0.32</b>		yes
2I	Post-hoc	genotype (condition=1 h delay)	FA	WT,msi-1(ff);:no array	t	<b>10.26</b>	<b>62</b>	<b>5.4e-15</b>	<b>4.9e-14</b>	yes
2I	Post-hoc	genotype (condition=naive)	FA	msi-1(ff);:Exp[prnc-47::msi-1+],msi-1(ff);:no array	t	<b>0.32</b>	<b>55</b>	<b>0.75</b>		yes
2I	Post-hoc	genotype (condition=cond.)	FA	msi-1(ff);:Exp[prnc-47::msi-1+],msi-1(ff);:no array	t	<b>0.54</b>	<b>57</b>	<b>0.59</b>		yes
2I	Post-hoc	genotype (condition=1 h delay)	FA	msi-1(ff);:Exp[prnc-47::msi-1+],msi-1(ff);:no array	t	<b>0.8</b>	<b>55</b>	<b>0.43</b>		yes
2I	Post-hoc	genotype (condition=naive)	FA	WT,msi-1(ff);:Exp[prnc-47::msi-1+]	t	<b>5.2</b>	<b>53</b>	<b>0.0023</b>	<b>0.021</b>	yes
2I	Post-hoc	genotype (condition=cond.)	FA	WT,msi-1(ff);:Exp[prnc-47::msi-1+]	t	<b>0.3</b>	<b>57</b>	<b>0.76</b>		yes
2I	Post-hoc	genotype (condition=1 h delay)	FA	WT,msi-1(ff);:Exp[prnc-47::msi-1+]	t	<b>8.57</b>	<b>55</b>	<b>1e-11</b>	<b>9.3e-11</b>	yes
2J	Anova	condition	FA	naive,cond.,1 h delay	F	<b>2000.05</b>	2 288	<1e-16		yes
2J	Anova	genotype	FA	WT,msi-1(ff);:Exp[prig-3::msi-1+],msi-1(ff);:no array	F	<b>17.76</b>	2 288	<b>5.8e-08</b>		yes
2J	Anova	condition:genotype	FA		F	<b>28.18</b>	4 288	<1e-16		yes
2J	Post-hoc	genotype (condition=naive)	FA	WT,msi-1(ff);:no array	t	<b>4.06</b>	<b>73</b>	<b>0.00012</b>	<b>0.0011</b>	yes
2J	Post-hoc	genotype (condition=cond.)	FA	WT,msi-1(ff);:no array	t	<b>1.25</b>	<b>70</b>	<b>0.22</b>		yes
2J	Post-hoc	genotype (condition=1 h delay)	FA	WT,msi-1(ff);:no array	t	<b>10.7</b>	<b>73</b>	<b>1.3e-16</b>	<b>1.2e-15</b>	yes
2J	Post-hoc	genotype (condition=naive)	FA	msi-1(ff);:Exp[prig-3::msi-1+],msi-1(ff);:no array	t	<b>-1.77</b>	<b>56</b>	<b>0.082</b>	<b>0.73</b>	yes
2J	Post-hoc	genotype (condition=cond.)	FA	msi-1(ff);:Exp[prig-3::msi-1+],msi-1(ff);:no array	t	<b>-0.66</b>	<b>58</b>	<b>0.51</b>		yes
2J	Post-hoc	genotype (condition=1 h delay)	FA	msi-1(ff);:Exp[prig-3::msi-1+],msi-1(ff);:no array	t	<b>9.37</b>	<b>57</b>	<b>3.9e-13</b>	<b>3.5e-12</b>	yes
2J	Post-hoc	genotype (condition=naive)	FA	WT,msi-1(ff);:Exp[prig-3::msi-1+]	t	<b>4.44</b>	<b>63</b>	<b>3.7e-05</b>	<b>0.00033</b>	yes
2J	Post-hoc	genotype (condition=cond.)	FA	WT,msi-1(ff);:Exp[prig-3::msi-1+]	t	<b>1.53</b>	<b>62</b>	<b>0.13</b>		yes
2J	Post-hoc	genotype (condition=1 h delay)	FA	WT,msi-1(ff);:Exp[prig-3::msi-1+]	t	<b>2.53</b>	<b>64</b>	<b>0.014</b>	<b>0.13</b>	yes
2K	Anova	condition	FA	naive,cond.,1 h delay	F	<b>1467.08</b>	2 249	<1e-16		yes
2K	Anova	genotype	FA	WT,msi-1(ff);:Exp[plim-4::msi-1+],msi-1(ff);:no array	F	<b>12.85</b>	2 249	<b>4.8e-06</b>		yes
2K	Anova	condition:genotype	FA		F	<b>22.68</b>	4 249	<b>5.6e-16</b>		yes
2K	Post-hoc	genotype (condition=naive)	FA	WT,msi-1(ff);:no array	t	<b>3.9</b>	<b>59</b>	<b>0.00025</b>	<b>0.0022</b>	yes
2K	Post-hoc	genotype (condition=cond.)	FA	WT,msi-1(ff);:no array	t	<b>-0.65</b>	<b>56</b>	<b>0.52</b>		yes
2K	Post-hoc	genotype (condition=1 h delay)	FA	WT,msi-1(ff);:no array	t	<b>10.32</b>	<b>58</b>	<b>9.4e-15</b>	<b>8.4e-14</b>	yes
2K	Post-hoc	genotype (condition=naive)	FA	msi-1(ff);:Exp[plim-4::msi-1+],msi-1(ff);:no array	t	<b>-0.42</b>	<b>49</b>	<b>0.67</b>		yes
2K	Post-hoc	genotype (condition=cond.)	FA	msi-1(ff);:Exp[plim-4::msi-1+],msi-1(ff);:no array	t	<b>-0.61</b>	<b>51</b>	<b>0.55</b>		yes
2K	Post-hoc	genotype (condition=1 h delay)	FA	msi-1(ff);:Exp[plim-4::msi-1+],msi-1(ff);:no array	t	<b>7.03</b>	<b>50</b>	<b>5.4e-09</b>	<b>4.9e-08</b>	yes
2K	Post-hoc	genotype (condition=naive)	FA	WT,msi-1(ff);:Exp[plim-4::msi-1+]	t	<b>3.41</b>	<b>58</b>	<b>0.0012</b>	<b>0.011</b>	yes
2K	Post-hoc	genotype (condition=cond.)	FA	WT,msi-1(ff);:Exp[plim-4::msi-1+]	t	<b>0.08</b>	<b>57</b>	<b>0.93</b>		yes
2K	Post-hoc	genotype (condition=1 h delay)	FA	WT,msi-1(ff);:Exp[plim-4::msi-1+]	t	<b>3.01</b>	<b>60</b>	<b>0.0038</b>	<b>0.034</b>	yes
2L	Anova	condition	FA	naive,cond.,1 h delay	F	<b>4218.6</b>	2 205	<1e-16		yes
2L	Anova	genotype	FA	WT,msi-1(ff);:Exp[pmnr-1::msi-1+],msi-1(ff);:no array	F	<b>0.4</b>	2 205	<b>0.67</b>		yes
2L	Anova	condition:genotype	FA		F	<b>42.57</b>	4 205	<1e-16		yes
2L	Post-hoc	genotype (condition=naive)	FA	WT,msi-1(ff);:no array	t	<b>0.62</b>	<b>43</b>	<b>0.54</b>		yes
2L	Post-hoc	genotype (condition=cond.)	FA	WT,msi-1(ff);:no array	t	<b>-0.89</b>	<b>43</b>	<b>0.38</b>		yes
2L	Post-hoc	genotype (condition=1 h delay)	FA	WT,msi-1(ff);:no array	t	<b>16.19</b>	<b>43</b>	<b>6.6e-20</b>	<b>6e-19</b>	yes
2L	Post-hoc	genotype (condition=naive)	FA	msi-1(ff);:Exp[pmnr-1::msi-1+],msi-1(ff);:no array	t	<b>-0.52</b>	<b>51</b>	<b>0.61</b>		yes
2L	Post-hoc	genotype (condition=cond.)	FA	msi-1(ff);:Exp[pmnr-1::msi-1+],msi-1(ff);:no array	t	<b>0.82</b>	<b>51</b>	<b>0.42</b>		yes
2L	Post-hoc	genotype (condition=1 h delay)	FA	msi-1(ff);:Exp[pmnr-1::msi-1+],msi-1(ff);:no array	t	<b>-1</b>	<b>52</b>	<b>0.32</b>		yes
2L	Post-hoc	genotype (condition=naive)	FA	WT,msi-1(ff);:Exp[pmnr-1::msi-1+]	t	<b>0.84</b>	<b>42</b>	<b>0.41</b>		yes
2L	Post-hoc	genotype (condition=cond.)	FA	WT,msi-1(ff);:Exp[pmnr-1::msi-1+]	t	<b>-1.42</b>	<b>42</b>	<b>0.16</b>		yes
2L	Post-hoc	genotype (condition=1 h delay)	FA	WT,msi-1(ff);:Exp[pmnr-1::msi-1+]	t	<b>13.63</b>	<b>43</b>	<b>3.3e-17</b>	<b>2.9e-16</b>	yes

Abbreviations:

IN: integrer

FA: factor

df: degrees of freedom

var/dent: model calculated accounts for heterogeneity of variance

P-values represented on the figure are highlighted in bold.

Table S3: Statistical Results for Figure 3

Figure	Model	Condition.tested	Class	Levels	Test	Test.statistic	df	p.value	p.value.bonf	varIdent
3C	Anova	condition	FA	naive,cond.,30 min recovery,1 h recovery,starved,adapted	F	19.11	5 117	7.3e-14		
3C	Post-hoc	condition	FA	starved,naive	t	1.24	36	0.22	1	no
3C	Post-hoc	condition	FA	adapted,naive	t	1.16	37	0.25	1	no
3C	Post-hoc	condition	FA	cond.,naive	t	7.51	43	2.4e-09	1.2e-08	no
3C	Post-hoc	condition	FA	30 min recovery,naive	t	5.63	38	1.8e-06	9.2e-06	no
3C	Post-hoc	condition	FA	1 h recovery,naive	t	4.24	39	0.00013	0.00067	no
3D	Anova		FA	naive,cond.,30 min recovery,1 h recovery,starved,adapted	F	31.72	5 110	<1e-16		
3D	Post-hoc	condition	FA	starved,naive	t	0.75	38	0.46	1	no
3D	Post-hoc	condition	FA	adapted,naive	t	0.74	32	0.47	1	no
3D	Post-hoc	condition	FA	cond.,naive	t	8.86	37	1.1e-10	5.6e-10	no
3D	Post-hoc	condition	FA	30 min recovery,naive	t	6.83	37	4.7e-08	2.4e-07	no
3D	Post-hoc	condition	FA	1 h recovery,naive	t	5.21	34	9.1e-06	4.6e-05	no
3E	Anova		FA	naive,cond.,30 min recovery,1 h recovery,starved,adapted	F	18.73	5 114	1.50E-13		
3E	Post-hoc	condition	FA	starved,naive	t	0.84	41	0.41	1	no
3E	Post-hoc	condition	FA	adapted,naive	t	2.78	40	0.0082	0.041	no
3E	Post-hoc	condition	FA	cond.,naive	t	6.99	46	9.3e-09	4.7e-08	no
3E	Post-hoc	condition	FA	30 min recovery,naive	t	6.67	46	2.8e-08	1.4e-07	no
3E	Post-hoc	condition	FA	1 h recovery,naive	t	4.63	41	3.7e-05	0.00018	no
3F	Anova	condition	FA	naive,cond.,30 min recovery,1 h recovery,starved,adapted	F	0.14	5 115	0.98		no
3G	Anova	condition	FA	naive,cond.,30 min recovery,1 h recovery,adapted,starved	F	0.39	5 92	0.85		no

**Abbreviations:**

IN: integer

FA: factor

df: degrees of freedom

varIdent: model calculated accounts for heterogeneity of variance

P-values represented on the figure are highlighted in bold.

Table S4: Statistical Results for Figure 4

Figure	Model	Condition tested	Class	Levels	Test	Test statistic	df	p value	p value bonf	varIdent
4A	Anova	genotype	FA	WT, <i>msi-1(lf)</i> , <i>msi-1(lf)</i> cond, <i>msi-1(lf)</i> ; <i>ls[msi-1+cDNA]</i>	F	79.32	4 101	<1e-16		no
4A	Post-hoc	genotype	FA	<b><i>msi-1(lf)</i>,WT</b>	t	<b>-8.94</b>	<b>41</b>	<b>3.60E-11</b>	<b>2.50E-10</b>	<b>no</b>
4A	Post-hoc	genotype	FA	<i>msi-1(lf)</i> cond,WT	t	-7.19	36	1.80E-08	1.30E-07	no
4A	Post-hoc	genotype	FA	<b><i>msi-1(lf)</i>;ls[msi-1+cDNA],WT</b>	t	<b>-0.17</b>	<b>47</b>	<b>0.87</b>	<b>1</b>	<b>no</b>
4A	Post-hoc	genotype	FA	<i>msi-1(lf)</i> ;ls[msi-1+cDNA] cond,WT	t	8.09	34	2.00E-09	1.40E-08	no
4A	Post-hoc	genotype	FA	<b><i>msi-1(lf)</i> cond,msi-1(lf)</b>	t	<b>-4.43</b>	<b>39</b>	<b>0.67</b>	<b>1</b>	<b>no</b>
4A	Post-hoc	genotype	FA	<i>msi-1(lf)</i> ;ls[msi-1+cDNA], <i>msi-1(lf)</i>	t	9.08	50	3.70E-12	2.60E-11	no
4A	Post-hoc	genotype	FA	<b><i>msi-1(lf)</i>;ls[msi-1+cDNA] cond,msi-1(lf);ls[msi-1+cDNA]</b>	t	<b>8.4</b>	<b>43</b>	<b>1.30E-10</b>	<b>9.10E-10</b>	<b>no</b>
4B	Anova	genotype	FA	WT, <i>msi-1(lf)</i> , <i>msi-1(lf)</i> cond, <i>msi-1(lf)</i> ; <i>ls[msi-1+cDNA]</i>	F	102.31	4 104	<1e-16		no
4B	Post-hoc	genotype	FA	<b><i>msi-1(lf)</i>,WT</b>	t	<b>-8.41</b>	<b>38</b>	<b>3.40E-10</b>	<b>2.20E-09</b>	<b>no</b>
4B	Post-hoc	genotype	FA	<i>msi-1(lf)</i> cond,WT	t	-9.94	38	4.00E-12	2.80E-11	no
4B	Post-hoc	genotype	FA	<b><i>msi-1(lf)</i>;ls[msi-1+cDNA],WT</b>	t	<b>0.99</b>	<b>37</b>	<b>0.33</b>	<b>1</b>	<b>no</b>
4B	Post-hoc	genotype	FA	<i>msi-1(lf)</i> ;ls[msi-1+cDNA] cond,WT	t	7.85	42	9.20E-10	6.40E-09	no
4B	Post-hoc	genotype	FA	<b><i>msi-1(lf)</i> cond,msi-1(lf)</b>	t	<b>-1.08</b>	<b>42</b>	<b>0.28</b>	<b>1</b>	<b>no</b>
4B	Post-hoc	genotype	FA	<i>msi-1(lf)</i> ;ls[msi-1+cDNA], <i>msi-1(lf)</i>	t	8.36	41	2.20E-10	1.50E-09	no
4B	Post-hoc	genotype	FA	<b><i>msi-1(lf)</i>;ls[msi-1+cDNA] cond,msi-1(lf);ls[msi-1+cDNA]</b>	t	<b>5.95</b>	<b>45</b>	<b>3.70E-07</b>	<b>2.60E-06</b>	<b>no</b>
4C	Anova	genotype	FA	WT, <i>msi-1(lf)</i> , <i>msi-1(lf)</i> cond, <i>msi-1(lf)</i> ; <i>ls[msi-1+cDNA]</i>	F	73.69	4 130	<1e-16		yes
4C	Post-hoc	genotype	FA	<b><i>msi-1(lf)</i>,WT</b>	t	<b>-4</b>	<b>64</b>	<b>0.00016</b>	<b>0.0012</b>	<b>yes</b>
4C	Post-hoc	genotype	FA	<i>msi-1(lf)</i> cond,WT	t	-3.54	58	0.00081	0.0057	yes
4C	Post-hoc	genotype	FA	<b><i>msi-1(lf)</i>;ls[msi-1+cDNA],WT</b>	t	<b>2.06</b>	<b>67</b>	<b>0.044</b>	<b>0.3</b>	<b>yes</b>
4C	Post-hoc	genotype	FA	<i>msi-1(lf)</i> ;ls[msi-1+cDNA] cond,WT	t	8.58	70	1.60E-12	1.10E-11	yes
4C	Post-hoc	genotype	FA	<b><i>msi-1(lf)</i> cond,msi-1(lf)</b>	t	<b>0.71</b>	<b>36</b>	<b>0.48</b>	<b>1</b>	<b>yes</b>
4C	Post-hoc	genotype	FA	<i>msi-1(lf)</i> ;ls[msi-1+cDNA], <i>msi-1(lf)</i>	t	5.99	45	3.30E-07	2.30E-06	yes
4C	Post-hoc	genotype	FA	<b><i>msi-1(lf)</i>;ls[msi-1+cDNA] cond,msi-1(lf);ls[msi-1+cDNA]</b>	t	<b>7.33</b>	<b>51</b>	<b>1.60E-09</b>	<b>1.10E-08</b>	<b>yes</b>
4D	Anova	genotype	FA	WT, <i>msi-1(lf)</i> , <i>msi-1(lf)</i> cond, <i>msi-1(lf)</i> ; <i>ls[msi-1+cDNA]</i>	F	0.61	4 109	0.65		no
4E	Anova	genotype	FA	WT, <i>msi-1(lf)</i> , <i>msi-1(lf)</i> cond, <i>msi-1(lf)</i> ; <i>ls[msi-1+cDNA]</i>	F	0.48	4 84	0.75		no
4G	Anova	condition	FA	naive,cond, 1h delay no CHX, 1h delay with CHX	F	383.31	3 114	<1e-16		yes
4G	Anova	genotype	FA	WT, <i>msi-1(lf)</i> , <i>msi-1(lf)</i> ; <i>ls[msi-1+cDNA]</i>	F	3.81	2 114	0.025		yes
4G	Anova	condition:genotype	FA		F	11.11	6 114	9.80E-10		yes
4G	Post-hoc	genotype (condition=naive)	FA	<i>msi-1(lf)</i> ,WT	t	2.81	22	0.01	0.081	yes
4G	Post-hoc	genotype (condition=cond.)	FA	<i>msi-1(lf)</i> ,WT	t	0.26	22	0.79	1	yes
4G	Post-hoc	genotype (condition=1h delay no CHX)	FA	<b><i>msi-1(lf)</i>,WT</b>	t	<b>8.96</b>	<b>22</b>	<b>8.50E-09</b>	<b>6.80E-08</b>	<b>yes</b>
4G	Post-hoc	genotype (condition=1h delay with CHX)	FA	<b><i>msi-1(lf)</i>,WT</b>	t	<b>-0.78</b>	<b>16</b>	<b>0.44</b>	<b>1</b>	<b>yes</b>
4G	Post-hoc	genotype (condition=naive)	FA	<i>msi-1(lf)</i> ;ls[msi-1+cDNA],WT	t	4.26	22	0.00032	0.0025	yes
4G	Post-hoc	genotype (condition=cond.)	FA	<i>msi-1(lf)</i> ;ls[msi-1+cDNA],WT	t	-0.36	22	0.72	1	yes
4G	Post-hoc	genotype (condition=1h delay no CHX)	FA	<i>msi-1(lf)</i> ;ls[msi-1+cDNA],WT	t	0.31	22	0.76	1	yes
4G	Post-hoc	genotype (condition=1h delay with CHX)	FA	<i>msi-1(lf)</i> ;ls[msi-1+cDNA],WT	t	1.2	16	0.25	1	yes
4H	Anova	genotype	FA	1h delay no CHX, 1h delay with CHX,cond. no CHX,cond. with CHX,naive no CHX,naive with CHX	F	328.83	5 174	<1e-16		yes
4H	Anova	genotype	FA	WT, <i>msi-1(lf)</i> , <i>msi-1(lf)</i> ; <i>ls[msi-1+cDNA]</i>	F	8.52	2 174	0.00029		yes
4H	Anova	condition:genotype	FA		F	7.77	10 174	3.10E-10		yes
4H	Post-hoc	genotype (condition=1h delay no CHX)	FA	<b><i>msi-1(lf)</i>,WT</b>	t	<b>11.65</b>	<b>22</b>	<b>7.00E-11</b>	<b>1.00E-09</b>	<b>yes</b>
4H	Post-hoc	genotype (condition=1h delay with CHX)	FA	<b><i>msi-1(lf)</i>,WT</b>	t	<b>2.06</b>	<b>22</b>	<b>0.051</b>	<b>0.77</b>	<b>yes</b>
4H	Post-hoc	genotype (condition=cond. no CHX)	FA	<i>msi-1(lf)</i> ,WT	t	-0.93	22	0.36	1	yes
4H	Post-hoc	genotype (condition=cond. with CHX)	FA	<b><i>msi-1(lf)</i>,WT</b>	t	<b>1.08</b>	<b>22</b>	<b>0.29</b>	<b>1</b>	<b>yes</b>
4H	Post-hoc	genotype (condition=naive no CHX)	FA	<i>msi-1(lf)</i> ,WT	t	2.26	22	0.034	0.51	yes
4H	Post-hoc	genotype (condition=naive with CHX)	FA	<i>msi-1(lf)</i> ,WT	t	1.18	16	0.26	1	yes
4H	Post-hoc	genotype (condition=1h delay no CHX)	FA	<i>msi-1(lf)</i> ;ls[msi-1+cDNA], <i>msi-1(lf)</i>	t	-6.52	19	3.00E-06	4.50E-05	yes
4H	Post-hoc	genotype (condition=1h delay with CHX)	FA	<i>msi-1(lf)</i> ;ls[msi-1+cDNA], <i>msi-1(lf)</i>	t	-1.45	19	0.16	1	yes
4H	Post-hoc	genotype (condition=cond. no CHX)	FA	<i>msi-1(lf)</i> ;ls[msi-1+cDNA], <i>msi-1(lf)</i>	t	1.21	19	0.24	1	yes
4H	Post-hoc	genotype (condition=cond. with CHX)	FA	<i>msi-1(lf)</i> ;ls[msi-1+cDNA], <i>msi-1(lf)</i>	t	-0.41	19	0.69	1	yes
4H	Post-hoc	genotype (condition=naive no CHX)	FA	<i>msi-1(lf)</i> ;ls[msi-1+cDNA], <i>msi-1(lf)</i>	t	-2.36	19	0.029	0.44	yes
4H	Post-hoc	genotype (condition=naive with CHX)	FA	<i>msi-1(lf)</i> ;ls[msi-1+cDNA], <i>msi-1(lf)</i>	t	-2.06	16	0.056	0.84	yes
4H	Post-hoc	condition (genotype=WT)	FA	<b>cond. no CHX,cond. with CHX</b>	t	<b>-5.09</b>	<b>22</b>	<b>4.20E-05</b>	<b>0.00064</b>	<b>yes</b>
4H	Post-hoc	condition (genotype= <i>msi-1(lf)</i> )	FA	cond. no CHX,cond. with CHX	t	-6.89	22	6.40E-07	9.50E-06	yes
4H	Post-hoc	condition (genotype= <i>msi-1(lf)</i> ;ls[msi-1+cDNA])	FA	cond. no CHX,cond. with CHX	t	-5.56	16	4.30E-05	0.00064	yes

## Abbreviations:

IX: integrer

FA: factor

df: degrees of freedom

varIdent: model calculated accounts for heterogeneity of variance

P-values represented on the figure are highlighted in bold.

Table S5: Statistical Results for Figure 5

Figure	Model	Condition tested	Class	Levels	Test	Test statistic	df	p value	p value bonf	varIdent	
5A	<i>nre-1 lin15b</i>	treatment	FA	<i>gfp1,arx-2i</i>	F	0.17	1164	0.688		no	
5A	<i>nre-1 lin15b</i>	condition	FA	naive,cond_1 h delay	F	<b>000.01</b>	2164	<1e-16		no	
5A	<i>nre-1 lin15b</i>	treatment condition	FA		F	<b>0.28</b>	2164	<b>0.76</b>		no	
5A	<i>msi-1(lf);nre-1 lin15b</i>	treatment	FA	<i>gfp1,arx-2i</i>	F	6.07	1164	<b>0.016</b>		no	
5A	<i>msi-1(lf);nre-1 lin15b</i>	condition	FA	naive,cond_1 h delay	F	<b>197.45</b>	2164	<1e-16		no	
5A	<i>msi-1(lf);nre-1 lin15b</i>	treatment condition	FA		F	<b>10.27</b>	2164	<b>0.00014</b>		no	
5A	<i>msi-1(lf);nre-1 lin15b</i>	Post-hoc	treatment (condition=naive)	FA	<i>arx-2i;gfp1</i>	t	<b>0.69</b>	<b>72</b>	<b>0.5</b>	<b>7</b>	no
5A	<i>msi-1(lf);nre-1 lin15b</i>	Post-hoc	treatment (condition=cond)	FA	<i>arx-2i;gfp1</i>	t	1.31	21	0.2	0.61	no
5A	<i>msi-1(lf);nre-1 lin15b</i>	Post-hoc	treatment (condition=1h delay)	FA	<i>arx-2i;gfp1</i>	t	<b>-4.66</b>	<b>21</b>	<b>0.00014</b>	<b>0.00041</b>	<b>no</b>
5B	<i>nre-1 lin15b</i>	treatment	FA	<i>gfp1,arx-1i,arx-3i,arx-4i,arx-6i</i>	F	3.48	4112	0.0099		no	
5B	<i>nre-1 lin15b</i>	condition	FA	naive,cond_1 h delay	F	307.73	2112	<1e-16		no	
5B	<i>nre-1 lin15b</i>	treatment condition	FA		F	2.25	8112	0.029		no	
5B	<i>msi-1(lf);nre-1 lin15b</i>	treatment	FA	<i>gfp1,arx-1i,arx-3i,arx-4i,arx-6i</i>	F	4.17	498	0.0035		no	
5B	<i>msi-1(lf);nre-1 lin15b</i>	condition	FA	naive,cond_1 h delay	F	290.82	298	<1e-16		no	
5B	<i>msi-1(lf);nre-1 lin15b</i>	treatment condition	FA		F	2.56	898	0.014		no	
5B	<i>msi-1(lf);nre-1 lin15b</i>	Post-hoc	treatment (condition=naive)	FA	<i>arx-1i;gfp1</i>	t	-2.06	14	0.058	0.7	no
5B	<i>msi-1(lf);nre-1 lin15b</i>	Post-hoc	treatment (condition=cond)	FA	<i>arx-1i;gfp1</i>	t	-0.48	13	0.64		no
5B	<i>msi-1(lf);nre-1 lin15b</i>	Post-hoc	treatment (condition=1h delay)	FA	<i>arx-1i;gfp1</i>	t	<b>-4.43</b>	<b>11</b>	<b>0.001</b>	<b>0.012</b>	<b>no</b>
5B	<i>msi-1(lf);nre-1 lin15b</i>	Post-hoc	treatment (condition=naive)	FA	<i>arx-1i;gfp1</i>	t	-0.7	14	0.49	1	no
5B	<i>msi-1(lf);nre-1 lin15b</i>	Post-hoc	treatment (condition=cond)	FA	<i>arx-1i;gfp1</i>	t	0.02	14	0.98	1	no
5B	<i>msi-1(lf);nre-1 lin15b</i>	Post-hoc	treatment (condition=1h delay)	FA	<i>arx-1i;gfp1</i>	t	<b>-5.35</b>	<b>12</b>	<b>0.00017</b>	<b>0.0021</b>	<b>no</b>
5B	<i>msi-1(lf);nre-1 lin15b</i>	Post-hoc	treatment (condition=naive)	FA	<i>arx-1i;gfp1</i>	t	-2.37	13	0.034	0.41	no
5B	<i>msi-1(lf);nre-1 lin15b</i>	Post-hoc	treatment (condition=cond)	FA	<i>arx-1i;gfp1</i>	t	0.69	14	0.5	1	no
5B	<i>msi-1(lf);nre-1 lin15b</i>	Post-hoc	treatment (condition=1h delay)	FA	<i>arx-1i;gfp1</i>	t	<b>-4.6</b>	<b>11</b>	<b>0.00076</b>	<b>0.0092</b>	<b>no</b>
5B	<i>msi-1(lf);nre-1 lin15b</i>	Post-hoc	treatment (condition=naive)	FA	<i>arx-1i;gfp1</i>	t	-0.88	14	0.39	1	no
5B	<i>msi-1(lf);nre-1 lin15b</i>	Post-hoc	treatment (condition=cond)	FA	<i>arx-1i;gfp1</i>	t	-0.14	14	0.89	1	no
5B	<i>msi-1(lf);nre-1 lin15b</i>	Post-hoc	treatment (condition=1h delay)	FA	<i>arx-1i;gfp1</i>	t	<b>-4.01</b>	<b>11</b>	<b>0.002</b>	<b>0.025</b>	<b>no</b>
5C	<i>msi-1(lf);nre-1 lin15b</i>	treatment	FA	<i>gfp1,wsp-1i</i>	F	14.15	190	3e-04		no	
5C	<i>msi-1(lf);nre-1 lin15b</i>	condition	FA	naive,cond_1 h delay	F	160.87	290	<1e-16		no	
5C	<i>msi-1(lf);nre-1 lin15b</i>	treatment condition	FA		F	4.52	290	0.013		no	
5C	<i>msi-1(lf);nre-1 lin15b</i>	Post-hoc	treatment (condition=naive)	FA	<i>gfp1,wsp-1i</i>	t	-1.87	31	0.071	0.21	no
5C	<i>msi-1(lf);nre-1 lin15b</i>	Post-hoc	treatment (condition=cond)	FA	<i>gfp1,wsp-1i</i>	t	-0.24	29	0.81	1	no
5C	<i>msi-1(lf);nre-1 lin15b</i>	Post-hoc	treatment (condition=1h delay)	FA	<i>gfp1,wsp-1i</i>	t	<b>-5.33</b>	<b>30</b>	<b>9.10E-06</b>	<b>2.70E-05</b>	<b>no</b>
5C	<i>nre-1 lin15b</i>	treatment	FA	<i>gfp1,wsp-1i</i>	F	4.53	188	0.036		no	
5C	<i>nre-1 lin15b</i>	condition	FA	naive,cond_1 h delay	F	130.72	288	<1e-16		no	
5C	<i>nre-1 lin15b</i>	treatment condition	FA		F	0.27	288	0.77		no	
5D	Anova	condition	FA	naive,cond_1 h delay	F	725.86	2200	<1e-16		no	
5D	Anova	genotype	FA	WT, <i>msi-1(lf);msi-1(lf);Exp[plm-4::wsp-1 VCA],no array</i>	F	11.92	3200	3.10E-07		no	
5D	Anova	condition genotype	FA		F	22.39	6200	<1e-16		no	
5D	Post-hoc	genotype (condition=naive)	FA	WT, <i>msi-1(lf)</i>	t	4.45	25	0.00016	0.0019	no	
5D	Post-hoc	genotype (condition=cond)	FA	WT, <i>msi-1(lf)</i>	t	0.63	25	0.53	1	no	
5D	Post-hoc	genotype (condition=1h delay)	FA	WT, <i>msi-1(lf)</i>	t	6.25	25	1.80E-06	1.80E-05	no	
5D	Post-hoc	genotype (condition=naive)	FA	WT, <i>msi-1(lf);Exp[plm-4::wsp-1 VCA]</i>	t	1.28	31	0.21	1	no	
5D	Post-hoc	genotype (condition=cond)	FA	WT, <i>msi-1(lf);Exp[plm-4::wsp-1 VCA]</i>	t	-1.81	31	0.08	0.96	no	
5D	Post-hoc	genotype (condition=1h delay)	FA	WT, <i>msi-1(lf);Exp[plm-4::wsp-1 VCA]</i>	t	<b>4.78</b>	<b>30</b>	<b>4.40E-05</b>	<b>0.0052</b>	<b>no</b>	
5D	Post-hoc	genotype (condition=naive)	FA	no array,WT	t	4.76	39	2.70E-05	0.00032	no	
5D	Post-hoc	genotype (condition=cond)	FA	no array,WT	t	0.52	39	0.6		no	
5D	Post-hoc	genotype (condition=1h delay)	FA	no array,WT	t	<b>-2.07</b>	<b>39</b>	<b>0.045</b>	<b>0.54</b>	<b>no</b>	
5D	Post-hoc	genotype (condition=naive)	FA	<i>msi-1(lf);msi-1(lf);Exp[plm-4::wsp-1 VCA]</i>	t	-3.48	28	0.0017	0.02	no	
5D	Post-hoc	genotype (condition=cond)	FA	<i>msi-1(lf);msi-1(lf);Exp[plm-4::wsp-1 VCA]</i>	t	-2.83	28	0.0086	0.1	no	
5D	Post-hoc	genotype (condition=1h delay)	FA	<i>msi-1(lf);msi-1(lf);Exp[plm-4::wsp-1 VCA]</i>	t	-0.73	27	0.47	1	no	
5E	Anova	condition	FA	naive,cond_1 h delay	F	831.04	2192	<1e-16		no	
5E	Anova	genotype	FA	WT, <i>msi-1(lf);msi-1(lf);Exp[prig-3::wsp-1 VCA],no array</i>	F	12.75	3192	1.20E-07		no	
5E	Anova	condition genotype	FA		F	10.64	6192	3.40E-10		no	
5E	Post-hoc	genotype (condition=naive)	FA	WT, <i>msi-1(lf)</i>	t	3.09	22	0.0054	0.064	no	
5E	Post-hoc	genotype (condition=cond)	FA	WT, <i>msi-1(lf)</i>	t	1.03	22	0.31	1	no	
5E	Post-hoc	genotype (condition=1h delay)	FA	WT, <i>msi-1(lf)</i>	t	6.97	22	5.40E-07	6.50E-06	no	
5E	Post-hoc	genotype (condition=naive)	FA	WT, <i>msi-1(lf);Exp[prig-3::wsp-1 VCA]</i>	t	0.47	28	0.64	1	no	
5E	Post-hoc	genotype (condition=cond)	FA	WT, <i>msi-1(lf);Exp[prig-3::wsp-1 VCA]</i>	t	-0.45	28	0.65	1	no	
5E	Post-hoc	genotype (condition=1h delay)	FA	WT, <i>msi-1(lf);Exp[prig-3::wsp-1 VCA]</i>	t	<b>3.83</b>	<b>28</b>	<b>0.00066</b>	<b>0.0079</b>	<b>no</b>	
5E	Post-hoc	genotype (condition=naive)	FA	no array,WT	t	3.04	36	0.0044	0.053	no	
5E	Post-hoc	genotype (condition=cond)	FA	no array,WT	t	0.06	36	0.96	1	no	
5E	Post-hoc	genotype (condition=1h delay)	FA	no array,WT	t	<b>-0.81</b>	<b>36</b>	<b>0.42</b>	<b>1</b>	<b>no</b>	
5E	Post-hoc	genotype (condition=naive)	FA	<i>msi-1(lf);msi-1(lf);Exp[prig-3::wsp-1 VCA]</i>	t	-2.19	28	0.037	0.44	no	
5E	Post-hoc	genotype (condition=cond)	FA	<i>msi-1(lf);msi-1(lf);Exp[prig-3::wsp-1 VCA]</i>	t	-1.64	28	0.11	1	no	
5E	Post-hoc	genotype (condition=1h delay)	FA	<i>msi-1(lf);msi-1(lf);Exp[prig-3::wsp-1 VCA]</i>	t	-2.17	28	0.039	0.46	no	
5F	Anova	condition	FA	naive,cond_1 h delay	F	493.62	295	<1e-16		no	
5F	Anova	genotype	FA	WT, <i>msi-1(lf);add-1(lf);add-1(lf);msi-1(lf)</i>	F	14.92	395	4.10E-08		no	
5F	Anova	condition genotype	FA		F	11.01	695	2.80E-09		no	
5F	Post-hoc	genotype (condition=naive)	FA	WT, <i>msi-1(lf)</i>	t	3.56	16	0.0026	0.031	no	
5F	Post-hoc	genotype (condition=cond)	FA	WT, <i>msi-1(lf)</i>	t	2.03	16	0.059	0.71	no	
5F	Post-hoc	genotype (condition=1h delay)	FA	WT, <i>msi-1(lf)</i>	t	6.43	15	1.10E-05	0.00014	no	
5F	Post-hoc	genotype (condition=naive)	FA	WT, <i>add-1(lf)</i>	t	2.81	16	0.013	0.15	no	
5F	Post-hoc	genotype (condition=cond)	FA	WT, <i>add-1(lf)</i>	t	1.76	16	0.098	1	no	
5F	Post-hoc	genotype (condition=1h delay)	FA	WT, <i>add-1(lf)</i>	t	<b>-5.26</b>	<b>15</b>	<b>9.70E-05</b>	<b>0.0012</b>	<b>no</b>	
5F	Post-hoc	genotype (condition=naive)	FA	WT, <i>msi-1(lf);add-1(lf)</i>	t	4.28	16	0.00058	0.0069	no	
5F	Post-hoc	genotype (condition=cond)	FA	WT, <i>msi-1(lf);add-1(lf)</i>	t	2.2	16	0.043	0.51	no	
5F	Post-hoc	genotype (condition=1h delay)	FA	WT, <i>msi-1(lf);add-1(lf)</i>	t	1.22	15	0.24	1	no	
5F	Post-hoc	genotype (condition=naive)	FA	<i>add-1(lf);msi-1(lf);add-1(lf)</i>	t	1.63	16	0.12	1	no	
5F	Post-hoc	genotype (condition=cond)	FA	<i>add-1(lf);msi-1(lf);add-1(lf)</i>	t	0.82	16	0.43	1	no	
5F	Post-hoc	genotype (condition=1h delay)	FA	<i>add-1(lf);msi-1(lf);add-1(lf)</i>	t	<b>6.92</b>	<b>16</b>	<b>3.50E-06</b>	<b>4.10E-05</b>	<b>no</b>	
5G	Anova	genotype	FA	WT, <i>msi-1(lf);gfr-1(lf);msi-1(lf);gfr-1(lf);gfr-1(lf);msl25;gfr-1(lf);Exp[prig-3::GFPhp];msi-1(lf);gfr-1(lf);gfr-1(lf);msl25;msi-1(lf);gfr-1(lf);Exp[prig-3::GFPhp]</i>	F	10.38	7241	1.90E-11		yes	
5G	Anova	condition	FA	naive,cond_1 h delay	F	1754.81	2241	<1e-16		yes	
5G	Anova	genotype condition	FA		F	31.01	14241	<1e-16		yes	
5G	Post-hoc	genotype (condition=naive)	FA	WT, <i>gfr-1(lf)</i>	t	0.14	21	0.89	1	yes	
5G	Post-hoc	genotype (condition=cond)	FA	WT, <i>gfr-1(lf)</i>	t	<b>-8.95</b>	<b>21</b>	<b>1.30E-08</b>	<b>1.90E-07</b>	<b>yes</b>	
5G	Post-hoc	genotype (condition=1h delay)	FA	WT, <i>gfr-1(lf)</i>	t	-2.19	22	0.039	0.59	yes	
5G	Post-hoc	genotype (condition=naive)	FA	<i>gfr-1(lf);msi-1(lf);gfr-1(lf)</i>	t	2.02	14	0.063	0.95	yes	
5G	Post-hoc	genotype (condition=cond)	FA	<i>gfr-1(lf);msi-1(lf);gfr-1(lf)</i>	t	1.62	14	0.13	1	yes	
5G	Post-hoc	genotype (condition=1h delay)	FA	<i>gfr-1(lf);msi-1(lf);gfr-1(lf)</i>	t	-0.78	14	0.45	1	yes	
5G	Post-hoc	genotype (condition=naive)	FA	WT, <i>gfr-1(lf);msl25</i>	t	-0.48	23	0.63	1	yes	
5G	Post-hoc	genotype (condition=cond)	FA	WT, <i>gfr-1(lf);msl25</i>	t	-0.09	23	0.93	1	yes	
5G	Post-hoc	genotype (condition=1h delay)	FA	WT, <i>gfr-1(lf);msl25</i>	t	<b>0.22</b>	<b>23</b>	<b>0.82</b>	<b>1</b>	<b>yes</b>	
5G	Post-hoc	genotype (condition=naive)	FA	<i>gfr-1(lf);Exp[prig-3::GFPhp];gfr-1(lf);msl25</i>	t	-0.36	21	0.72	1	yes	
5G	Post-hoc	genotype (condition=cond)	FA	<i>gfr-1(lf);Exp[prig-3::GFPhp];gfr-1(lf);msl25</i>	t	0.71	21	0.48	1	yes	
5G	Post-hoc	genotype (condition=1h delay)	FA	<i>gfr-1(lf);Exp[prig-3::GFPhp];gfr-1(lf);msl25</i>	t	<b>-5.44</b>	<b>21</b>	<b>2.10E-05</b>	<b>0.00032</b>	<b>yes</b>	
5G	Post-hoc	genotype (condition=naive)	FA	<i>gfr-1(lf);Exp[prig-3::GFPhp];msi-1(lf);gfr-1(lf);Exp[prig-3::GFPhp]</i>	t	2.17	28	0.039	0.58	yes	
5G</											

Table S6: Statistical Results for Figure 6

Figure	Model	Condition tested	Class	Levels	Test	Test statistic	df	p value	p value bonf	varIdent
6A	Anova	condition	FA	naive,cond,2 h delay	F	12.48	2 80	1.8e-05		yes
6A	Anova	genotype	FA	WT,msi-1(ff),msi-1(ff);ls[msi-1+cDNA]	F	26.37	2 80	1.3e-09		yes
6A	Anova	condition:genotype	FA		F	3.74	4 80	0.0077		yes
6A	Post-hoc	condition	FA	naive,cond.	t	5.75	58	3.4e-07	2.4e-06	yes
6A	Post-hoc	genotype (condition=naive)	FA	WT,msi-1(ff)	t	0	16	1	1	yes
6A	Post-hoc	genotype (condition=cond.)	FA	WT,msi-1(ff)	t	0.17	22	0.87	1	yes
6A	Post-hoc	genotype (condition=2 h delay)	FA	WT,msi-1(ff)	t	6.78	16	4.5e-06	3.1e-05	yes
6A	Post-hoc	genotype (condition=naive)	FA	msi-1(ff);ls[msi-1+cDNA];msi-1(ff)	t	0.18	16	0.86	1	yes
6A	Post-hoc	genotype (condition=cond.)	FA	msi-1(ff);ls[msi-1+cDNA];msi-1(ff)	t	0.37	21	0.71	1	yes
6A	Post-hoc	genotype (condition=2 h delay)	FA	msi-1(ff);ls[msi-1+cDNA];msi-1(ff)	t	7.05	16	2.8e-06	1.9e-05	yes
6B naive	Anova	treatment	FA	DMSO,5 µM,10 µM	F	0.22	2 90	0.81		no
6B naive	Anova	genotype	FA	WT,msi-1(ff),msi-1(ff);ls[msi-1+cDNA]	F	10.56	2 90	7.3e-05		no
6B naive	Anova	treatment:genotype	FA		F	0.14	4 90	0.97		no
6B conditioned	Anova	treatment	FA	DMSO,5 µM,10 µM	F	2.2	2 85	0.12		yes
6B conditioned	Anova	genotype	FA	WT,msi-1(ff),msi-1(ff);ls[msi-1+cDNA]	F	5.25	2 85	0.007		yes
6B conditioned	Anova	treatment:genotype	FA		F	1.18	4 85	0.33		yes
6B 1h delay	Anova	treatment	FA	DMSO,5 µM,10 µM	F	1.95	2 90	0.15		yes
6B 1h delay	Anova	genotype	FA	WT,msi-1(ff),msi-1(ff);ls[msi-1+cDNA]	F	18.16	2 90	2.2e-07		yes
6B 1h delay	Anova	treatment:genotype	FA		F	8.82	4 90	4.7e-06		yes
6B 1h delay	Post-hoc	treatment (genotype=WT)	FA	5 µM,DMSO	t	0.18	22	0.86	1	yes
6B 1h delay	Post-hoc	treatment (genotype=msi-1(ff))	FA	5 µM,DMSO	t	6.01	22	4.8e-06	4.3e-05	yes
6B 1h delay	Post-hoc	treatment (genotype=msi-1(ff);ls[msi-1+cDNA])	FA	5 µM,DMSO	t	0.1	16	0.92	1	yes
6B 1h delay	Post-hoc	treatment (genotype=WT)	FA	10 µM,DMSO	t	0.68	22	0.5	1	yes
6B 1h delay	Post-hoc	treatment (genotype=msi-1(ff))	FA	10 µM,DMSO	t	6.91	22	6.1e-07	5.5e-06	yes
6B 1h delay	Post-hoc	treatment (genotype=msi-1(ff);ls[msi-1+cDNA])	FA	10 µM,DMSO	t	0.08	16	0.94	1	yes
6B 1h delay	Post-hoc	treatment (genotype=WT)	FA	5 µM,10 µM	t	0.67	22	0.51	1	yes
6B 1h delay	Post-hoc	treatment (genotype=msi-1(ff))	FA	5 µM,10 µM	t	-0.64	22	0.53	1	yes
6B 1h delay	Post-hoc	treatment (genotype=msi-1(ff);ls[msi-1+cDNA])	FA	5 µM,10 µM	t	-0.02	16	0.98	1	yes
6C	Anova	condition	FA	1 h delay 10 µM,1 h delay 5 µM,1 h delay DMSO,cond,naive	F	264.46	4 120	<1e-16		yes
6C	Anova	genotype	FA	WT,msi-1(ff),msi-1(ff);ls[msi-1+cDNA]	F	5.68	2 120	0.0043		yes
6C	Anova	condition:genotype	FA		F	12.04	8 120	1.6e-12		yes
6C	Post-hoc	condition (genotype=WT)	FA	1 h delay 5 µM,1 h delay DMSO	t	1.06	16	0.31	1	yes
6C	Post-hoc	condition (genotype=msi-1(ff))	FA	1 h delay 5 µM,1 h delay DMSO	t	7.87	16	6.8e-07	6.1e-06	yes
6C	Post-hoc	condition (genotype=msi-1(ff);ls[msi-1+cDNA])	FA	1 h delay 5 µM,1 h delay DMSO	t	0.39	16	0.7	1	yes
6C	Post-hoc	condition (genotype=WT)	FA	1 h delay 10 µM,1 h delay DMSO	t	0.75	16	0.46	1	yes
6C	Post-hoc	condition (genotype=msi-1(ff))	FA	1 h delay 10 µM,1 h delay DMSO	t	8.52	16	2.4e-07	2.2e-06	yes
6C	Post-hoc	condition (genotype=msi-1(ff);ls[msi-1+cDNA])	FA	1 h delay 10 µM,1 h delay DMSO	t	-0.02	16	0.99	1	yes
6C	Post-hoc	condition (genotype=WT)	FA	1 h delay 5 µM,1 h delay 10 µM	t	-0.47	16	0.64	1	yes
6C	Post-hoc	condition (genotype=msi-1(ff))	FA	1 h delay 5 µM,1 h delay 10 µM	t	2.23	16	0.041	0.37	yes
6C	Post-hoc	condition (genotype=msi-1(ff);ls[msi-1+cDNA])	FA	1 h delay 5 µM,1 h delay 10 µM	t	-0.37	16	0.72	1	yes
6D	Anova	condition	FA	24 h delay ARP2/3 inh 1,24 h delay DMSO 1,cond. 0,naive 0	F	188.33	3 95	<1e-16		no
6D	Anova	genotype	FA	WT,msi-1(ff),msi-1(ff);ls[msi-1+cDNA]	F	16.96	2 95	4.5e-07		no
6D	Anova	condition:genotype	FA		F	18.32	6 95	5e-14		no
6D	Post-hoc	condition (genotype=WT)	FA	24 h delay ARP2/3 inh 1,24 h delay DMSO 1	t	-0.75	16	0.47	1	no
6D	Post-hoc	condition (genotype=msi-1(ff))	FA	24 h delay ARP2/3 inh 1,24 h delay DMSO 1	t	7.89	16	6.6e-07	2e-06	no
6D	Post-hoc	condition (genotype=msi-1(ff);ls[msi-1+cDNA])	FA	24 h delay ARP2/3 inh 1,24 h delay DMSO 1	t	-0.97	16	0.35	1	no

Abbreviations:

*lf*: integer

*FA*: factor

*df*: degrees of freedom

*varIdent*: model calculated accounts for heterogeneity of variance

*P-values* represented on the figure are highlighted in **bold**.

Table S7: Statistical Results for Figure 7

Figure	Model	Condition tested	Class	Levels	Test	Test statistic	df	p value	p.value bonf	varIdent
7A	Anova	condition	FA	naive,cond.,3h,6h,12h,24h	F	43.45	514599	<1e-16		yes
7A	Anova	genotype	FA	nuls25,nuls25;msi-1(f),nuls25	F	9.98	214599	2.3e-09		yes
7A	Anova	condition:genotype	FA	msi-1(f);ls[msi-1+cDNA]	F	5.8	1014599	4e-05		yes
7A	Post-hoc	genotype (condition=naive)	FA	nuls25;msi-1(f),nuls25	t	0.41	839	0.68	1	yes
7A	Post-hoc	genotype (condition=cond.)	FA	nuls25;msi-1(f),nuls25	t	0.15	868	0.88	1	yes
7A	Post-hoc	genotype (condition=30)	FA	nuls25;msi-1(f),nuls25	t	0.98	278	0.33	1	yes
7A	Post-hoc	genotype (condition=60)	FA	nuls25;msi-1(f),nuls25	t	1.48	302	0.14	1	yes
7A	Post-hoc	genotype (condition=120)	FA	nuls25;msi-1(f),nuls25	t	4.77	569	2.3e-06	2.8e-05	yes
7A	Post-hoc	genotype (condition=240)	FA	nuls25;msi-1(f),nuls25	t	5.52	625	5.1e-08	6.1e-07	yes
7A	Post-hoc	genotype (condition=naive)	FA	nuls25 msi-1(f);ls[msi-1+cDNA],nuls25	t	0.18	627	0.86	1	yes
7A	Post-hoc	genotype (condition=cond.)	FA	nuls25 msi-1(f);ls[msi-1+cDNA],nuls25	t	0.38	735	0.7	1	yes
7A	Post-hoc	genotype (condition=30)	FA	nuls25 msi-1(f);ls[msi-1+cDNA],nuls25	t	0.18	203	0.86	1	yes
7A	Post-hoc	genotype (condition=60)	FA	nuls25 msi-1(f);ls[msi-1+cDNA],nuls25	t	0.06	249	0.96	1	yes
7A	Post-hoc	genotype (condition=120)	FA	nuls25 msi-1(f);ls[msi-1+cDNA],nuls25	t	0.65	512	0.51	1	yes
7A	Post-hoc	genotype (condition=240)	FA	nuls25 msi-1(f);ls[msi-1+cDNA],nuls25	t	0.99	567	0.32	1	yes
7B nuls25	Anova	treatment	FA	DMSO,ARP2/3 inh	F	0.06	111305	0.8		no
7B nuls25	Anova	condition	FA	naive,cond.,2h rec,4h rec	F	22.1	311305	5.8e-14		no
7B nuls25	Anova	treatment:condition	F		F	0.83	311305	0.48		no
7B nuls25	Post-hoc	treatment (condition=naive)	FA	ARP2/3 inh,DMSO	t	1.38	401	0.17	0.67	no
7B nuls25	Post-hoc	treatment (condition=cond.)	FA	ARP2/3 inh,DMSO	t	0.45	546	0.65	1	no
7B nuls25	Post-hoc	treatment (condition=2h rec)	FA	ARP2/3 inh,DMSO	t	0.24	285	0.81	1	no
7B nuls25	Post-hoc	treatment (condition=4h rec)	FA	ARP2/3 inh,DMSO	t	0.47	273	0.64	1	no
7B nuls25;msi-1(f)	Anova	treatment	FA	DMSO,ARP2/3 inh	F	22.04	11940	5.1e-06		no
7B nuls25;msi-1(f)	Anova	condition	FA	naive,cond.,2h rec,4h rec	F	13.44	31940	7.4e-08		no
7B nuls25;msi-1(f)	Anova	treatment:condition	F		F	5.12	31940	0.0016		no
7B nuls25;msi-1(f)	Post-hoc	treatment (condition=naive)	FA	ARP2/3 inh,DMSO	t	1.13	216	0.26	1	no
7B nuls25;msi-1(f)	Post-hoc	treatment (condition=cond.)	FA	ARP2/3 inh,DMSO	t	0.36	238	0.72	1	no
7B nuls25;msi-1(f)	Post-hoc	treatment (condition=2h rec)	FA	ARP2/3 inh,DMSO	t	4.41	224	1.6e-05	6.3e-05	no
7B nuls25;msi-1(f)	Post-hoc	treatment (condition=4h rec)	FA	ARP2/3 inh,DMSO	t	4.24	262	3.1e-05	0.00013	no
7B nuls25;msi-1(f);ls[msi-1+]	Anova	treatment	FA	DMSO,ARP2/3 inh	F	0.84	111266	0.36		no
7B nuls25;msi-1(f);ls[msi-1+]	Anova	condition	FA	naive,cond.,2h rec,4h rec	F	11.73	311266	1.4e-07		no
7B nuls25;msi-1(f);ls[msi-1+]	Anova	treatment:condition	F		F	0.06	311266	0.98		no
7B nuls25;msi-1(f);ls[msi-1+]	Post-hoc	treatment (condition=naive)	FA	ARP2/3 inh,DMSO	t	-0.51	305	0.61	1	no
7B nuls25;msi-1(f);ls[msi-1+]	Post-hoc	treatment (condition=cond.)	FA	ARP2/3 inh,DMSO	t	-0.25	303	0.8	1	no
7B nuls25;msi-1(f);ls[msi-1+]	Post-hoc	treatment (condition=2h rec)	FA	ARP2/3 inh,DMSO	t	-0.78	356	0.44	1	no
7B nuls25;msi-1(f);ls[msi-1+]	Post-hoc	treatment (condition=4h rec)	FA	ARP2/3 inh,DMSO	t	-0.25	302	0.8	1	no
7C	Anova	genotype	FA	nuls25,nuls25;msi-1(f),nuls25	F	15.67	212364	1.7e-07		no
7C	Anova	condition	FA	2h rec -,2h rec +,4h rec -,4h rec +,cond.naive	F	23.01	512364	<1e-16		no
7C	Anova	genotype:condition	F		F	2.64	1012364	0.0034		no
7C	Post-hoc	condition (genotype=nuls25)	FA	2h rec +,2h rec -	t	0.5	256	0.62	1	no
7C	Post-hoc	condition (genotype=nuls25 msi-1(f))	FA	2h rec +,2h rec -	t	3.75	220	0.00023	0.0014	no
7C	Post-hoc	condition (genotype=nuls25 msi-1(f);ls[msi-1+cDNA])	FA	2h rec +,2h rec -	t	0.31	207	0.75	1	no
7C	Post-hoc	condition (genotype=nuls25)	FA	4h rec +,4h rec -	t	1.27	290	0.21	1	no
7C	Post-hoc	condition (genotype=nuls25 msi-1(f))	FA	4h rec +,4h rec -	t	3.96	252	9.7e-05	0.00058	no
7C	Post-hoc	condition (genotype=nuls25 msi-1(f);ls[msi-1+cDNA])	FA	4h rec +,4h rec -	t	-1	228	0.32	1	no

Abbreviations:  
*IN*: integer  
*FA*: factor  
*df*: degrees of freedom  
*varIdent*: model calculated accounts for heterogeneity of variance  
*P-values* represented on the figure are highlighted in **bold**.

† data has been log transformed for the statistical analysis

Table S8: Statistical Results for the Supplementary Figures ¶

Figure	Model	Condition tested	Class	Levels	Test	Test statistic	df	p.value	p.value.bonf	var/ident
S1A diacetyl	Anova	dilution	FA	10-2,10-3	F	9.72	1 81	0.0025		no
S1A diacetyl	Anova	genotype	FA	WT,msi-1(ff)	F	1.13	1 81	0.29		no
S1A diacetyl	Anova	dilution:genotype	FA		F	0.03	1 81	0.87		no
S1A benzaldehyde	Anova	dilution	FA	10-2,10-3	F	55.31	1 32	1.1e-06		no
S1A benzaldehyde	Anova	genotype	FA	WT,msi-1(ff)	F	0.25	1 32	0.62		no
S1A benzaldehyde	Anova	dilution:genotype	FA		F	0.71	1 32	0.4		no
S1A octanol	Anova	dilution	FA	10-2,10-3	F	0	1 32	0.98		yes
S1A octanol	Anova	genotype	FA	WT,msi-1(ff)	F	0.44	1 32	0.51		yes
S1A octanol	Anova	dilution:genotype	FA		F	0	1 32	0.99		yes
S1A isomylalcohol	Anova	dilution	FA	10-2,10-3	F	46.37	1 32	5.1e-08		yes
S1A isomylalcohol	Anova	genotype	FA	WT,msi-1(ff)	F	0.15	1 32	0.7		yes
S1A isomylalcohol	Anova	dilution:genotype	FA		F	0.17	1 32	0.68		yes
S1B	Anova	condition	FA	F>F,F>E,S>F	F	115.18	2 96	<1e-16		no
S1B	Anova	genotype	FA	WT,msi-1(ff)	F	0.05	1 96	0.82		no
S1B	Anova	condition:genotype	FA		F	0.49	2 96	0.61		no
S1C	Anova	condition	FA	naive_starved,diacetyl only,cond.	F	326.49	3 162	<1e-16		yes
S1C	Anova	genotype	FA	WT,msi-1(ff)	F	12.73	1 162	0.00047		yes
S1C	Anova	condition:genotype	FA		F	1.56	3 162	0.2		yes
S1D	Anova	time	numeric		F	535.86	1 228	<1e-16		yes
S1D	Anova	genotype	FA	WT,msi-1(ff)	F	58.09	1 228	1.2e-14		yes
S1D	Anova	time:genotype	FA		F	5.29	1 228	0.071		yes
S1D	Post-hoc	genotype (time=10)	FA	WT,msi-1(ff)	t	0.67	12	0.52		yes
S1D	Post-hoc	genotype (time=20)	FA	WT,msi-1(ff)	t	2.8	11	0.017	0.19	yes
S1D	Post-hoc	genotype (time=30)	FA	WT,msi-1(ff)	t	2.82	11	0.017	0.18	yes
S1D	Post-hoc	genotype (time=40)	FA	WT,msi-1(ff)	t	5.19	11	0.0087	0.096	yes
S1D	Post-hoc	genotype (time=50)	FA	WT,msi-1(ff)	t	5.54	10	0.0054	0.059	yes
S1D	Post-hoc	genotype (time=60)	FA	WT,msi-1(ff)	t	4.16	10	0.002	0.022	yes
S1D	Post-hoc	genotype (time=70)	FA	WT,msi-1(ff)	t	4.6	10	0.00098	0.011	yes
S1D	Post-hoc	genotype (time=90)	FA	WT,msi-1(ff)	t	5.22	8	0.0029	0.032	yes
S1D	Post-hoc	genotype (time=110)	FA	WT,msi-1(ff)	t	3.26	7	0.014	0.15	yes
S1D	Post-hoc	genotype (time=120)	FA	WT,msi-1(ff)	t	3.44	9	0.0074	0.082	yes
S1D	Post-hoc	genotype (time=240)	FA	WT,msi-1(ff)	t	3.07	7	0.018	0.2	yes
S3A	Anova	condition	FA	naive,cond.	F	26.73	1 108	1.1e-06		no
S3A	Anova	genotype	FA	WT,msi-1(ff);,ls[msi-1+cDNA]	F	77.29	2 108	<1e-16		no
S3A	Anova	condition:genotype	FA		F	4.57	2 108	0.012		no
S3A	Post-hoc	genotype (condition=naive)	FA	WT,msi-1(ff)	t	-5.99	42	4.2e-07	3.7e-06	no
S3A	Post-hoc	genotype (condition=cond.)	FA	WT,msi-1(ff)	t	-10.13	36	4.5e-12	4e-11	no
S3A	Post-hoc	genotype (condition=naive)	FA	msi-1(ff);,ls[msi-1+cDNA],msi-1(ff)	t	5.92	38	7.4e-07	6.6e-06	no
S3A	Post-hoc	genotype (condition=cond.)	FA	msi-1(ff);,ls[msi-1+cDNA],msi-1(ff)	t	8.74	28	1.7e-09	1.5e-08	no
S3A	Post-hoc	genotype (condition=naive)	FA	WT,msi-1(ff);,ls[msi-1+cDNA]	t	-0.01	38	0.99	1	no
S3A	Post-hoc	genotype (condition=cond.)	FA	WT,msi-1(ff);,ls[msi-1+cDNA]	t	1.26	34	0.22	1	no
S3A	Post-hoc	condition (genotype=WT)	FA	naive,cond.	t	4.84	42	1.8e-05	0.0016	no
S3A	Post-hoc	condition (genotype=msi-1(ff))	FA	naive,cond.	t	0.52	36	0.6	1	no
S3A	Post-hoc	condition (genotype=msi-1(ff);,ls[msi-1+cDNA])	FA	naive,cond.	t	4.97	30	2.5e-05	0.0023	no
S3B	Anova	condition	FA	naive,cond.	F	94.13	1 122	<1e-16		yes
S3B	Anova	genotype	FA	WT,msi-1(ff);,ls[msi-1+cDNA]	F	185.48	2 122	<1e-16		yes
S3B	Anova	condition:genotype	FA		F	6.61	2 122	0.0019		yes
S3B	Post-hoc	genotype (condition=naive)	FA	WT,msi-1(ff)	t	-9.88	41	2.1e-12	1.9e-11	yes
S3B	Post-hoc	genotype (condition=cond.)	FA	WT,msi-1(ff)	t	-17.62	38	7e-20	6.3e-19	yes
S3B	Post-hoc	genotype (condition=naive)	FA	msi-1(ff);,ls[msi-1+cDNA],msi-1(ff)	t	11.6	42	1.1e-14	1e-13	yes
S3B	Post-hoc	genotype (condition=cond.)	FA	msi-1(ff);,ls[msi-1+cDNA],msi-1(ff)	t	17.34	41	1.7e-20	1.6e-19	yes
S3B	Post-hoc	genotype (condition=naive)	FA	WT,msi-1(ff);,ls[msi-1+cDNA]	t	1.56	39	0.13	1	yes
S3B	Post-hoc	genotype (condition=cond.)	FA	WT,msi-1(ff);,ls[msi-1+cDNA]	t	-1	43	0.32	1	yes
S3B	Post-hoc	condition (genotype=WT)	FA	naive,cond.	t	8.86	39	7e-11	6.3e-10	yes
S3B	Post-hoc	condition (genotype=msi-1(ff))	FA	naive,cond.	t	0.34	40	0.74	1	yes
S3B	Post-hoc	condition (genotype=msi-1(ff);,ls[msi-1+cDNA])	FA	naive,cond.	t	5.84	43	6.1e-07	5.5e-06	yes
S3C	Anova	condition	FA	naive,cond.	F	47.62	1 127	2.1e-10		no
S3C	Anova	genotype	FA	WT,msi-1(ff);,ls[msi-1+cDNA]	F	201.86	2 127	<1e-16		no
S3C	Anova	condition:genotype	FA		F	8.25	2 127	0.00043		no
S3C	Post-hoc	genotype (condition=naive)	FA	WT,msi-1(ff)	t	-10.52	44	1.4e-13	1.2e-12	no
S3C	Post-hoc	genotype (condition=cond.)	FA	WT,msi-1(ff)	t	-13.59	36	9.6e-16	8.6e-15	no
S3C	Post-hoc	genotype (condition=naive)	FA	msi-1(ff);,ls[msi-1+cDNA],msi-1(ff)	t	8.87	38	8.5e-11	7.6e-10	no
S3C	Post-hoc	genotype (condition=cond.)	FA	msi-1(ff);,ls[msi-1+cDNA],msi-1(ff)	t	14.72	45	8.2e-19	7.4e-18	no
S3C	Post-hoc	genotype (condition=naive)	FA	WT,msi-1(ff);,ls[msi-1+cDNA]	t	0.25	44	0.81	1	no
S3C	Post-hoc	genotype (condition=cond.)	FA	WT,msi-1(ff);,ls[msi-1+cDNA]	t	-1.43	47	0.16	1	no
S3C	Post-hoc	condition (genotype=WT)	FA	naive,cond.	t	9.33	44	5.4e-12	4.9e-11	no
S3C	Post-hoc	condition (genotype=msi-1(ff))	FA	naive,cond.	t	0.4	36	0.69	1	no
S3C	Post-hoc	condition (genotype=msi-1(ff);,ls[msi-1+cDNA])	FA	naive,cond.	t	6.54	47	4.1e-08	3.7e-07	no
S3D	Anova	condition	FA	naive,cond.	F	0.5	1 118	0.48		no
S3D	Anova	genotype	FA	WT,msi-1(ff);,ls[msi-1+cDNA]	F	3.89	2 118	0.023		no
S3D	Anova	condition:genotype	FA		F	0.14	2 118	0.87		no
S3E	Anova	condition	FA	naive,cond.	F	3.45	1 85	0.067		no
S3E	Anova	genotype	FA	WT,msi-1(ff);,ls[msi-1+cDNA]	F	7.42	2 85	0.0011		no
S3E	Anova	condition:genotype	FA		F	0.23	2 85	0.8		no
S5G	Anova	genotype	FA	msi25,msi25,msi-1(ff)	F	1.22	1 179	0.27		yes
S5G	Anova	condition	FA	naive,cond	F	0.19	1 179	0.66		yes
S5G	Anova	genotype:condition	FA		F	0.32	1 179	0.57		yes
S5H	Anova	genotype	FA	msi25,msi25,msi-1(ff);,msi25 msi-1(ff);,ls[msi-1+cDNA]	F	3.37	2 199	0.035		yes
S5H	Anova	condition	FA	naive_starved,adapted,cond	F	39.42	3 199	<1e-16		yes
S5H	Anova	genotype:condition	FA		F	0.39	6 199	0.89		yes
S5H	Post-hoc	condition	FA	starved,naive	t	-0.93	1183	0.35	1	yes
S5H	Post-hoc	condition	FA	adapted,naive	t	-0.35	1009	0.72	1	yes
S5H	Post-hoc	condition	FA	cond,naive	t	-9.49	1265	1.1e-20	3.2e-20	yes

Abbreviations:

IN: integer

FA: factor

df: degrees of freedom

var/ident: model calculated accounts for heterogeneity of variance

P-values represented on the figure are highlighted in bold.

¶ data has been log transformed for the statistical analysis



## Supplementary References

- Bolte, S., and Cordelières, F.P. (2006). A guided tour into subcellular colocalization analysis in light microscopy. *J Microsc* 224, 213–232.
- Kimble, J. (1981). Alterations in cell lineage following laser ablation of cells in the somatic gonad of *Caenorhabditis elegans*. *Dev Biol* 87, 286–300.
- Ollion, J., Cochenne, J., Loll, F., Escudé, C., and Boudier, T. (2013). TANGO: a generic tool for high-throughput 3D image analysis for studying nuclear organization. *Bioinformatics* 29, 1840–1841.
- Pinheiro, J., Bates, D., DebRoy, S., Sarkar, D., & R Core Team. (2012). nlme: Linear and Nonlinear Mixed Effects Models. Retrieved from <http://cran.r-project.org/web/packages/nlme/>
- R Core Team. (2012). R: A Language and Environment for Statistical Computing. Vienna, Austria. Retrieved from <http://www.r-project.org/>
- Roy, P.J., Stuart, J.M., Lund, J., and Kim, S.K. (2002). Chromosomal clustering of muscle-expressed genes in *Caenorhabditis elegans*. *Nature* 418, 975-979.
- Schneider, C.A., Rasband, W.S., and Eliceiri, K.W. (2012). NIH Image to ImageJ: 25 years of image analysis. *Nat Methods* 9, 671–675.
- Sulston, J.E., White, J.G. (1980). NIH Regulation and cell autonomy during postembryonic development of *Caenorhabditis elegans*. *Dev Biol* 78, 577–97.
- Thévenaz, P., Ruttimann, U.E., and Unser, M. (1998). A pyramid approach to subpixel registration based on intensity. *IEEE Trans Image Process* 7, 27–41.
- Tian, L., Hires, S.A., Mao, T., Huber, D., Chiappe, M.E., Chalasani, S.H., Petreanu, L., Akerboom, J., McKinney, S.A., Schreiter, E.R., Bargmann, C.I., Jayaraman, V., Svoboda, K., and Looger, L.L. (2009). Imaging neural activity in worms, flies and mice with improved GCaMP calcium indicators. *Nat Methods*. 6, 875-81.

**Declaration by candidate**

I hereby declare that I autonomously carried out the PhD-thesis entitled “Molecular mechanisms of forgetting in *Caenorhabditis elegans*” and that it has not been submitted anywhere for any award. Where other sources of information have been used, they have been acknowledged. This PhD-thesis consists of an original research article that has been accepted for publication and was written in cooperation with the listed co-authors.

Signature: .....

Date: .....

## Curriculum Vitae

### Dr. med. Nils Omar Hadziselimovic

---

Address: Holderstüdeliweg 57  
4132 Muttenz  
E-mail: nils@hadziselimovic.net  
Telephone: 0765104981  
0615549055  
Date of birth: 28.04.1980 in Basel  
Nationality: Swiss  
Civil status: Married, one child

### Professional experience:

---

Since 2009 PhD-student in molecular neuroscience at the Biozentrum of the University of Basel in the laboratory of Prof. A. Papassotiropoulos  
2008 – 2009 Research fellow at the institute of andrology in Liestal

### Medical dissertation:

---

2009 „Der Zusammenhang zwischen der verminderten Expression von FGFR1 und TGFBR1 und der Ätiologie des Kryptorchismus“, submitted to the medical faculty of the University of Basel.

### Academic studies:

---

2000 – 2008 Medicine at the University of Basel

### Publications:

---

- de Quervain DJ, Kolassa IT, Ackermann S, Aerni A, Boesiger P, Demougin P, Elbert T, Ertl V, Gschwind L, Hadziselimovic N, Hanser E, Heck A, Hieber P, Huynh KD, Klarhöfer M, Luechinger R, Rasch B, Scheffler K, Spalek K, Stippich C, Vogler C, Vukojevic V, Stetak A, Papassotiropoulos A.: PKC $\alpha$  is genetically linked to memory capacity in healthy subjects and to risk for posttraumatic stress disorder in genocide survivors. Proc Natl Acad Sci U S A. 2012 May 14.
- Hadziselimovic F, Hadziselimovic N, Demougin P, Krey G, Oakeley EJ.: Deficient expression of genes involved in the endogenous defense system against transposons in cryptorchid boys with impaired mini-puberty. Sex Dev. 2011;5(6):287-93.
- Hadziselimovic F, Hadziselimovic N, Demougin P, Oakeley EJ.: Testicular gene expression in cryptorchid boys at risk of azoospermia. Sex Dev. 2011;5(2):49-59.
- Hadziselimovic N, Demougin P, Oakley EJ, Hadziselimovic F: Decreased expression of FGFR1, SOS1, RAF1 genes in cryptorchidism. Urol Int. 2010;84 (3):353-61.
- Hadziselimovic F, Hadziselimovic N, Demougin P, Krey G, Hoecht B, Oakeley EJ: EGR4 Is a Master Gene Responsible for Fertility in Cryptorchidism. Sex Dev. 2009;3 (5):253-263.